The Hong Kong

POLYTECHNIC UNIVERSITY

香港理工大学

The Department of Applied Biology and Chemical Technology

The Studies of Ultrasound Enhancement on Ultrafiltration for *Radix astragalus* Extracts and Cleaning of Fouled Membrane

CAI Ming

A thesis submitted in partial fulfillment of the requirements for

the degree of

DOCTOR OF PHILOSOPHY

May, 2010

Certificate of Originality

I hereby declare that this thesis is my own work and that, to the best of my knowledge and belief, it reproduces no material previously published or written, nor material that has been accepted for the award of any other degree of diploma, except where due acknowledgement has been made in the text.

(Signature)

CAI Ming

May, 2010

TO

My parents and my wife

May 2010

Abstract

This study investigated the effects of operational parameters on both ultrafiltration (UF) and ultrasound-assisted UF (USUF) processes of a natural product, *Radix astragalus* (*RA*) extracts. Dead-end flat sheet (DEFS) and cross-flow hollow fiber (CFHF) membranes were used in the processes.

Permeate flux and fouling resistances were investigated in the UF of *RA* extracts, in both DEFS and CFHF modules. Transmembrane pressure (TMP) was an important factor which could significantly influence the flux and resistances either in the DEFS or CFHF mode. 10 k or 30 k Da molecular weight cut-off (MWCO) of membrane was suitable for clarifying the *RA* aqueous extracts. By analyzing the fouling resistances, it was found that concentration polarization and reversible fouling were two main resistances which could significantly affect the performance of UF process. The quality of *RA* extracts has been improved after UF because of lower soluble solid and higher total polysaccharides. Polysaccharides and proteins were demonstrated as the main substances of membrane foulants in UF of *RA* extracts.

US technique was introduced to both DEFS and CFHF UF processes of *RA* extracts. Effects of ultrasonic parameters, including frequency, power and irradiation mode, on permeate flux and fouling resistances during both UF

processes were investigated. Ultrasonic irradiation made strong impacts on the UF processes, especially at low frequency and high output power. In DEFS, 12-15% enhancement in flux was observed at the US of 28 or 45 kHz frequency. Upon ultrasonic irradiation, the reversible resistance, including concentration polarization and cake layer, was sufficiently reduced as revealed by the quantitative resistance analysis using the resistance-in-series model. In CFHF, the flux enhancement could be up to 42% at the US of 45 kHz and 120 W, but it was 29% only at the US of 100 kHz and 600 W. Concentration polarization and cake layer resistances could be effectively decreased by US, which led to exciting flux performance. Though satisfactory enhancements were obtained, hollow fiber UF membrane was more susceptible to the US irradiation of high power and low frequency than the flat sheet membrane. It is necessary to carefully control the US power when it is applied to the UF process.

Response surface methodology (RSM) with a central composite rotatable design (CCRD) was employed to optimize the process of USUF for *RA* mixtures with hollow fiber membrane. The effects and mutual interactions of various parameters, namely ultrasonic power, ultrasonic irradiation mode, TMP and temperature, on flux reduction (Y_1) and process duration (Y_2) were investigated, simultaneously. The results showed that TMP was the most significant parameter, followed by the temperature, ultrasonic power and irradiation mode. The optimum conditions were found to be ultrasonic power of 120 W, continued

ultrasonic irradiation mode, TMP of 0.64 bar and temperature of 20 ºC. The two predicted response values were 55.3% and 53 minutes for Y_1 and Y_2, respectively, which were in good agreement with the results obtained from the confirmation experiments, about 57.0-60.3% and 53-58 minutes.

The kinetics of various resistances, including adsorption, pore blocking and cake layer resistances, were quantified as functions of time or time and TMP in UF and USUF processes. Mechanisms for the effects of US irradiation on membrane fouling were demonstrated by comparing with the dynamics of different resistances in these two processes. Semi-empirical models were developed for predicting flux decline in UF and USUF of *RA* extracts. According to the analysis on the fouling resistances and the phenomena of US irradiated hollow fiber membranes, acoustic cavitation, bubble collapse and micro-jet were believed to be the main mechanisms leading to membrane fouling reduction and permeate flux improvement.

Publications

1. **M. Cai**, S.N. Zhao, H.H. Liang, Mechanisms for the enhancement of ultrafiltration and membrane cleaning by different ultrasonic frequencies, *Desalination*, 263(2010) 133-138
2. **M. Cai**, S.J. Wang, H.H. Liang, Effect of ultrasound on ultrafiltration of *Radix astragalus* extracts and fouled membrane cleaning, *Separation and Purification Technology* 68(2009) 351-356
3. **M. Cai**, S.J. Wang, H.H. Liang, Effects of Ultrasound on the Ultrafiltration of *Radix Astragalus* Extracts with Cross-flow Hollow Fiber Module, poster presentation at *the 15th World Congress of Food Science and Technology*, Cape Town, South Africa, 22-26 August, 2010
4. **M. Cai**, H.H. Liang, Effect of operational factors on flux and resistances in ultrafiltration of *Radix Astragalus* aqueous extracts, poster presentation at *Euromembrane 2009 conference*, Montpellier, France, 6-10 September 2009
5. **M. Cai**, S.N. Zhao, H.H. Liang, Effect of ultrasound on the separation of dextran aqueous solution by polyethersulfone ultrafiltration membrane, poster presentation at *the 18th International Congress of Chemical and Process Engineering*, Prague, Czech Republic, 24th-28th August 2008

Acknowledgements

This thesis comprises my work at the Department of Applied Biology and Chemical Technology, the Hong Kong Polytechnic University during the year 2007-2010. The funding was supported by the Research Grants Council of the Hong Kong Special Administrative Region and the Research Committee of the Hong Kong Polytechnic University.

This work would not have been possible without the contributions from many individuals.

Above all, I would like to thank my advisor Dr. Hanhua Liang for the opportunity for me to pursue the Degree of Philosophy. He demonstrated trust and space for my skills and work. And also he gave kind guidance and suggestion during the entire period of this work.

I would thank the fellow members in Dr. Liang's research group and the department at PolyU. I am also happy to thank my friends in PolyU for giving me a colorful life in Hong Kong.

Finally, I will give my thanks to my parents and my wife. They give their support, encouragement and patience to let me finish my study.

Table of contents

List of Figures

List of Tables

List of abbreviations

ANOVA	Analysis of variance
CCRD	Central composite rotatable design
CFHF	Cross-flow hollow fiber
CIP	Cleaning-in-place
COP	Cleaning-out-of-place
Da	Dalton
DEFS	Dead-end flat sheet
DI	Deionized
FTIR	Fourier transform infrared spectroscopy
MAE	Microwave-assisted extraction
MF	Microfiltration
MWCO	Molecular weight cut off
NF	Nanofitration
NOM	Natural organic material
PES	Polyethersulfone
PS	Polysulfone
RA	Radix astragalus
R_c	Cake layer resistance
R_m	Intrinsic membrane resistance
R_{tot}	Total resistance

RO	Reverse osmosis
RSM	Response surface methodology
SEM	Scanning electron microscope
SFE	Supercritical fluid extraction
TMP	Transmembrane pressure
UAE	Ultrasound-assisted extraction
UF	Ultrafiltration
US	Ultrasound
USUF	Ultrasound-assisted ultrafiltration
VSEP	Vibratory shear enhanced filtration process

Chapter 1

Introduction

1.1 Problem statement

Radix astragalus (*RA*) is one of the typical and most widely used natural plants, and its main active constituents are polysaccharides, saponins and flavonoids, which have pharmacological and nutritional activities [1]. The main active constituents in the *RA* are usually extracted and separated by various technologies, such as heat reflux extraction, precipitation with ethanol and chromatography. However, technologies for clarification or separation of *RA* aqueous mixtures are still limited; thus it is necessary to find some more feasible techniques to apply to this area.

Membrane technology gradually applied in clarification or separation of *RA* extracts in the recent decade, especially the ultrafiltration (UF) [2, 3]. But the characteristics of flux performance and fouling in this process have not been systematically investigated. UF membrane is a porous membrane with the average pore size from 0.005 to 0.1 μm and operated at low pressure from 5 to 150 psi as the driving force [4]. It can be made from inorganic and organic materials, and has types of flat sheet, tubular, spiral wound and hollow fiber. Dead-end and cross-flow processes are two main operational modes, of which the latter is more commonly used. UF technology has been applied to the environment, food industry and biotechnology [5]. Though UF technology is a promising unit in the separation process, there are still some crucial problems which hinder its development and application. Membrane fouling is a critical problem in all

membrane processes, which can cause flux decline and affect the process efficiency. In order to minimize this fouling problem, some methods have been introduced into the membrane filtration process to enhance the permeate flux. Pretreatment of feed solution, modification of the membrane surface and optimization of process conditions have been greatly studied and satisfactory results were obtained [6]. Various additional techniques have also been introduced to the process, such as backflushing/backwashing, pulsatile flow, gas sparging, vibration and electrical field. However, besides these satisfactory techniques, it is still urgent to find some more effective methods to minimize the fouling problem.

Ultrasound (US) technique has been used in many areas, such as extraction and drying, because of its characteristics of cavitation, acoustic streaming, microstreaming, liquid micro-jet and radiation force in the liquid medium [7]. In recent years, it is found that US has the ability to enhance the flux during membrane filtration process. Obvious improvement of flux in the dead-end UF system was obtained due to a decrease of the boundary layer resistance on the membrane surface [8]. Effects of some ultrasonic parameters on flux have been investigated in cross-flow flat sheet membrane filtration process by Kobayashi and his group [9-12]. However, most studies used the dextran or peptone as a model solution, and they have not used a more complicated solution such as the natural product mixture. The permeate flux and fouling characteristics in the US-assisted UF (USUF) process, especially for *RA* extracts, have not been systematically

investigated and identified. Additionally, there is no published report found in the area of USUF process for *RA* aqueous mixtures, both in dead-end flat sheet (DEFS) and cross-flow hollow fiber (CFHF) modes.

1.2 Objectives

The overall purpose of this study is to introduce the US technique into both DEFS and CFHF UF processes for *RA* aqueous mixtures, and to investigate the effects of US on these two processes. Effects of ultrasonic parameters, including ultrasonic frequency, power and irradiation mode on the flux and fouling resistances in the UF and USUF processes will be investigated. The mechanisms of US induced fouling reduction and flux enhancement will be demonstrated and identified. The specific objectives are to:

a) study the effects of operational factors on the permeate flux and fouling resistances in both DEFS and CFHF UF processes for *RA* extracts;

b) study the effects of ultrasonic parameters on both US-assisted DEFS and CFHF UF processes for *RA* extracts and cleaning of fouled membrane;

c) optimize the operational conditions in the US-assisted CFHF UF process of *RA* extracts using response surface methodology;

d) identify the possible mechanisms for US induced flux enhancement and develop a feasible model for USUF process of *RA* extracts.

1.3 Dissertation overview

This thesis includes nine chapters. Chapters 1, 2, 8 and 9 are introduction, literature review, conclusions and future studies, respectively. Chapters 3 to 7 are the research works have been done in our study. Contents of these chapters are briefly summarized below:

Chapter 3 investigates the effects of some parameters, including temperature, transmembrane pressure (TMP), molecular weight cut-off (MWCO) or flow rate, on permeate flux and fouling resistances in both DEFS and CFHF UF of *RA* extracts. After UF with 10 kDa, the quality of *RA* extracts has been improved with lower soluble solid and higher total polysaccharides. Flux performances will be compared at different process conditions. Fouling resistances, including concentration polarization, cake layer and irreversible fouling will be calculated and analyzed based on the resistance-in-series model. The main constituents in membrane foulants will be analyzed by the FTIR technique.

Chapter 4 evaluates the effects of ultrasonic parameters on the DEFS UF process of *RA* extracts and fouled membrane cleaning processes. Amicon type UF cell with stirring will be modified by introducing US transducer probe. Influences of

various ultrasonic parameters in terms of ultrasonic frequency, power and irradiation mode on permeate flux and fouling resistances in the USUF process, and flux recovery in cleaning of fouled membranes will be investigated.

Chapter 5 studies the effects of ultrasonic parameters, such as ultrasonic frequency, power and irradiation mode, on permeate flux and fouling resistances during the USUF process for *RA* extracts with CFHF module. US power intensity inside the hollow fiber module will be measured. The feasibility of introduction of US to the membrane filtration process is going to be studied.

Chapter 6 optimizes the US-assisted CFHF UF process of *RA* mixtures using the response surface methodology (RSM) with a central composite rotatable design (CCRD). The effects and mutual interaction of some operational parameters, namely ultrasonic power, ultrasonic irradiation mode, TMP and temperature, on the USUF process of *RA* mixtures will be investigated. The optimum conditions of the process for minimizing both flux reduction and process duration will be obtained.

Chapter 7 develops semi-empirical models which are composed of the kinetics of various resistances, including adsorption, pore blocking and cake layer resistances. These resistances are quantified as functions of time or time and TMP, respectively. The mechanisms of US irradiation on the membrane fouling can be demonstrated by a comparison of the kinetics of different resistances in UF and USUF processes,

and the US irradiated UF membranes.

Reference

1. K.J. Kemper, Rebecca Small. Astragalus (*Astragalus membranaceus*). http://www. mcp.du/herbal/default.htm
2. Z.W. Yang, H.D. Liu, Z.G. Qu, The experimental study of astragalus injection between water-alcohol and ultrafiltration method, Lishizhen Medicine and Materia Medica Research 15 (2004) 837-838
3. G.L. Jiao, Y. Yang, B.H. He, Research on the extraction of astragalus polysaccharides by ultrafiltration, Chemistry and Bioengineering 27 (2010) 58-61
4. R.W. Baker, Membrane technology and applications, second edition, Wiley
5. A.K. Pabby, S.S.H. Rizvi, A.M. Sastre, Handbook of Membrane Separations, CRC Press, New York
6. N. Hilal, O.O. Ogunbiyi, N.J. Miles, R. Nigmatullin, Methods employed for control of fouling in MF and UF membranes: A comprehensive review, Separation Science and Technology 40 (2005) 1957-2005
7. K.S. Suslick, Ultrasound: Its Chemical, Physical, and Biological Effects, VCH, New York, 1988, pp65
8. A. Simon, N. Gondrexon, S. Taha, J. Cabon, G. Dorange, Low-frequency ultrasound to improve dead-end ultrafiltration performance, Separation Science and Technology, 35 (2000) 2619-2637
9. X. Chai, T. Kobayashi, N. Fujii, Ultrasound effect on cross-flow filtration of polyacrylonitrile ultrafiltration membranes, Journal of Membrane Science, 148

(1998) 129-135

10. T. Kobayashi, X. Chai, N. Fujii, Ultrasound enhanced cross-flow membrane filtration, Separation and Purification Technology, 17 (1999) 31-40
11. T. Kobayashi, T. Kobayashi, Y. Hosaka, N. Fujii, Ultrasound-enhanced membrane-cleaning processes applied water treatments: influence of sonic frequency on filtration treatments, Ultrasonics, 41 (2003) 185-190
12. K.K. Latt, T. Kobayashi, Ultrasound-membrane hybrid processes for enhancement of filtration properties, Ultrasonic Sonochemistry, 13 (2006) 321-328

Chapter 2

Literature Review

2.1 *Radix astragalus*

Astragalus memebranaceus (Fisch.) Bunge, known as *Huangqi* in China, is a classic plant from the Fabaceae family (legumes) and belongs to the subfamily Papilionoideae [1]. The roots of *astragalus* are cylindrical, not usually branched, 30-90 cm long and covered with a tough, yellowish-brown skin with a sweet white inner pulp [2]. Figure 2.1 shows the slice and grinded materials of *radix astragalus* (*RA*). The main active constituents of *RA* are polysaccharides, saponins, flavonoids and some other components such as amino acids and trace elements. The polysaccharides of *RA*, called astragalans or astragaloglucans, are present in a relative large quantity. It has been reported that the mass distribution of polysaccharides is wide and asymmetric, and most polysaccharides, about 57.6%, were distributed above 150 k Da and the content of polysaccharides between 3 k and 150 k Da was 13.2% only [3]. Different methods of extraction and purification have been used to extract polysaccharides, saponins and isoflavonoids according to their nature. Reflux extraction, Soxhlet extraction, UAE, MAE and matrix solid-phase dispersion extraction have been used in *RA* extraction [4-6]. These polysaccharides are mainly extracted by water or ethanol. Because most of the polysaccharides in *RA* are soluble in water, thus hot water extraction is usually used. There are two means: extract with hot water directly and extract with hot water after degreasing using some organic solvent like ethanol, ether, etc. Ni et al. [7] reported that it was easy and reasonable to extract using hot water directly at the optimum conditions, 12 mL g^{-1} water extracted for 1.5

hours and 3 times. Luo et al. [8] optimized the water extraction technologies for *RA*, and the content of polysaccharides was about 10.3013 $g \cdot mL^{-1}$ at the optimum condition. Fiber is a major ingredient in the herbs and may prevent the polysaccharides to be extracted easily and thoroughly. Extraction assisted with cellulase has been found as an effective method to maximize the extraction yield of polysaccharides [9, 10].

Figure 2.1 Slice and powder of *Radix astragulus*

The crude polysaccharides are usually precipitated by ethanol and then purified by sevage method [11] or polyamide resins [12] to remove proteins and collagen. A water soluble polysaccharide named as APS was isolated from *RA* by hot water extraction, anion-exchange and gel-permeation chromatography [13]. Wang et al. [14] isolated a water soluble hetero-polysaccharide, APSID3, from the crude polysaccharide by hot water extraction followed by precipitation with 95% alcohol and chromatography. In recent years, ultrafiltration technology has been applied

to clarify or separate the *RA* extract mixtures [15, 16].

2.2 Ultrafiltration membrane technology

2.2.1 Introduction

Membrane technology takes a crucial role in separation and purification processes and has been applied to many areas. The studies of membrane can be traced back to the eighteenth century when Abbé Nolet [17] first defined the word ‘osmosis’ in 1748. Membrane technology is basically like a sieving in terms of the pore size from 0.001 to 1000 μm and operated under a variety of driving forces such as pressure. According to the pore size, membrane technology can be divided into reverse osmosis (RO), nanofiltration (NF), ultrafiltration (UF), microfiltration (MF) and conventional filtration with the increased pore size. Figure 2.2 shows the applications of different membrane technologies in the separation of different substances. RO is commonly used to remove dissolved salts and organisms for the desalination of water, which is also considered as a dewatering technology. Pore size of membrane used in this separation process must be larger than 0.003μm. NF membrane is larger than RO membrane in pore size, and the permeation can be monovalent salts and undissociated acids. MF membrane technology is to separate suspended particles with porous diameters between 0.1 and 10 μm. It has been widely used in sterile filtration of pharmaceutical and wine, and treatment of drinking water.

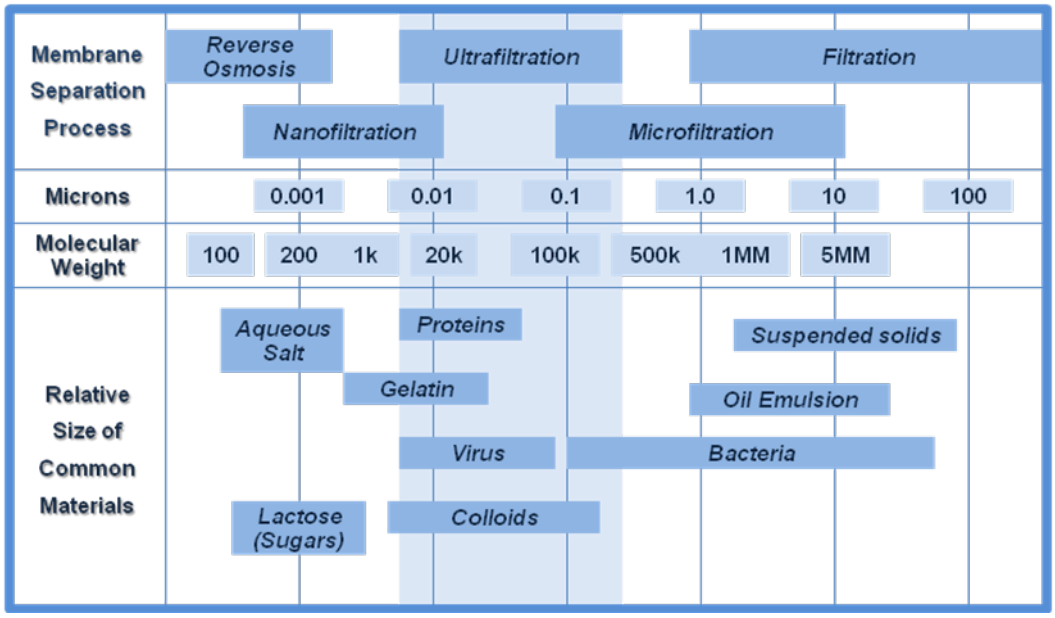

Figure 2.2 Membrane separation technology and its applications

2.2.2 Ultrafiltration technology

UF membrane is a porous membrane with the average pore size from 0.005 to 0.1 μm and operated at low pressure from 5 to 150 psi as the driving force. Bechhold [18] first synthesized a UF membrane from collodion and defined the term 'ultrafilter' in 1907. In 1969, Abcor [19] installed the first commercially successful industrial UF system equipped with tubular membrane modules to recover electrocoat paint from the rinse water in automobile paint shop. Today, UF membrane can be made from ceramic, regenerated cellulose, polysulfone, polyethersulfone, polyamide, etc. UF membrane usually has an asymmetric structure as shown in Figure 2.3. Dissolved macromolecules and particles, whose size is larger than the membrane pore, will be retained whilst the substances with smaller size can pass.

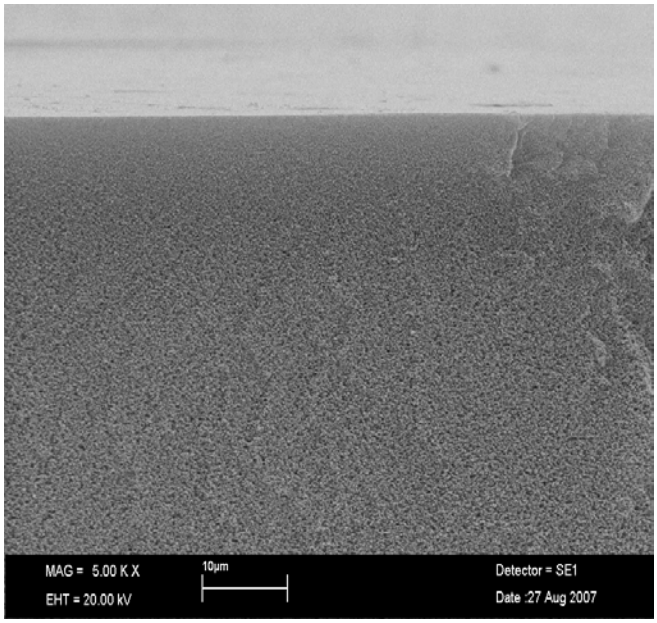

(a)

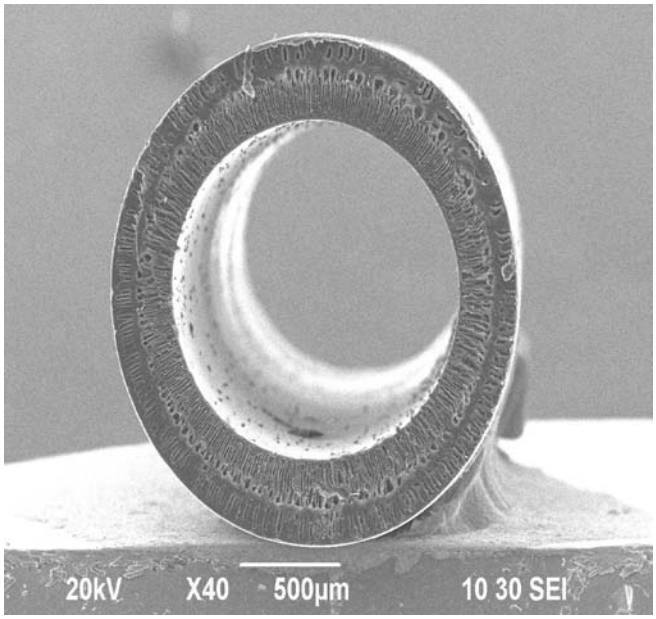

(b)

Figure 2.3 Structure of ultrafiltration membranes: (a) cross-section of a flat sheet UF membrane (PES); (b) cross-section of a hollow fiber UF membrane (PS)

Conventional UF process is operated in dead-end mode which is similar to the filter paper filtration. Because the critical fouling problem in dead-end filtration, UF becomes more widely operated in cross-flow (tangential) mode in which the flow is parallel to the membrane surface hence the permeation can be higher.

Figure 2.4 shows the two filtration modes.

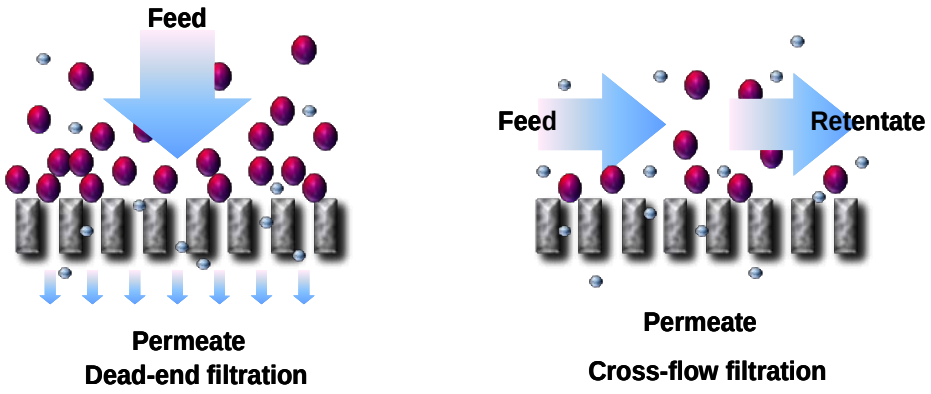

Figure 2.4 Dead-end and cross flow filtration modes

The principal types of UF module are plate-and-frame, tubular, spiral wound and hollow fiber [17]. Plate-and-frame module is one of the earliest types of membrane system, which primarily consists of a flat sheet membrane and a membrane holder. It is used in some small industries only because of its serious fouling problem and low efficiency. Tubular module is now generally limited to UF application, for which the benefit of resistance to membrane fouling due to good fluid hydrodynamics outweighs their high cost. Spiral wound module consists of a membrane envelope of spacer and membrane wound around a perforated central collection tube. Hollow fiber module is made of a bundle of capillary fiber membranes and a shell. It has two typical designs, out-in and in-out. The advantage of hollow fiber module is the ability to pack a very large membrane area into a single module. All these modules are operated in cross-flow mode which can effectively decrease the fouling.

2.2.3 Application of UF membrane

UF membrane has the ability to separate soluble macromolecules from other soluble substances in terms of the molecular weight or size. Over the past decades, UF technology has been applied to various areas, especially in environment, food and biotechnology.

2.2.3.1 Environmental technology

UF technology can be directly used in two main environmental aspects; namely water or wastewater treatment, and gas or air separation. Because UF can efficiently remove suspended particles and colloids, turbidity, algae, bacteria, parasites and viruses for clarification and disinfection, it is typically applied to remove natural organic material (NOM) for drinking water treatment. Lowe and Hossain [20] once applied UF membranes to remove humic acid from drinking water and they found that all the membranes with MWCO of 3 k, 5 k and 10 k Da can effectively remove humic acid with an efficiency of about 90%. Aoustin et al. [21] investigated UF of drinking water. They found that humic acid was responsible for irreversible pore adsorption and plugging. UF is also used in the treatment of waste water from paper plant and electrocoat paint, especially the oil/water emulsion. Tubular ceramic membranes with MWCO of 50 k and 300 k Da were used in a model metalworking oil/water emulsion by Alberto et al. [22]. It was found that various factors such as pH values and cross flow velocity were effective on improving the UF efficiency.

2.2.3.2 Food industry

UF has main applications in the dairy industry and the production of cheese. Appropriate UF membrane can effectively fractionate, purify and concentrate whey components. The initial protein content of 10-12% (dry basis) in whey can be increased to 35%, 50% or 80% protein products after UF, while decreasing in lactose and some salts [23]. Castro and Gerla [24] reported that cheese whey could be concentrated 20 times by batch UF using hollow fiber and spiral membrane. It was found that both concentrates retained 99% proteins in the original whey.

UF has also been used for the clarification of fruit juice, such as apple, pineapple, pear, orange and grape. In the traditional process, pectin and starch in juice are hydrolyzed by certain enzymes, which make flocculation, turbidity and haze in juice. The UF process, however, can effectively displace the conventional method because of their higher yield, better and reliable quality of juice. The clarified apple juice after UF without enzyme and pasteurization pretreatment has very good quality in NTU, transmittance and color, and no starch, pectin and thermo-acidophilic bacteria [25]. Compared with alcohol precipitation, Yapo et al. [26] found the yield, purity, chemical, and physicochemical features of isolated pectin in UF process depended upon the type of procedure used.

2.2.3.3 Biotechnology

Because of the characteristics of its operation at low temperatures and pressures,

and no phase changes or chemical additives, UF has been applied to concentrate protein, exchange buffer systems, clarify suspensions for cell harvesting, and sterilize liquids to remove viruses and bacteria [27]. Plasmid DNA was purified or concentrated by the simple, robust and scalable UF technology. Arkhangelsky et al. [28] studied on UF of plasmid DNA and found that the transmitted DNA copies kept their integrity and infectious ability. Virus capture is critical in gene therapy and vaccine production. The Aedes aegypti densonucleosis virus with particle size about 26 nm was purified using ion exchange UF membranes by Czermak et al. [29]. It was found that virus particles could be retained by membranes with MWCO of 30 k, 50 k and 100 k Da whereas 300 k Da membranes could let some virus pass. Nevertheless, UF has become an important part of biotechnology and its application in this area becomes more prevalent.

2.2.4 Membrane fouling phenomena

During UF process, the permeate flux usually decline with time, which is caused by various factors such as adsorption, pore blocking, concentration polarization and formation of cake/gel layer. These factors are defined as resistances which can be described as follows:

$$R_{tot} = R_m + R_{cp} + R_{cg} + R_a + R_p \qquad (2\text{-}1)$$

where R_{tot} is the total resistance, R_m the intrinsic membrane resistance, R_{cp} the concentration polarization, R_{cg} the cake/gel layer, R_a the adsorption and R_p the pore blocking.

R_m is the property of a membrane which is the only resistance in an ideal case. In the initial period of UF process, some solutes can be adsorbed immediately on the membrane surface, but they do not block the pores. This fouling phenomenon is called adsorption resistance, R_a. Because the UF membrane is porous, it is possible that some solutes can block the pores which lead to the pore blocking resistance, R_p. When the process continues, some solutes in solution gradually accumulate near the membrane surface which results in a high concentrated layer, namely concentration polarization resistance, R_{cp}. When the concentration of accumulated solutes arrives at a critical level, a cake/gel layer will form to be a resistance, R_{cg}. Figure 2.5 shows the distribution of different resistances on a UF membrane.

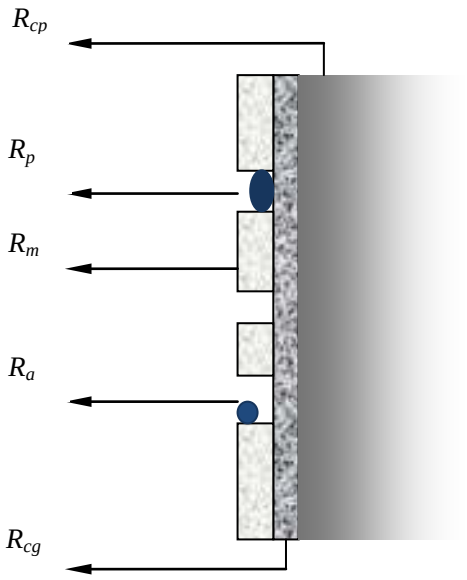

Figure 2.5 Different resistances on an ultrafiltration membrane. R_m, intrinsic membrane resistance; R_{cp}, concentration polarization; R_{cg}, cake/gel layer; R_a, adsorption; R_p, pore blocking.

Solutes in solution can be easily adsorbed on the membrane surface by the membrane-solute interactions. Some organic matters, such as proteins and polysaccharides in the solution, are the major substances which can be firstly adsorbed on the membrane surface by the interactions, especially on the hydrophobic membranes [30-33]. Some solutes, which are relatively similar or smaller size of the pores, can pass through and be adsorbed on the inside surface of membrane. Pore blocking is the phenomenon that membrane pores are plugged by the solutes which are similar in both shape and size [34, 35]. These two resistances are usually considered as irreversible fouling which can not be removed by water flushing and need further chemical cleaning. They usually occur at the initial stage during the membrane filtration process [36, 37].

Concentration polarization is one of the critical problems affecting the filtration. It always happens during the period of UF process, leading to the subsequent formation of cake/gel layer on the membrane surface. When solutes and solvent are carried towards the membrane surface, the solvent and solutes with small molecular weight permeate the membrane, while others like macromolecule or colloidal accumulate on the membrane surface. Thus the concentration of these macromolecules near the membrane surface is always 20-50 times higher than that of the original feed solution. Since concentration polarization is an important reason for the decline of permeate flux and subsequent fouling on the membrane, it is necessary to control or reduce it at the very beginning of UF process. In the past decades, concentration polarization has been studied by many researchers in different applications. Johnston et al. studied the concentration polarization in stirred UF cells using laminar boundary layer theory with a hybrid approach of applying locally the stagnant-film relationships but allowing the film thickness to vary with position [38]. In the dead-end UF process of dextran, the contribution of concentration polarization was found to be dependent on the applied pressures and initial bulk feed concentrations whereas the boundary layer thickness of concentration polarization was affected by feed concentration alone [39]. The role of concentration polarization and fouling in UF process can be different in terms of operational factors such as different UF membranes. Kwon et al. [40] found in UF of PEGylated proteins, the filtration behavior with the cellulose membranes was dominated by concentration polarization effects while significant fouling was observed with the polyethersulfone membranes.

A cake/gel layer forms when the concentration of solutes on the membrane surface reaches a critical level. The components of the cake/gel layer are primary the macromolecules or colloids in the solution. Natural organic matters (NOM) including microorganisms, bacteria and viruses are the major constituents in the cake layer fouling during drinking water treatment [20]. In most membrane purification processes of dairy and whey, protein is the major substance depositing on the membrane surface to form a cake/gel layer [41]. Besides some proteins, polysaccharides usually exist in the cake/gel layer in purification or clarification of fruit juice with UF technology. Saha et al. [42] used FTIR and SEM analytical techniques to study the polysaccharides fouling which contained arabinogalactan protein, phenolics and some lipids during the UF of sugarcane juice. All these substances in the cake/gel layer have high molecular weights larger than the pore size of membranes, as well as some that have the similar size with the membrane pore size.

2.2.5 Field Enhanced ultrafiltration process

The critical problem in UF process is flux decline which is primarily caused by the membrane fouling. In order to make the UF process more efficient, it is necessary to control the decline of flux more slowly. In other words, it should effectively reduce some of the various fouling resistances in the processes. Up to now, many methods have been employed into the membrane filtration process to enhance the permeate flux. Pretreatment of feed solution, modification of

membrane surface and optimization of the process conditions have been greatly studied and satisfactory results have been obtained [43]. In another aspect, some additional techniques have been introduced to the membrane separation process, such as backflushing/backwashing, pulsatile flow, gas sparging, vibration, electrical field and ultrasound [44-55].

Backflushing/backwashing is a common method used to reduce the concentration polarization and cake/gel layer fouling. It is mainly applied to cross-flow filtration processes and used to eliminate particle deposition which can enhance the permeate flux and flux recovery. The permeate flow is employed to the membrane in a reverse direction to filtration for a few seconds in every several minutes or longer in the backflushing cycle. The backflushing for cross-flow filtration is shown in Figure 2.6.

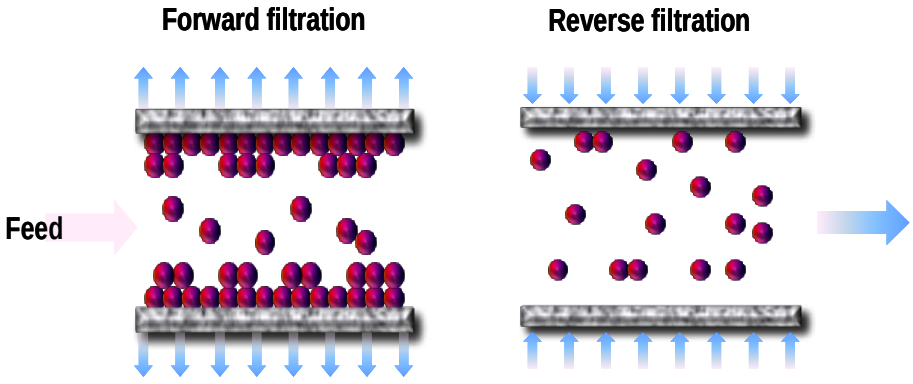

Figure 2.6 Backflushing on cross-flow membrane filtration

Pulsatile flow, which the pulsation is introduced into the feed or filtrate and permeate channels to obtain oscillations and unsteady flows, by usually alter TMP

or cross-flow velocity [44]. It can be more easily applied to the membrane configurations of tubular and hollow fiber. The mechanisms of pulsatile flow affecting membrane filtration are that backflushing and shear rate changes whereas backflushing achieved the greatest reductions [45]. Finnigan and Howell [46] found flux improvements of 300% when using periodically spaced, doughnut shaped, baffles in UF tubes together with pulsed flows with an oscillation frequency up to 2.5 Hz.

Gas sparging, using air or gas supplied to the UF system with feed solution to create a two phase flow, is effective in most modules such as flat-sheet, tubular, spiral wound and hollow fiber membranes. The concentration polarization and cake/gel layer can be reduced and the permeate flux will be enhanced, which mainly due to the promotional turbulence in flow by injected air or other gas. Figure 2.7 shows the two phase flow types in gas-liquid two phase system. Cui and his research group [47-51] have systemically and comprehensively studied the effects of gas sparging on different cross-flow UF modules. In tubular membrane, they found permeate flux increased by up to 60% for dextran, 113% for dyed dextran and 91% for BSA. The rejection ratios were also improved with an increase of between 5 and 10% [47]. In hollow fiber membrane, flux was enhanced almost 20-50% for dextran and 10-60% for albumin [48]. It was also found that flux enhancement was higher under continuous rather than intermittent gas sparging in hollow fiber UF process, up to 102% with a 10 g/L dextran feed concentration [49]. A 7% to 50% increase in permeate flux was observed in gas

sparged flat sheet UF of proteins [50].

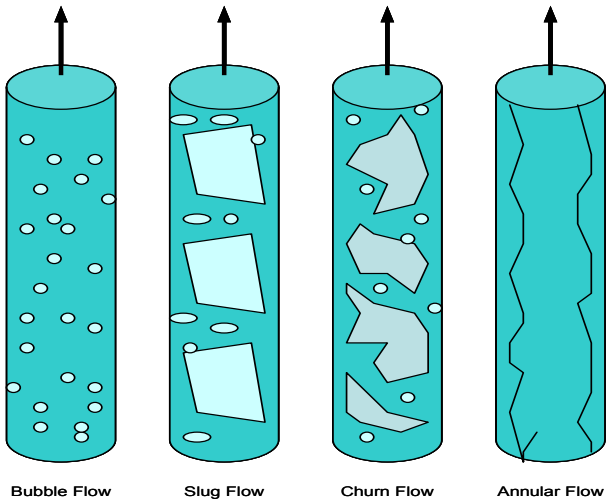

Figure 2.7 Flow types in gas liquid two phase filtration

Vibration technique has been coupled in filtration process as an integrated module, called vibratory shear enhanced filtration process (VSEP), which can reduce the fouling in both dead-end and cross-flow modes. Vibration can significantly improve the performance of UF process, simultaneously changes the morphology of foulants from a continuous layer into scattered clumps [52]. These modules have been developed and been proven to be able to ultrafilter extremely concentrated, viscous solutions which could not be treated by other conventional modules.

Electric field has been applied to cross-flow UF process to make charged particles move away from the membrane surface, leading to reduction in concentration polarization and cake/gel layer formation. Early in 1976, Klinkowski [53] proposed an electro UF process and apparatus. It is especially useful when used

in electrophoretic coating systems, because it can establish a stable bath composition and also tends to maintain the membrane in an essentially unfouled condition. It is also better to separate proteins because of their surface charge can be changed according to the pH of solution. Figure 2.8 shows the concentration polarization and cake/gel layer in the electro-UF process. Sarkar et al. [54] studied the process of cross-flow electro-UF of mosambi juice, a 32% enhancement of permeate flux was obtained by electric field. Iritani et al. [55] applied electric field to dead-end inclined and downward UF of protein solutions. Results showed that in downward electro-UF, the dynamical balanced filtration rate was directly proportional to the electric field strength, whilst in inclined electro-UF, the rate increases with the strength above the critical electric field strength.

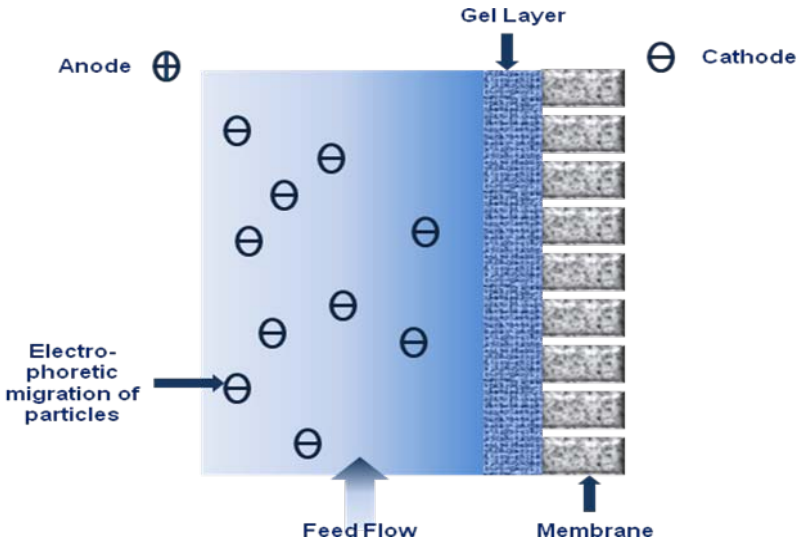

Figure 2.8 Concentration polarization and gel layers in electro-UF process

In recent years, US has been gradually employed to the membrane separation

process, especially in MF and UF processes. Primary studies have been carried out by some researchers, and results show that it is a promising assistant technique which can not only enhance the membrane filtration process but also improve the cleaning of fouled membrane. Detailed review will be shown in section 2.3.

2.2.6 Membrane cleaning

Membrane cleaning is an important step after UF process for regeneration and flux recovery of membrane. The fouled membranes can be cleaned by cleaning-in-place (CIP) or cleaning-out-of-place (COP). Because the COP method is not so convenient in pilot scale or industry, CIP is usually recommended. Cleaning procedure usually performs in three different forms: physical, chemical and biological.

Physical cleaning is firstly carried out after fouling process and before further chemical cleaning. It is used to remove concentration polarization and cake/gel layer formed on the membrane surface. The commonly used method is to rinse or flush the fouled membrane with water. In this step, temperature, TMP and rinse time are the most important factors which can affect the cleaning efficiency [56, 57]. Makardij et al. [56] found the optimum cleaning temperature was 55 ºC since the higher temperature led to a greater disintegration or solubilization of the deposit which provided smaller foulants. The best TMP in physical cleaning was suggested at 0.15 MPa, higher or lower pressure did not result in any improvement

of the rinsing efficiency [57]. Some assistant techniques have been introduced to the physical cleaning to improve the cleaning efficiency. Electric field assisted physical cleaning was carried out in the UF of a biological solution [58]. The plasma proteins above the isoelectric point were negatively charged so when the field was applied the particles were taken off the membrane surface, producing a fast increase of the permeate flux.

Generally, the flux recovery of membrane is not so satisfactory even after physical cleaning. Thus further chemical cleaning is needed. Appropriate chemical agents should be first selected in terms of the foulant type and the compatibility of the membrane with the agent at the cleaning temperature [44]. Sodium hydroxide, sodium hypochlorite, EDTA, SDS and citric acid have been widely used in cleaning fouled membranes as chemical solutions. Sodium hydroxide solution is an alkaline cleaner which can increase the solution pH, and therefore increase the negative charge and solubility of the organic foulant [59]. It is primarily used to clean organic foulant, such as bacteria and endotoxins, by hydrolysis and solubilization as well as sodium hypochlorite solution which is a disinfection agent. EDTA is a metal chelating agent which can effectively remove metal ions, such as calcium ion, from the complex organic molecules. Inorganic foulants are always removed by acids such as citric acid. The SDS is a surfactant agent which can attribute to cleaning strength of emulsifiers due to altering interfacial tension of water [60]. Because the foulants of membrane in dairy industry are proteins, sodium hydroxide or combined with sodium hypochlorite solution and EDTA is

usually used as the cleaning agents [60].

Enzymatic cleaners can clean the irreversible foulants by breaking the network chains of proteins or lipids, or the bonds between the foulants and the membrane surface, whereas the basic alkaline cleaning only removes isolated proteins from the membrane surface [61, 62]. The enzyme should be at an optimal concentration, higher or lower does not increase the enzymatic cleaning efficiency. Enzymatic cleaning is operated at low temperature, usually 25-40 ºC, thus avoiding membrane damage and saving energy. At the optimal condition, flux recovery of the membrane can achieve up to 100% [61-63]. Using enzymatic cleaner should firstly identify the foulants in/on the membrane; otherwise, it might be not effective. For example, if metal complexes are formed in the foulants, it is better to use an acid cleaning before the enzymatic cleaning [62].

2.2.7 Conclusion

UF membrane technology is an efficient process in water/wastewater treatment, juice/beverage clarification and biotechnology. Membrane fouling is the critical problem which makes the UF technology stagnant and curtailing its wide application. Fortunately, various assistant techniques have been introduced into the membrane separation technology to reduce concentration polarization and other membrane fouling, accordingly to improve the permeate flux and process efficiency. But further studies and improvements are still needed to be developed

in UF separation technology and cleaning of fouled membrane.

2.3 Ultrasound technique

2.3.1 Introduction

US is defined in terms of human hearing and is the sound having a higher frequency (> 20 kHz) that the human ear can respond. The basis for the generation of US was established as far back as 1880 with the discovery of the piezoelectric effect by the Curies [64, 65]. The earliest form of an ultrasonic transducer was a whistle developed by Francis Galton [66] in 1883 to investigate the threshold frequency of human hearing.

The use of US in this large frequency range is divided into two areas [67]. Figure 2.9 shows the ranges of sound frequency. The first area involves low amplitude sound and concerned with the physical effect of the medium on the wave and is commonly referred to as “low power” or “high frequency ultrasound”. Low amplitude waves are typically used for analytical purposes to measure the velocity and absorption coefficient of the wave in a medium in the range of 2 M to 10 M Hz. The second area involves high energy waves, known as “power ultrasound”, and lies between 20 k and 100 k Hz. It is used for cleaning, plastic welding and sonochemistry.

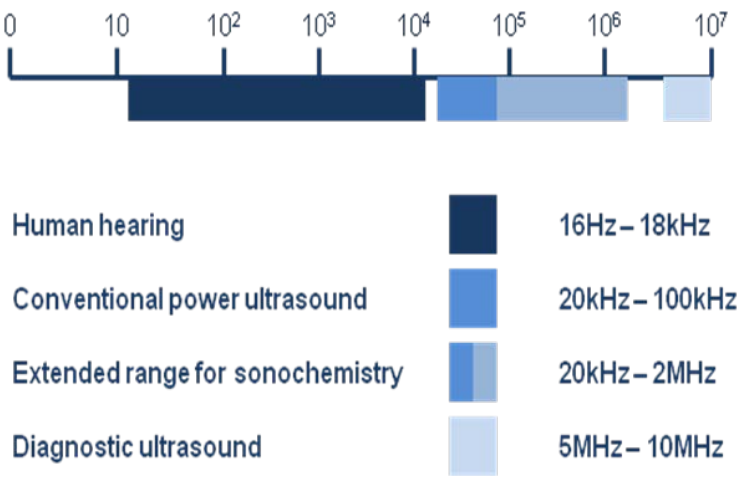

Figure 2.9 The ranges of sound frequency

The power US generation needs two essential components exist simultaneously, a medium and a source of high energy vibration. Ultrasonic transducer, source of the vibration energy, is to convert either mechanical or electrical energy into high frequency sound. Gas driven, liquid driven and electromechanical are the three main types of transducer.

2.3.2 Mechanisms

2.3.2.1 Introduction

US can propagate through any substance, such as solid, liquid and gas, by inducing vibratile motion of the molecules in which it is travelling. For liquids and gases, particle oscillation occurs in the direction of the wave and produces longitudinal waves. However, solids can also support tangential stresses bring on transverse waves. The sound motional waves represented by line and shaded colour are shown in Figure 2.10.

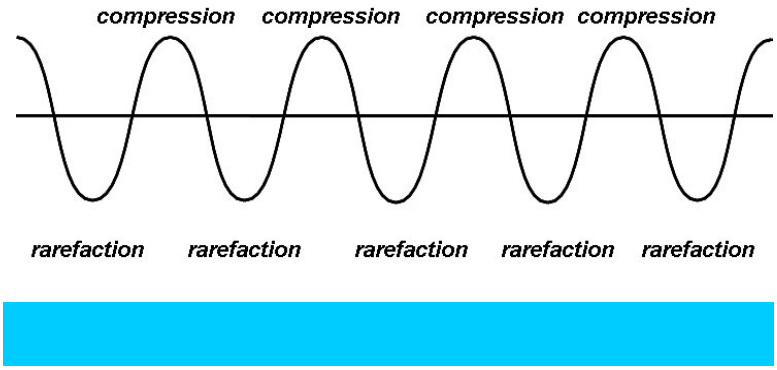

Figure 2.10 Sound motional waves

Because the sound is a form of energy, which is derived from the wave itself, the intensity of the sound wave can be expressed as follows:

$$I = \frac{P_A^{\,2}}{2\rho c} \tag{2-2}$$

where P_A is the amplitude of the oscillating acoustic pressure, ρ the density of medium and c the velocity of sound in the medium. According to Equation (2-2), the ultrasonic intensity can be measured by using a hydrophone and an oscillograph [68].

When ultrasonic wave propagates through a medium, intensity of the wave weakens as the distance from the radiation source increases. This attenuation can be caused by reflection, refraction, diffraction or scattering of the wave or it may be the result of converting some of the mechanical energy into heat [69]. A calorimetric method can be used to determine the ultrasonic power intensity by detecting the temperature rise ratio (dT/dt), assuming no heat lost as following

equation.

$$I = \frac{mC_p}{\pi r^2}\frac{dT}{dt} \tag{2-3}$$

where m is the total mass of medium, C_p the specific heat of the solvent and r the transducer probe tip radius.

2.3.2.2 Effects of ultrasound

Cavitation, acoustic streaming, microstreaming, liquid micro-jet, radiation force, etc. are considered as the main effects induced by US irradiation in liquid medium [68]. Cavitation is defined as the formation and the subsequent dynamic life of bubbles in liquids [70]. The cavitation is generally described as two types: transient and stable. The stable cavitation can lead to transient cavitation, whilst transient cavitation collapses to smaller stable bubbles. When the bubble collapses, the localized hot spot temperature can be up to about 5000 K, peak core temperature of 17000 K, as well as the pressure of about 2000 atm [68, 71]. These high temperature and pressure can induce both the physical and chemical effects. Figure 2.11 shows the effects of acoustic cavitation in different mediums.

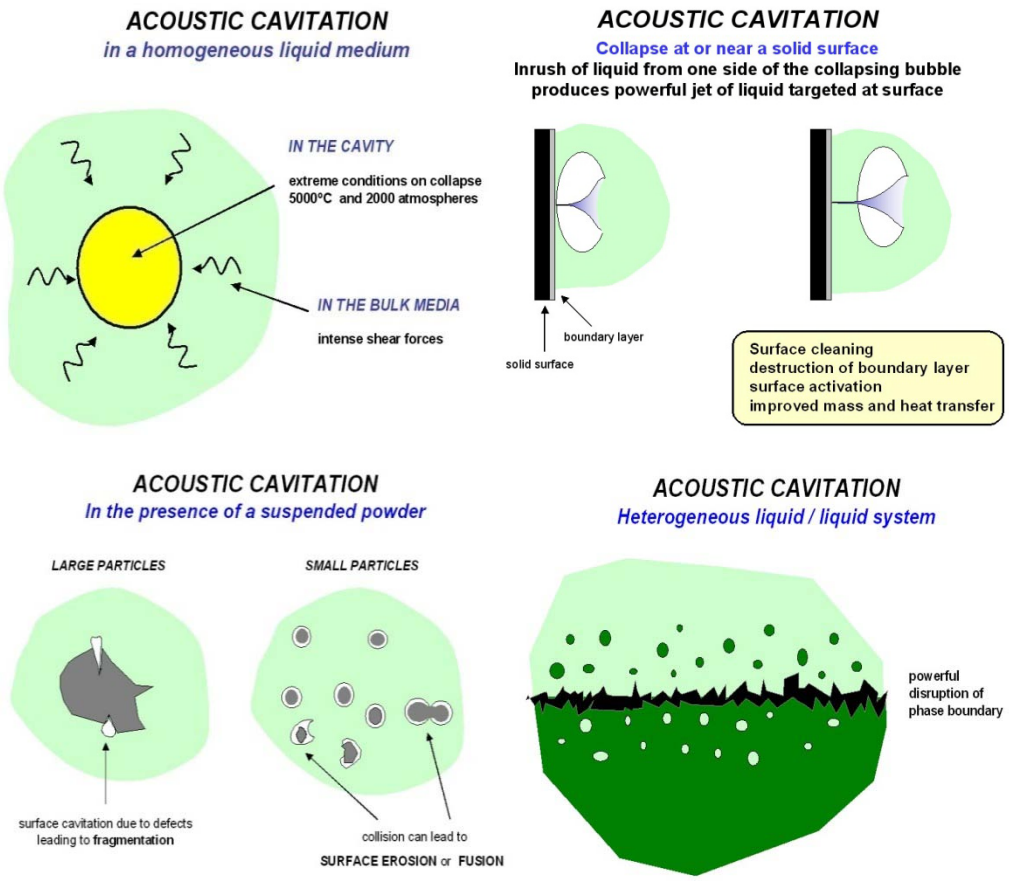

Figure 2.11 Effects of acoustic cavitation in different mediums [72]

Bubble dynamics is another aspect that can affect the US effects caused by acoustic cavitation in liquid medium. The spherical bubble contains gas and vapor and the liquid-bubble interface continually changes shape and size. Acoustic streaming, the time-independent flow of fluid induced by the US [68], makes velocity gradients, shearing stresses and related properties which has been proven useful for US application. It always present in the fluid away from the transducer, closely to the cross-section area of the transducer. Microstreaming exists around a small obstacle, especially the bubble. Micro-jet appears immediately when the bubble collapse with an estimated velocity of 100-200 ms^{-1} [74]. Figure 2.12 shows some effects in liquid induced by US irradiation.

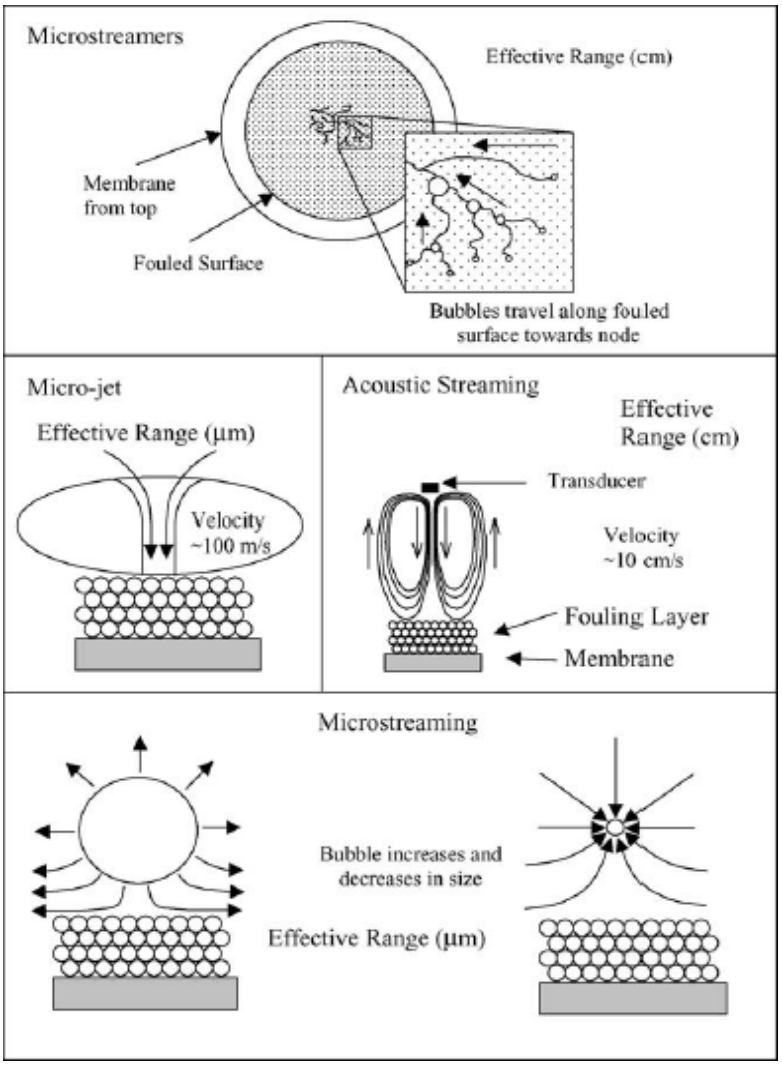

Figure 2.12 Some effects of liquid dynamic induced by ultrasound irradiation [73]

2.3.3 Application

US is a useful technique and has been effectively applied to some areas, as shown in Table 2.1, some typical applications. Based on these applications, there are two main equipments, ultrasonic bath and probe transducer. Bath equipment is usually designed as a tank with transducers outside of the stainless steel. This kind equipment can be used in laboratory and industry scales for cleaning and other uses. Probe system usually involves a transducer horn and an ultrasonic

generator. It is generally at 20 kHz frequency and is the best for laboratory uses like cell disruption and welding. In this section, applications of US in extraction, drying/adsorption, and membrane filtration and cleaning will be reviewed in detail.

Table 2.1 Some applications of ultrasound [75]

Application	**Examples**
Machining of materials	welding; cutting; drilling; soldering
Cleaning	General surface cleaning; washing of soil and ores
Homogenisation/Spraying	Emulsification and atomization of liquids
Separation	Crystallization; sieving; filtration
Degassing	Treatment of HPLC eluents
Water treatment	Removal of chemical and biological pollution
Biological uses	Cell disruption
Medical uses	Dental descaling; scalpels; lithptripsy; HIFU; preparation of protein microspheres; nebulisers

2.3.3.1 Ultrasound-assisted extraction

US has been effectively applied to liquid-liquid or liquid-solid extraction processes due to its efficient effects on improving the diffusion or mass transfer rate [76, 77]. US can be used in heterogeneous liquid-liquid systems especially in analytical chemistry, producing stable emulsions and facilitating the transfer [78]. In liquid-solid systems, US has been used especially in extraction of oil, protein and

other active components from foods or plants [79-81]. In these systems, US can enhance the selectivity, increase the yield and shorten the extraction time. Compared with steam distillation and superheated liquid extraction, US-assisted dynamic extraction was 176-165 min shorter than the first and 31-20 min shorter than the latter [82].

In recent years, US technique has been combined with some extraction technology to enhance the extraction efficiency. Hu et al. [83] applied US to conventional supercritical fluid extraction to extract oil and coixenolide from adlay seed. Results showed that with the US assistant, it reduced the temperature, pressure, CO_2 flow rate, as well as extraction time. 14% increase in the yield was obtained in this technology compared with supercritical fluid extraction. US was also combined with microwave extraction technology by Zhang and Liu [84]. At the optimum extraction conditions, the percentage of lycopene yield was 97.4% and 89.4% for ultrasonic and microwave-assisted extraction, and US-assisted extraction, respectively, which showed that US could efficiently enhance the extraction yield.

2.3.3.2 Ultrasound-assisted drying/ adsorption

During conventional drying processes, the structure of active components may change due to high temperature treatment. US can enhance the drying efficiency, especially in food drying, by not only mass transfer but also product quality due to no significant heat needed [85]. Acoustic intensity of US significantly affected

the drying process [86]. US can also make some components lose in food. Fernandes et al. [87, 88] found the pineapples and bananas lost sugar during the ultrasonic treatment, though the drying time was reduced by 8% for pineapples and 11% for bananas.

Generally, the regeneration of adsorbent resins is done by chemical solutions, which requires using organic solvents or inorganic chemicals and involves a difficult secondary separation step. US is found can not only promote desorption but also enhance the mass transfer of sorption processes [89, 90]. Ji et al. [91] studied the effect of US on adsorption of geniposide on polymeric resin. Results showed pulsed US could enhance both liquid film diffusion and intraparticle diffusion, in addition, the adsorption equilibrium constant decreased with increased ultrasonic intensity and pulse duty ratio.

2.3.3.3 Ultrasound-assisted filtration and fouled membrane cleaning

Actually, the application of US in filtration can be traced back to 1970s, Bjørnø et al [92] reported some studies on US-assisted pressure filtration rates in 1978. Though its application started long ago, the effects of US on filtration have not been widely studied. In recent years, some studies on US enhanced MF or UF membrane separation processes have been just reported. The enhancement of filtration process induced by US has been studied [93, 94].

US has been introduced to dead-end and cross-flow flat sheet MF or UF processes.

Simon et al. developed an US-assisted dead-end UF system using ultrasonic probe at 20 kHz [95]. Obvious improvement of flux was obtained due to a decrease of the boundary layer resistance on the membrane surface. Kobayashi and his group [96-99] systematically studied the effects of US on cross-flow flat sheet membrane filtration. Factors of ultrasonic frequency, module position, ultrasonic intensity and irradiation direction on membrane filtration were investigated. But most of these studies used dextran or peptone as a model solution, US-assisted filtration has not been widely applied to pilot or industry scale, except Muthukumaran et al. [100, 101] reported a study on US cleaning of UF membrane in dairy industry. Cleaning efficiencies using US were improved by 5-10% at all experimental conditions.

2.3.4 Conclusion

Because of the characteristics and effects of US, US technique can be applied to many areas for the improvement purpose. US-assisted extraction has been widely used due to its advantages of higher yield, short time and almost no structure damage. Though US was applied to filtration early, it has not been widely studied until recent years. However, there are still many existed problems should be resolved in its application. US is an effective assistant technique that can be applied to many conventional processes.

Reference

1. Subhuti Dharmananda. Astragalus: Practical Aspects of Administering the Herb. http://www.itmonling.org/arts/astragalus/htm
2. K.J. Kemper, Rebecca Small. Astragalus (*Astragalus membranaceus*). http://www. mcp.du/herbal/default.htm
3. Q.J. Yan L.J. Han, Z.Q. Jiang et al. Molecular Mass Distribution of Astragalus Polysaccharrides, Food Science 8 (2004) 27-30 (in Chinese)
4. H.B. Xiao, M. Krucker K. Albert, X.M. Liang, Determination and identification of isoflavonoids in Radix astragali by matrix solid-phase dispersion extraction and high performance liquid chromatograohy with photodiode array and mass spectrometric detection, Journal of Chromatography A 1-2 (2004) 117-124
5. J.Z. Song, S.F. Mo, Y.K. Yip, C.F. Qiao, Q.B. Han, H.X. Xu, Development of microwave assisted extraction for the simultaneous determination of isoflavonoids and saponins in *Radix Astragali* by high performance liquid chromatography. Journal of Separation Science 30 (2007) 819-824
6. W.H. Mao, L.J. Han, B. Shi, Optimization of microwave-assisted extraction of flavonoid from *Radix Astragali* using response surface methodology, Separation Science and Technology 3 (2008) 671-681
7. Y. Ni, Q. Su, X. Liu, X.R. Li, Optimization of water extraction technology of astragalus membranaceus polysaccharides, China Journal of Chinese Materia Medica 5 (1998) 284-286

8. Y. Luo, G. Liu, B.H. Zhou, S.D. Luo, Study on water extraction techniques for Radix astragali by the synthetical mark, China Hospital Pharmacy Journal 11 (2004) 667-669
9. Q.J. Yan, L.J. Han, Z.Q. Jiang, Extraction of Astragalus polysaccharides by cellulose, Chinese Traditional and Herbal Drugs 12 (2005) 1804-1807
10. X.W. Zhang, P.Z. Zhang, W. Gong, C.F. Chen, Optimization of Extraction Technology for Astragalus Polysaccharides by Cellulase, Food and Fermentation Industries 2007 (5) 158-161
11. J.J. Shan, S.C. Wang, D. Liu et al. Comparison of polysaccharides between hairy root of Astragalus membranaceus and its cultivation, China Traditional Herb Drugs 5 (2001) 413
12. R.M. Wang, X.R. Li, Determination of polysaccharides in the stalk and leaves of Astragalus, China Traditional Pat Med 5 (1999) 254
13. S.G. Li, Y.Q. Zhang, Characterization and renal protective effect of a polysaccharide from *Astragalus membranaceus*, Carbohydrate Polymers 78 (2009) 343-348
14. S.C. Wang, J.J. Shan, Z.T. Wang, Z.B. Hu, Isolation and structural analysis of an acidic polysaccharide from *Astragalus membranaceus* (Fisch.) Bunge, Journal of Integrative Plant Biology 48 (2006) 1379-1384
15. Z.W. Yang, H.D. Liu, Z.G. Qu, The experimental study of astragalus injection between water-alcohol and ultrafiltration method, Lishizhen Medicine and Materia Medica Research 15 (2004) 837-838
16. G.L. Jiao, Y. Yang, B.H. He, Research on the extraction of astragalus

polysaccharides by ultrafiltration, Chemistry and Bioengineering 27 (2010) 58-61

17. R.W. Baker, Membrane technology and applications, second edition, Wiley, pp.1
18. R.W. Baker, Membrane technology and applications, second edition, Wiley, pp.237
19. R.L. Goldsmith, R.P. deFilippi, S. Hossain and R.S. Timmins, Industrial Ultrafiltration, Membrane Processes in Industry and Biomedicine, M. Bier, Plenum Press, New York, pp. 267-300, 1971
20. J. Lowe and Md.M. Hossain, Application of ultrafiltration membranes for removal of humic acid from drinking water, Desalination 218 (2008) 343-354
21. E. Aoustin, A.I. Schafer, A.G. Fane, T.D. Waite, Ultrafiltration of natural organic matter, Separation and Purification Technology 22-23 (2001) 63-78
22. A. Lobo, Á. Cambiella, J.M. Benito, C. Pazos, J. Coca, Ultrafiltration of oil-in-water emulsions with creamic membranes: Influence of pH and crossflow velocity, Journal of Membrane Science 278 (2006) 328-334
23. B. Cancino, V. Espina, C. Orellana, Whey concentration using microfiltration and ultrafiltration, Desalination 200 (2006) 557-558
24. B.N. Castro, P.E. Gerla, Hollow fiber and spiral cheese whey ultrafiltration: minimizing controlling resistances, Journal of Food Engineering 69 (2005) 495-502
25. Y.S. He, Z.J. Ji, S.X. Li, Effective clarification of apple juice using membrane filtration without enzyme and pasteurization pretreatment, Separation and

Purification Technology 57 (2007) 366-373

26. B.M. Yapo, B. Wathelet, M. Paquot, Comparison of alcohol precipitation and membrane filtration effects on sugar beet pulp pectin chemical features and surface properties, Food Hydrocolloids 21 (2007) 245-255
27. C. Charcosset, Membrane processes in biotechnology: An overview, Biotechnology Advances 24 (2006) 482-492
28. E. Arkhangelsky, B. Steubing, E. Ben-Dov, A. Kushmaro, V. Gitis, Influence of pH and ionic strength on transmission of plasmid DNA through ultrafiltration membranes, Desalination 227 (2008) 111-119
29. P. Czermak, D.L. Grzenia, A. Wolf, J.O. Carlson, R. Specht, B. Han, S.R. Wickramasinghe, Purification of the densonucleosis virus by tangential flow ultrafiltration and by io exchange membranes, Desalination 224 (2008) 23-27
30. A.G. Fane, C.J.D. Fell, A.G. Waters, Ultrafiltration of protein solutions through partially permeable membranes-the effect of adsorption and solution environment, Journal of Membrane Science, 16 (1983) 211-224
31. M. Ulbricht, W. Ansorge, I. Danielzik, M. König, O. Schuster, Fouling in microfiltration of wine: The influence of the membrane polymer on adsorption of polyphenols and polysaccharides, Separation and Purification Technology, 68 (2009) 335-342
32. L.C. Koh, W.Y. Ahn, M.M. Clark, Selective adsorption of natural organic foulants by polysulfone colloids: Effect on ultrafiltration fouling, Journal of Membrane Science, 281 (2006) 472-479
33. G. Crozes, C. Anselme, J. Mallevialle, Effect of adsorption of organic matter

on fouling of ultrafiltration membranes, Journal of Membrane Science 84 (1993) 61-77

34. G. Belfort, R.H. Davis, A.L. Zydney, The behavior of suspensions and macromolecular solutions in crossflow microfiltration, Journal of Membrane Science, 96 (1994) 1-58
35. L. Song, Flux decline in crossflow microfiltration and ultrafiltration: mechanisms and modeling of membrane fouling, Journal of Membrane Science, 139 (1998) 183-200
36. M.K. Purkait, S. DasGupta, S.De, Resistance in series model for micellar enhanced ultrafiltration of eosin dye, Journal of Colloid and Interface Science 270 (2004) 496-506
37. T. Mohammadi, A. Kohpeyma, M. Sadrzadeh, Mathematical modeling of flux decline in ultrafiltrtion, Desalination, 184 (2005) 367-375
38. S.T. Johnston, K.A. Smith, W.M. Deen, Concentration polarization in stirred ultrafiltration cells, AIChE Journal, 47 (2001) 1115-1125
39. S.K. Zaidi, A. Kumar, Experimental studies in the dead-end ultrafiltration of dextran: analysis of concentration polarization, Separation and Purification Technology 36 (2004) 115-130
40. B. Kwon, J. Molek, A.L. Zydney, ultrafiltration of PEGylate proteins: Fouling and concentration polarization effects, Journal of Membrane Science 319 (2008) 206-213
41. A.D. Maechall, P.A. Munro, G. trägårdh, The effect of protein fouling in microfiltration and ultrafiltration on permeate flux, protein retention and

selectivity: A literature review, Desalination 91 (1993) 65-108

42. N.K. Saha, M. Balakrishnan, M. Ulbricht, Sugarcane juice ultrafiltration: FTIR and SEM analysis of polysaccharide fouling, Journal of Membrane Science 306 (2007) 287-297
43. N. Hilal, O.O. Ogunbiyi, N.J. Miles, R. Nigmatullin, Methods employed for control of fouling in MF and UF membranes: A comprehensive review, Separation Science and Technology 40 (2005) 1957-2005
44. R.J. Wakeman, C.J. Williams, Additional techniques to improve microfiltration, Separation and Purification Technology 2006 (2002) 3-18
45. H.Y. Li, C.D. Bertram, D.E.Wiley, Mechanisms by which pulsatile flow affects cross-flow microfiltration, AIChE Journal 44 (1998) 1950-1961
46. S.M. Finnigan, J.A. Howell, The effect of pulsatile flow on ultrafiltration fluxes in a baffled tubular membrane system, Chemical Engineering Research & Design 67 (1989) 278-282
47. Z.F. Cui, K.I.T. Wright, Gas-liquid two-phase cross-flow ultrafiltration of BSA and dextran solutions, Journal of Membrane Science 90 (1994) 183-189
48. S.R. Smith, Z.F. Cui, D.S. Pepper, Gas sparging to enhance permeate flux in ultrafiltration using hollow fiber membranes, Journal of Membrane Science 121 (1996) 175-184
49. S.R. Smith, Z.F. Cui, Gas-slug enhanced hollow fibre ultrafiltration-an experimental study, Journal of Membrane Science 242 (2004) 117-128
50. Q.Y. Li, R. Ghosh, S.R.Bellara, Z.F. Cui, D.S. Pepper, Enhancement of ultrafiltration by gas sparging with flat sheet membrane modules, Separation

and Purification Technology 14 (1998) 79-83

51. Z.F. Cui, T. Taha, Enhancement of ultrafiltration using gas sparging: a comparison of different membrane modules, Journal of Chemical Technology and Biotechnology 78 (2003) 249-253
52. W. Shi, M.M. Benjamin, Membrane interactions with NOM and an adsorbent in a vibratory shear enhanced filtration process (VSEP) system, Journal of Membrane Science 312 (2008) 23-33
53. P.R. Klinkowski, Electro ultrafiltration process and apparatus, US Patent 3945900
54. B. Sarkar, S. DasGupta, S. De, Cross-flow electro-ultrafiltration of mosambi (Citrus sinensis (L.) Osbeck) juice, Journal of Food Engineering 89 (2008) 241-245
55. E. Iritani, Y. Mukai, Y. Kiyotomo, Effects of electric field on dynamic behaviors of dead-end inclined and downward ultrafiltration of protein solutions, Journal of Membrane Science 164 (2000) 51-57
56. A. Makardij, X.D. Chen, M.M. Farid, Microfiltration and ultrafiltration of milk: some aspects of fouling and cleaning, Trans IchemE 77 (1999) 107-113
57. M.L Cabero, F.A. Riera, R. Álvarez, Rinsing of ultrafiltration ceramic membranes fouled with whey proteins: effects on cleaning procedures, Journal of Membrane Science 154 (1999) 239-250
58. C.C. Tarazaga, M.E. Campderrós, A.P. Padilla, Physical cleaning by means of electric field in the ultrafiltration of a biological solution, Journal of Membrane Science 278 (2006) 219-224

59. W.S. Ang, S. Lee, M. Elimelech, Chemical and physical aspects of cleaning of organic-fouled reverse osmosis membranes, Journal of Membrane Science 272 (2006) 198-210

60. M. Kazemimoghadam, T. Mohammadi, Chemical cleaning of ultrafiltration membranes in milk industry, Desalination 204 (2007) 213-218

61. M.J. Muñoz-Aguado, D.E. Wiley, A.G. Fane, Enzymatic and detergent cleaning of a polysulfone ultrafiltration membrane fouled with BSA and whey, Journal of Membrane Science 117 (1996) 175-187

62. S.T. Poele, J.V.D. Graaf, Enzymatic cleaning in ultrafiltration of wastewater treatment plant effluent, Desalination 179 (2005) 73-81

63. A. Maartens, P. Swart, E.P. Jacobs, An enzymatic approach to the cleaning of ultrafiltration membranes fouled in abattoir effluent, Journal of Membrane Science 119 (1996) 9-16

64. J. Curie, P. Curie, Développement par pression de lélectricité polaire dans le cristaux hémíèdres ã faces inclinées, C.R. Acad. Sci. Paris 91 (1880) 294

65. J. Curie, P. Curie, Contractions et dilatations produites par des tensions électriques dans les cristaux hémíèdres ã faces inclines, C.R. Acad. Sci., Paris 93 (1881) 1137

66. F. Galton, Inquiries into Human Faculty and its Development. AMS Press, New York, 1883

67. T.J. Mason, J.P. Lorimer, Applied Sonochemistry: The uses of power ultrasound in chemistry and processing, WILEY-VCH, Weinheim, 2002, pp3

68. K.S. Suslick, Ultrasound: Its Chemical, Physical, and Biological Effects, VCH,

New York, 1988, pp65

69. T.J. Mason, J.P. Lorimer, Applied Sonochemistry: The uses of power ultrasound in chemistry and processing, WILEY-VCH, Weinheim, 2002, pp34
70. K.S. Suslick, Ultrasound: Its Chemical, Physical, and Biological Effects, VCH, New York, 1988, pp65
71. M. Ashokkumar, F. Grieser, A comparison between multibubble sonoluminescence intensity and the temperature within cavitation bubbles, Journal of American Chemical Society 127 (2005) 5326
72. http://www.sonochemistry.info/introdution.htm
73. M.O. Lamminen, H.W. Walker, L.K. Weavers, Mechanisms and factors influencing the ultrasonic cleaning of particle-fouled ceramic membranes, Journal of Membrane Science 237 (2004) 213-223
74. T.G. Leighton, The Acoustic Bubble, Academic Press, London, 1994
75. T.J. Mason, D. Peters, Practical Sonochemistry: Power ultrasound uses and applications, 2nd, Horwood, England, 2002
76. M.D. Luque de Castro, F. Priego-Capote, Ultrasound assistance to liquid-liquid extraction: A debatable analytical tool, Analytica Chimica Acla 583 (2007) 2-9
77. M. Romdhane, C. Gourdon, Investigation in solid-liquid extraction: influence of ultrasound, Chemical Engineering Journal 87 (2002) 11-19
78. M.D. Luque de Castro, F. Priego-Capote, Ultrasound-assisted preparation of liquid samples, Talanta 72 (2007) 321-334
79. K. Vilkhu, R. Mawson, L. Simons, D. Bates, Applications and opportunities for ultrasound assisted extraction in the food industry – A review, Innovative Food

Science and Emerging Technologies 9 (2008) 161-169

80. .S. Zhang, L.J. Wang, D. Li, S.S. Jiao, X.D. Chen, Z.H. Mao, Ultrasound-assisted extraction of oil from flaxseed, Separation and Purification Technology 62 (2008) 192-198
81. S. Boonkird, C. Phisalaphong, M. Phisalaphong, Ultrasound-assisted extraction of capsaicinoids from capsicum frutescens on a lab- and pilot-plant scale, Ultrasonics Sonochemistry 15 (2008) 1075-1079
82. J.M. Roldán-Gutiérrez, J. Ruiz-Jiménez, M.D. Luque de Castro, Ultrasound-assisted dynamic extraction of valuable compounds from aromatic plants and flowers as compared with steam distillation and superheated liquid extraction, Talanta 75 (2008) 1369-1375
83. A. Hu, S. Zhao, H. Liang, T. Qiu, G. chen, Ultrasound assisted supercritical fluid extraction of oil and coixenolide from adlay seed, Ultrasound Sonochemistry 14 (2007) 219-224
84. L. Zhang, Z. Liu, Optimization and comparison of ultrasound/microwave assisted extraction (UMAE) and ultrasonic assisted extraction (UAE) of lycopene from tomatoes, Ultrasonics Sonochemistry 15 (2008) 731-737
85. J.V. García-Pérez, J.A. Cárcel, J. Benedito, A. Mulet, Power ultrasound mass transfer enhancement in food drying, IChemE 85 (C3) 247-254
86. S. de la Fuente-Blanco, E. Riera-Franco de Sarabia, V.M. Acosta-Aparicio, A. Blanco-Blanco, J.A. Gallego-Juárez, Food drying process by power ultrasound, Ultrasonics 44 (2006) e523-e527
87. F.A.N. Fernandes, F.E. Linhares Jr., S. Rodrigues, Ultrasound as pre-treatment

for drying of pineapple, Ultrasonics Sonochemistry 15 (2008) 1049-1054

88. F.A.N. Fernandes, S. Rodrigues, Ulrasound as pre-treatment for drying of fruits: Dehydration of bananas, Journal of Food Engineering 82 (2007) 261-267
89. M. Breitbach, D. Bathen, Influence of ultrasound on adsorption processes, Ultrasonics Sonochemistry 8 (2001) 277-283
90. M. Breitbach, D. Bathen, H. Schmidt-Traub, Effect of ultrasound on adsorption and desorption processes, Industry and Engineering Chemistry Research 42 (2003) 5635-5646
91. J. Ji, X. Lu, Z. Xu, Effect of ultrasound on adsorption of Geniposide on polymeric resin, Ultrasonics Sonochemistry 13 (2006) 463-470
92. L. Bjørnø, S. Gram, P.R. Steenstrup, Some studies of ultrasound assisted filtration rates, Ultrasonics, 16 (1978) 103-107
93. H.M. Kyllönen, P. Pirkonen, M. Nyström, Membrane filtration enhanced by ultrasound : a review, Desalination 181 (2005) 319-335
94. S. Muthukumaran, S.E. Kentish, G.W. Stevens, M. Ashokkumar, Application of ultrasound in membrane separation processes: A review, Reviews in Chemical Engineering 22 (2006) 155-194
95. A. Simon, N. Gondrexon, S. Taha, J. Cabon, G. Dorange, Low-frequency ultrasound to improve dead-end ultrafiltration performance, Separation Science and Technology 35 (2000) 2619-2637
96. X. Chai, T. Kobayashi, N. Fujii, Ultrasound effect on cross-flow filtration of polyacrylonitrile ultrafiltration membranes, Journal of Membrane Science 148 (1998) 129-135

97. T. Kobayashi, X. Chai, N. Fujii, Ultrasound enhanced cross-flow membrane filtration, Separation and Purification Technology 17 (1999) 31-40

98. T. Kobayashi, T. Kobayashi, Y. Hosaka, N. Fujii, Ultrasound-enhanced membrane-cleaning processes applied water treatments: influence of sonic frequency on filtration treatments, Ultrasonics 41 (2003) 185-190

99. K.K. Latt, T. Kobayashi, Ultrasound-membrane hybrid processes for enhancement of filtration properties, Ultrasonic Sonochemistry 13 (2006) 321-328

100. S. Muthukumaran, K. Yang, A. Seuren, S. Kentish, M. Ashokkumar, G.W. Stevens, F. Grieser, The use of ultrasonic cleaning for ultrfiltration membranes in the dairy industry, Separation and Purification Technology 39 (2004) 99-107

101. S. Muthukumaran, S. Kentish, S. Lalchandani, M. Ashokkumar, R. Mawson, G.W. Stevens, F. Grieser, The optimisation of ultrasonic cleaning procedures for dairy fouled ultrafiltration membranes, Ultrasonics Sonochemistry 12 (2005) 29-35

Chapter 3

Flux and Resistances Analysis in DEFS and CFHF UF Processes of *RA* Extracts

Abstract

Effects of various parameters on flux and resistances in both dead-end flat sheet (DEFS) and cross-flow hollow fiber (CFHF) UF of *RA* extracts were investigated. Temperature (20, 30, 40 and 50 ºC), transmembrane pressure (TMP) (0.4, 0.8, 1.0 and 1.2 bar), molecular weight cut-off (MWCO) of membranes (100 k, 30 k, 10 k, 5 k and 1 k Da) and flow rate (40, 95 and 145 $mL \cdot min^{-1}$) were employed in this study. TMP was an important factor that can significantly affect the flux and resistances either in DEFS or CFHF mode. 10 k or 30 k Da MWCO of membrane was suitable for clarifying the *RA* extracts but the 100 k Da membrane had the most serious fouling problem and the other two had very low fluxes. The quality of *RA* extracts has been improved after UF because of the lower soluble solid and higher total polysaccharides. The flux enhancements within the temperatures range from 20 to 50 ºC were slight, though it became a bit more significant near 60 ºC. The flow rate in our study range in CFHF UF had slight effect on flux performance. By analyzing resistances, concentration polarization and reversible fouling were two main resistances which could significantly affect the UF process. Polysaccharides and proteins were demonstrated as the main substances of membrane foulants in UF of *RA* extracts.

3.1 Introduction

Ultrafiltration (UF) is a useful separation technology used for clarification, concentration and fractionation in various areas, such as whey protein or polysaccharides concentration or fractionation [1], fruit juice purification [2,3], tea extracts clarification [4,5]. Fouling phenomenon, which causes the flux decline and membrane pollute, is a critical problem in all UF processes. Natural organic matter is recognized as the main substance fouled on the membrane in water purification processes [6]. In the food industry, proteins and polysaccharides accumulated on the membrane surface and some were blocked in the membrane pores, consequently reduce the efficiency of membrane [7-9]. Hence, it is necessary to understand the characteristics and mechanisms of the foulants formed on/in the membranes. Accordingly, some methods, such as gas sparging, vibration, electric field and ultrasound, can be effectively applied to reduce the foulants.

Radix astragalus (*RA*), an important natural product for use in medicine, contains polysaccharides, saponins and flavonoids as three major active components in its extracts. Traditionally, these active constituents were extracted by hot water and separated or purified with ethanol precipitation or resins [10]. However, the precipitation method usually needs to add some solvents which can make the downstream recycling costly and even lead to certain contamination in the extracts. UF is an appropriate and promising technology for clarification of natural product

mixtures. By using UF technology, macromolecules in the extracts with high molecular weight can be retained or concentrated and the permeate solution can be classified for further use.

The main objectives of this study are to clarify the *RA* aqueous extracts by using UF membrane technology, and to analyze the effects of some major factors on flux performance and fouling characteristics in both dead-end flat sheet (DEFS) and cross-flow hollow fiber (CFHF) UF processes. Temperature, transmembrane pressure (TMP), molecular weight cut-off (MWCO) of membrane, and flow rate were selected as the independent factors. Resistance-in-series model, FTIR and SEM analytical techniques were used to examine the structure and properties of foulants.

3.2 Materials and methods

3.2.1 *RA* extracts and reagents

Extracts of *RA* (purchased from a local market in Hong Kong) were prepared by putting 100 g pulverized *RA* into 1 L deionized water (DI) and extracted at 95-100 ^{o}C for 1 h first. The aqueous extracts were poured out and another 0.8 L fresh water was added for second 1 h extraction. These two aqueous extracts were combined, cooled down to room temperature and filtered through a filter paper before the UF experiments. The concentration of total polysaccharides in the

mixture is about 18-19 mg/mL.

3.2.2 UF membranes and modules

The polyethersulfone (PES) flat sheet UF membrane (Millipore, Bedford, USA), with respective MWCO of 1 k, 5 k, 10 k, 30 k or 100 k Da and effective area of 41.8 cm^2, was installed in a UF cell (Amicon model 8 400, Millipore, Bedford, USA) for dead-end UF experiments.

Hollow fiber UF modules (MidiKros, Spectrum, and Microza, Pall, USA), made from polysulfone (PS) with MWCO of 10 k Da and total effective area of 0.015 m^2, were used in this study.

3.2.3 UF process

3.2.3.1 Dead-end flat sheet UF process

The experimental set-up is shown in Figure 3.1. 100 mL *RA* extracts were put into the cell installed with a UF membrane. The effects of TMP at 0.4, 0.8, 1.0 or 1.2 bar on flux and resistances were investigated in the experiments. The experiments for temperature effects were conducted by immersing the UF cell into a temperature controlled water bath, while other experiments were carried out at room temperature with a stirred speed at 300 rpm. The permeate flux of *RA* extracts was continually measured by an electronic balance and the data were

recorded at an interval of 2 minutes. The fouled membrane was regenerated by rinsing with 200 mL DI water and immersing into 100 mL 0.1 M NaOH for 30 minutes.

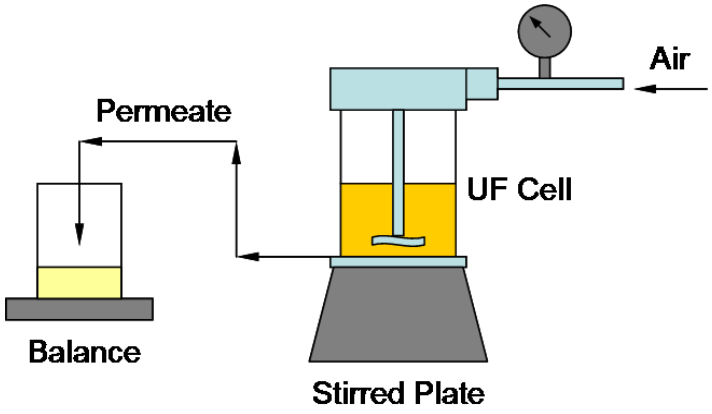

Figure 3.1 Experimental set up for DEFS UF of *RA* extracts

3.2.3.2 Cross-flow hollow fiber UF process

All experiments were carried out with a hollow fiber UF module with a bundle of 10 k Da MWCO PS membranes and total effective area of 0.015 m^2. The *RA* extracts were fed by a peristaltic pump (Masterflex, Cole-Parmer Ins. Co., USA) at various flow rates. The system TMP was adjusted at 0.4, 0.6 and 0.8 bar by controlling a valve on the retentate tube side. The feed container with a stirring bar inside was put on a heat plate with magnetic stirring function (Thermolyne Cimarec 1, Dubuque, USA). The schematic of the UF set-up is shown in Figure 3.2.

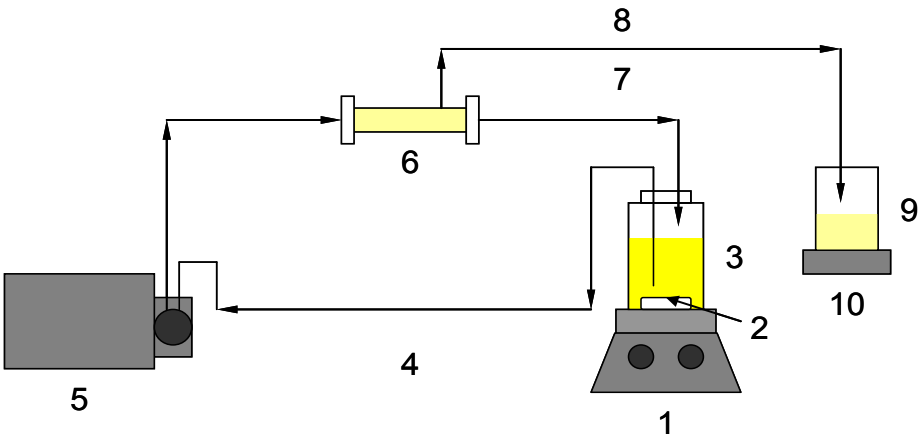

Figure 3.2 Experimental set-up of UF with hollow fiber membrane. 1) magnetic stirring and heat plate; 2) stirring bar; 3) feed container; 4) feed; 5) peristaltic pump; 6) hollow fiber module; 7) retentate; 8) permeate; 9) permeate container; 10) balance.

3.2.4 Determination of different resistances

3.2.4.1 Dead-end flat sheet UF process

The permeate flux can be expressed according to the following resistance-in-series model [11]:

$$J = \frac{\Delta P}{\mu R_{tot}} \tag{3-1}$$

where J is the permeate flux ($L \cdot m^{-2} \cdot h^{-1}$), ΔP the TMP (bar), μ the viscosity of solution (bar·h), and R_{tot} the total resistance (m^{-1}).

The total resistance R_{tot} in DEFS UF can be defined as

$$R_{tot} = R_m + R_{rev} + R_{irr} \tag{3-2}$$

where R_m is the intrinsic membrane resistance (m^{-1}), R_{rev} the reversible resistance (m^{-1}) including concentration polarization and cake/gel layer resistances, and R_{irr} the irreversible resistance (m^{-1}) which cannot be removed by water flushing.

Each resistance can be determined based on experimental measurements, according to the procedures described by Simon with modifications as follows [12]:

1) the flux of DI water was measured to obtain R_m;
2) the permeate flux of *RA* extracts solution was measured during the UF process to obtain R_{tot};
3) the *RA* extracts solution was removed and the reversible resistance was washed away by 200 mL DI water;
4) the flux of DI water was measured again in the UF process at the initial 5 minutes to obtain the value of R_m+R_{irr};
5) the membrane was chemically cleaned by 0.1 M NaOH for 30 minutes.

The value of R_{rev} can be obtained based on the Equation (3-2).

3.2.4.2 Cross-flow hollow fiber UF process

According to the resistance-in-series model, Equation (3-1), the resistances in hollow fiber UF process can be calculated. The total resistance in CFHF UF can be defined as follows:

$$R_{tot} = R_m + R_{cp} + R_{cg} + R_{frev} + R_{firr} \quad (3\text{-}3)$$

where R_{tot} is the total resistance (m^{-1}), R_m the intrinsic membrane resistance (m^{-1}), R_{cp} the concentration polarization (m^{-1}), R_{cg} the cake/gel layer resistance (m^{-1}), R_{frev} the reversible fouling which can be removed by chemical cleaning (m^{-1}), R_{firr} the irreversible fouling which cannot be removed by chemical cleaning (m^{-1}).

Each resistance can be determined using the procedures described by Jiraratananon [11] and Cassano [13] with modifications as follows:

1) R_m Water flux, J_w, can be measured in fixed conditions of temperature (room temperature) and flow rate at different TMPs, by Equation (3-1);
2) R_{tot} Permeate flux of *RA* extracts, J_{tot}, can be measured at different conditions, by Equation (3-1);
3) R_{cp} After the filtration of extracts, DI water was recirculated through the module at a low flow rate (13 mL·min^{-1}) and without pressure for 10 minutes. Water flux, J_{cp}, was measured;

$$R_{cg} + R_{frev} + R_{firr} + R_m = \frac{\Delta P}{J_{cp}\mu_w} \quad (3\text{-}4)$$

$$R_{cp} = R_{tot} - (R_{cg} + R_{frev} + R_{firr} + R_m) \quad (3\text{-}5)$$

4) R_{cg} A high water flow rate (200 mL·min^{-1}) was used at the same

procedure as in the measurement step of R_{cp}. After cleaning, water flux, J_f, was measured;

$$R_{cg} = \frac{\Delta P}{J_{cp}\mu_w} - (R_{frev} + R_{firr} + R_m) \quad (3\text{-}6)$$

$$R_{frev} + R_{firr} + R_m = \frac{\Delta P}{J_f \mu_w} \quad (3\text{-}7)$$

5) R_{frev}, R_{firr} 0.1 M NaOH solution was used to remove the foulant, recirculating and filtering for 30 minutes, respectively. DI water was used to remove the NaOH solution and then water flux, J_{firr}, was measured;

$$R_{firr} = \frac{\Delta P}{J_{firr}\mu_w} - R_m \quad (3\text{-}8)$$

$$R_{frev} = \frac{\Delta P}{J_f \mu_w} - \frac{\Delta P}{J_{firr}\mu_w} = \frac{\Delta P}{\mu_w}(\frac{1}{J_f} - \frac{1}{J_{firr}}) \quad (3\text{-}9)$$

3.2.5 FTIR spectroscopy and SEM analysis

The solutions of extracts, retentate, permeate and foulants were first evaporated and then dried for 2 days at -60 ºC in a vacuum freeze dryer (Alpha 1-4 LD2, Christ, Germany). Information about the presence of specific functional groups in the extracts, retentate, permeates and foulants on membrane surface was obtained by FTIR (Nicolet Avatar 360, Thermo Fisher, USA). KBr pellets

containing 0.5% (dry powder) of the sample were prepared. A total of 64 scans were performed at a resolution of 2 cm^{-1}, the optical path difference velocity was set at 0.2 cm^{-1}.

The fouled and washed flat sheet and hollow fiber membranes were freeze dried at -60 °C, sputter-coated with gold, and then imaged using a scanning electron microscope (SEM) (Stereoscan 440, Leica, UK).

3.3 Results and Discussion

3.3.1 Effect of UF on properties of *RA* extracts

The permeate solution in UF process looked much clearer and brighter than the extracts, as shown in Figure 3.3. The retentate solution looked whiter than the original extracts. This is because that most of the macromolecules such as polysaccharides and proteins being retained in the retentate by the UF membrane. Another reason is that the flavonoids and some pigments in extracts, which have low molecular weight and contribute a yellow color to the roots [14], can readily pass through the UF membrane as part of the permeate. The changes of soluble solid and total polysaccharides are shown in Table 3.1. As a result, the soluble solid of permeate was nearly 10% lower than that of the original extract of *RA* since some ingredients was retained by the membrane. Accordingly, the quality of the *RA* extracts has been improved after UF.

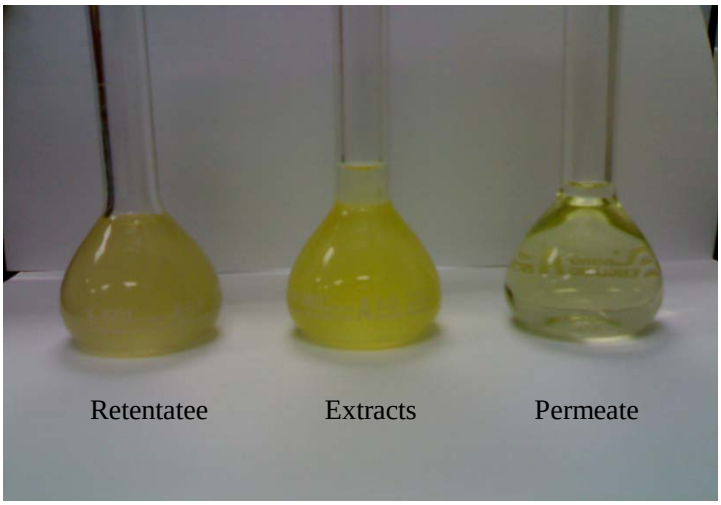

Figure 3.3 The extracts, retentate and permeate parts in UF process of *RA* extracts

Table 3.1 Changes of soluble solid and total polysaccharides in permeate of UF with different MWCO membranes

	Soluble Solid ($g \cdot L^{-1}$)	Changes (%)	Total Polysaccharides ($g \cdot L^{-1}$)	Changes (%)
Extracts	23.85		19.56	
100 kDa	23.01	3.40	19.08	2.43
30 kDa	21.78	8.11	18.06	7.67
10 kDa	21.90	8.03	18.08	7.57
5 kDa	19.97	16.14	18.01	7.92
1 kDa	19.87	16.78	17.79	9.05

3.3.2 Effect of temperature

The extracts temperature was kept from 20 to 60 ºC to investigate the effects of temperature on the permeate flux performance. Figure 3.4 showed the flux performances at different operational temperatures in both DEFS and CFHF

processes, which demonstrated that the flux could be improved by increasing the temperature. As shown in the figure, the improvements of flux from 20 to 50 ºC were slight, but it became relatively significant when the temperature rose to about 60 ºC. In DEFS mode, the enhancements of flux were only 4%, 13% and 15% at 30, 40 and 50 ºC, respectively. In CFHF mode, the enhancements of flux were 18% and 27% at 39 and 47 ºC, respectively, and it was up to almost 45% at 57 ºC. The changes of flux at different temperatures may be mainly caused by the changes of diffusion coefficient and viscosities of the *RA* extracts. Though the flux around 60 ºC was relatively high, the high temperature might cause membrane damage or shorten its service life in the same time. Moreover, the flux reductions during the UF of *RA* extracts were all around 30% from about 20 to 50 ºC, but became nearly 40% at 57 ºC in CFHF mode. Consequently, it was more convenient and economical to operate UF processes at room temperature due to only the slight effect on flux improvement exited in this temperature range.

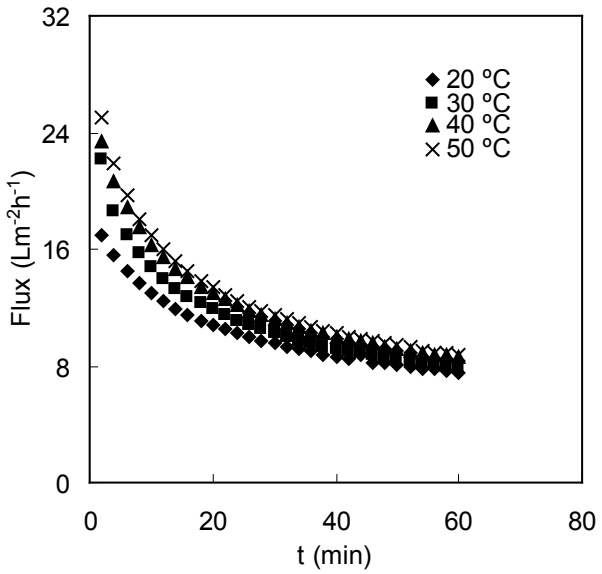

(a)

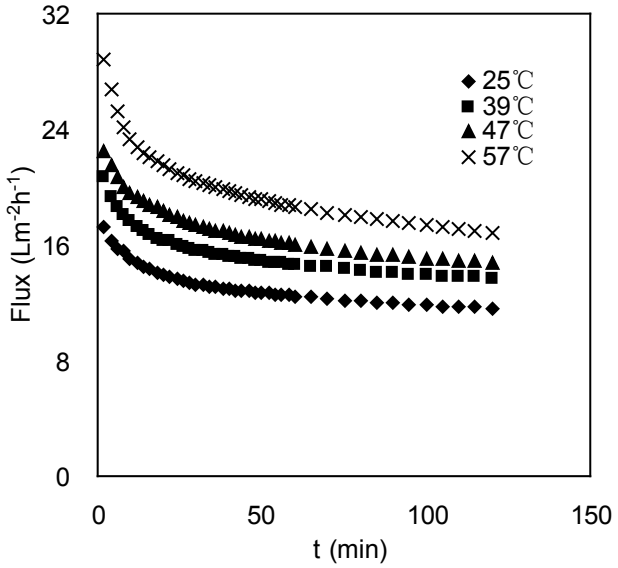

(b)

Figure 3.4 Effects of temperature on flux performance in UF process of *RA* extracts: (a) DEFS; (b) CFHF

3.3.3 Effect of TMP

TMP is the driving force in UF process and considered as one of the main factors that can affect both permeate flux and fouling resistances. Figure 3.5 shows the flux performances at different TMPs in DEFS and CFHF modes. In DEFS UF

mode, the flux enhancements were 40%, 71% and 81% when the TMP increased from 0.4 bar to 0.8, 1.0 and 1.2 bar, respectively. Flux reduction in UF process, which was all around 65%, was not significantly affected by the TMP change. In CFHF UF mode, the flux enhancements were 75%, 123% and 166% at 0.6, 0.8 and 1.0 bar, respectively. Flux reduction in this mode, which was from about 40% to 55% with the increased TMP, was smaller than that in DEFS mode. The relationships between fluxes and TMP demonstrates that higher TMP can cause higher flux, while the flux reduction becomes more serious, caused by the fouling formation on/in the membranes. Therefore, it is not appropriate to increase the TMP unlimitedly and there can be an optimum TMP for obtaining both maximum flux and minimum membrane fouling.

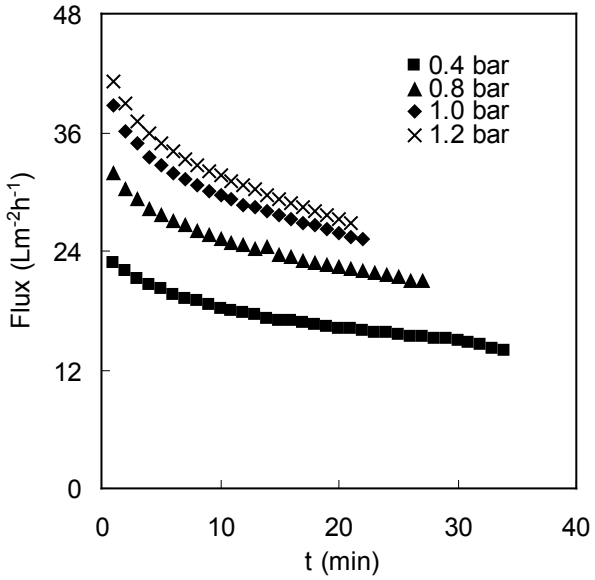

(a)

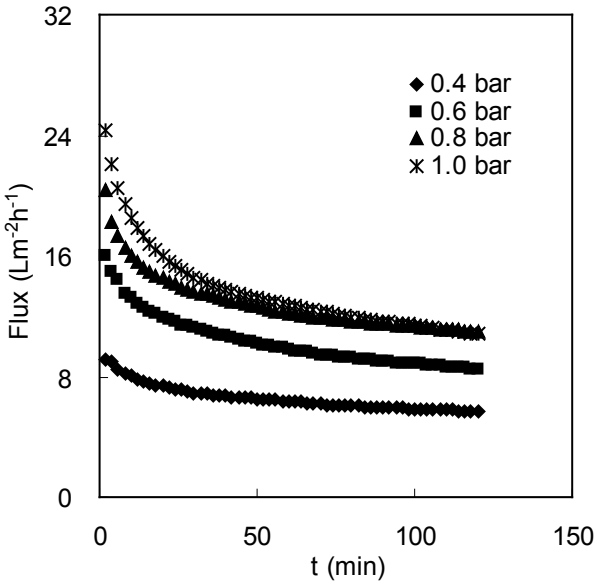

(b)

Figure 3.5 Effects of TMP on flux in DEFS and CFHF UF of *RA* extracts: (a) DEFS; (b) CFHF

The values of resistance, including R_m, R_{irr}, R_{rev} and R_{tot} in the DEFS, and R_m, R_{firr}, R_{frev}, R_p, R_c and R_{tot} in the CFHF at different TMPs, were calculated in terms of the resistance-in-series model. Figure 3.6 shows the contributions of each resistance at different TMPs in these two modes. Figure 3.6a shows that at low TMP, such

as 0.4 bar, the contributions of R_m, R_{irr} and R_{rev} were almost identical; when the TMP increased, the contribution of R_{rev} became significant, especially at TMP of 1.2 bar, it could be up to almost 60%. This indicated that higher TMP would cause higher concentration polarization and cake layer. By contrast, the contribution of R_{irr} became less significant at high TMP, though the values also increased but only slightly with the increased TMP. This might be caused by those substances in the extracts, which had molecular weights similar to the pore size of the membrane, thus passed through or stuck in the membrane pores more easily at higher TMP. In the CFHF UF process, concentration polarization and reversible fouling were the two main resistances, as shown in Figure 3.6b. Concentration polarization became significant as the pressure increased, contributing nearly 50% at 1.0 bar. The contribution of cake/gel layer resistance remained almost the same at all pressure levels. Irreversible fouling, like pore blocking or adsorption, showed the same trend as that in the DEFS. The results from both systems confirmed that higher TMP could make concentration polarization more serious and cake/gel layer thicker, leading to more dramatic flux reduction. The concentration polarization and cake/gel layer played important roles in the UF process of *RA* extracts.

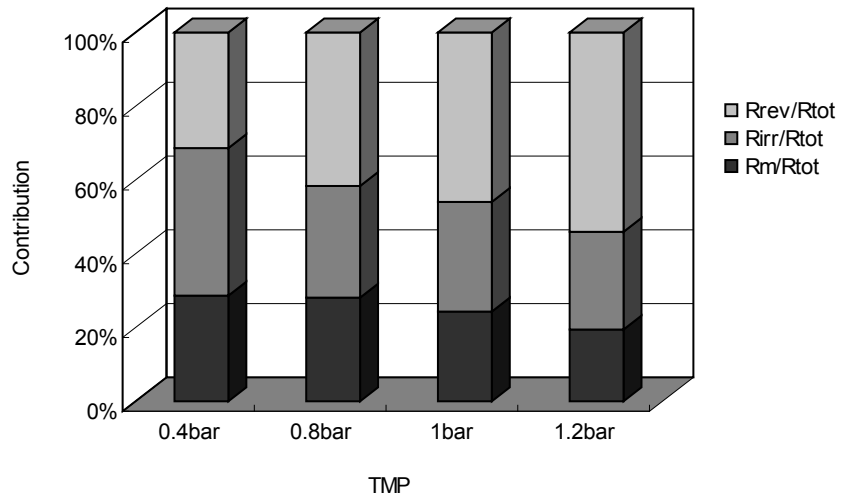

(a)

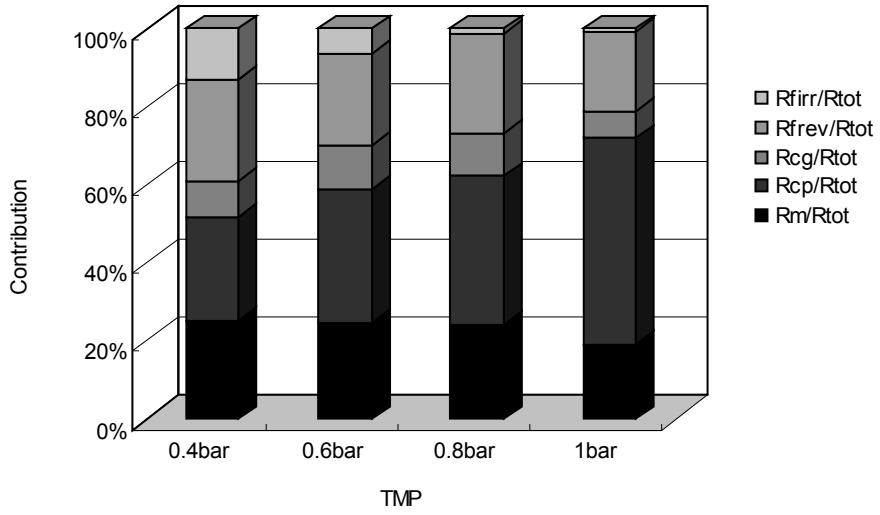

(b)

Figure 3.6 Effects of TMP on resistances contributions in DEFS (a) and CFHF (b) UF processes of *RA* extracts.

3.3.4 Effect of MWCO of membrane

Experiments for the effect of different MWCO of membranes on flux and resistance were carried out in DEFS only. The molecular weight distribution of the constituents in *RA* extracts is wide and asymmetric, therefore appropriate membranes with different MWCO should be selected. Figure 3.7a shows the flux

performances with different MWCO membranes in the UF process. At the beginning, the flux with 100 k Da membrane was much higher than that with the others, and over triple than that with 30 k and 10 k Da membranes; but it dropped sharply during the process, with almost 70% reduction in 20 minutes. It indicated that the fouling phenomenon in 100 k Da membrane was serious. Flux performances with 30 k and 10 k Da membranes were almost the same, indicating that the substances in the extracts with a molecular weight between 10 k and 30 k were quite less. With the membrane of 5 k and 1 k Da, flux performance declined slightly, almost forming a horizontal line as shown in Figure 3.7a. Table 3.2 shows the flux reductions for DI water (before and after fouling) and *RA* extracts with different MWCO membranes. These results indicated that pore plugging or adsorbing might be one of the important causes of membrane fouling in the UF process of *RA* extracts.

Resistances, namely R_m, R_{irr} and R_{rev}, were calculated based on each experimental results with different MWCO membranes, and their contributions were plotted in Figure 3.7b. As seen in the figure, the contribution of R_m gradually increased from 100 k to 1 k Da, but R_{irr} and R_{rev} showed different trends. Contributions of R_{rev} for 100 k, 30 k and 10 k were all significant and similar, nearly to 60%. It indicated the amount of substances with molecular weight between 10 k and 100 k Da in the extracts of *RA* was small, which was approximately the same as that reported by Yan et al. [15]. For the membrane of 5 k Da, the contributions of R_{irr} and R_{rev} were similar, about 35-40%, but R_{irr} was increased almost twice of that

with 30 k and 10 k Da membrane. This suggested that the substances in extracts having a molecular weight around 5 k Da could be more easily blocked in the membrane pores. The R_{irr} was too small while R_m played a very important role in the resistances of 1 k Da membrane, which could be the reason that the flux performance showed a horizontal line during the UF process.

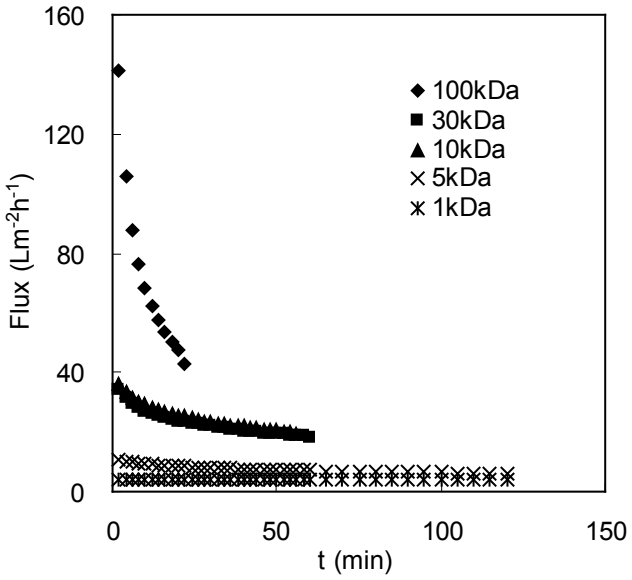

(a)

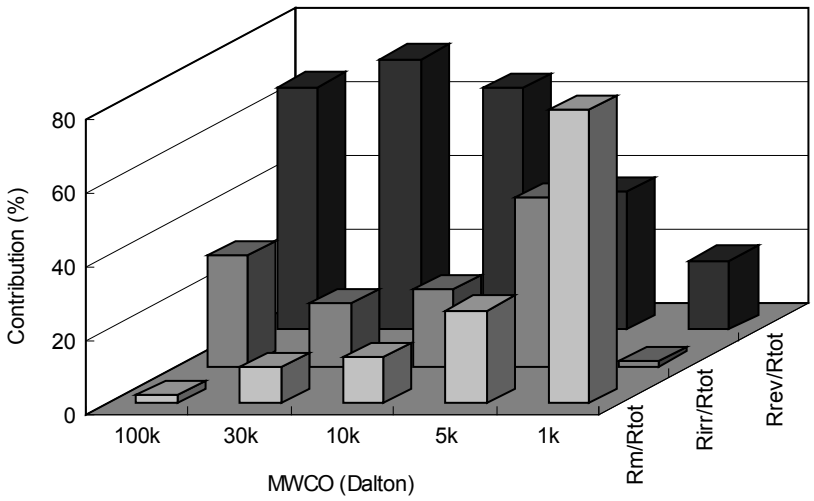

(b)

Figure 3.7 Flux performances (a) and contribution of resistances (b) in UF of *RA* extracts at different MWCO membranes (1bar, room temperature, 300 rpm)

Table 3.2 Flux reduction for DI water (after fouled) and *RA* extracts with different MWCO membranes

	Flux Reduction (%)				
	100 k Da	30 k Da	10 k Da	5 k Da	1 k Da
DI Water	93.52	63.05	62.53	64.48	1.63
Extracts	69.82	46.80	45.39	41.65	7.83

3.3.5 Effect of flow rate in CFHF UF of *RA* extracts

This study was carried out on the CFHF UF process only. Figure 3.8 shows the effect of various feed flow rates on flux and resistance in the CFHF UF of *RA* extracts. The flow velocities are about 0.09, 0.22 and 0.34 $m \cdot s^{-1}$ at the flow rates of 40, 95 and 145 $mL \cdot min^{-1}$, respectively. The flux changed slightly at different flow rates, and the contributions of resistance altered little too. Only at the flow rate of 145 $mL \cdot min^{-1}$ did the contribution of concentration polarization become a little smaller, whilst contributions of irreversible and reversible fouling became more significant. This result indicates that higher flow rate can increase the hydrodynamic of feed, thus reduce concentration polarization.

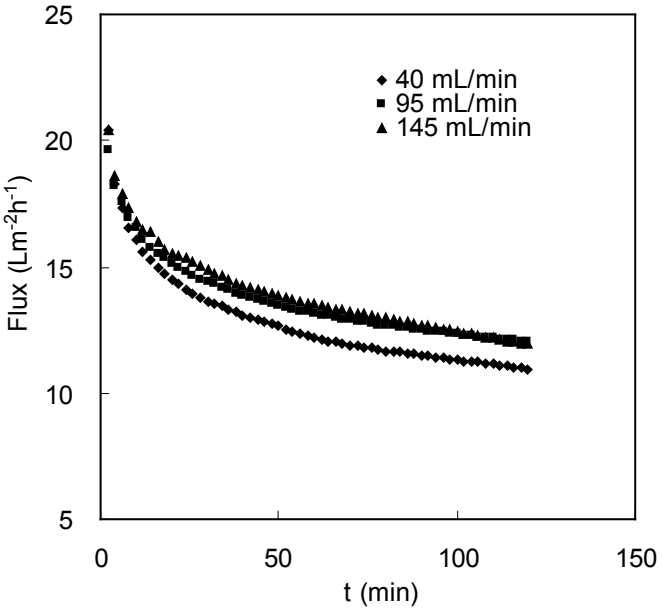

(a)

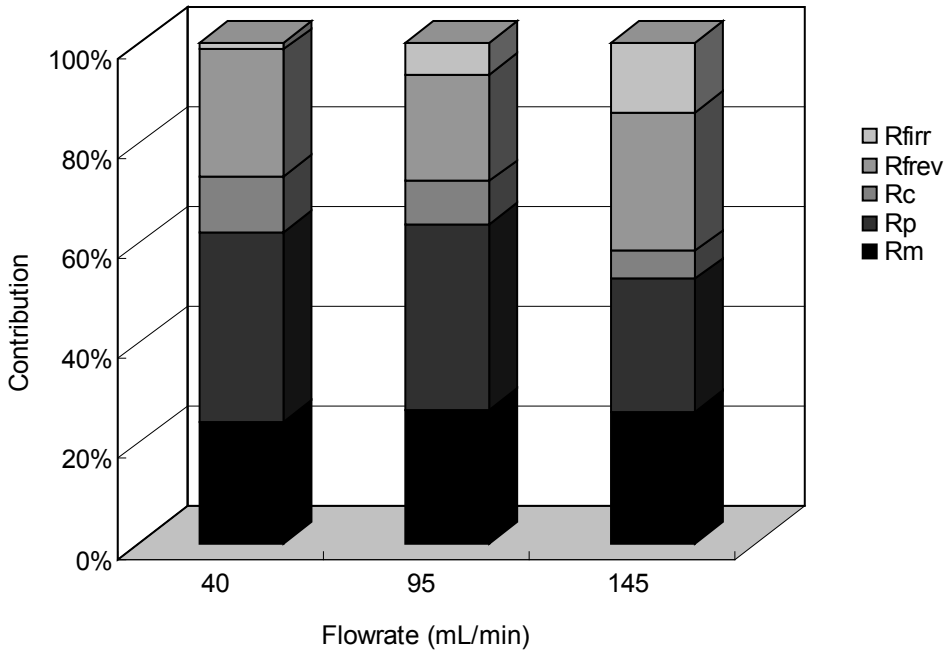

(b)

Figure 3.8 Flux performances (a) and contribution of resistances (b) of hollow fiber membrane ultrafiltration of *RA* ectracts

3.3.6 FTIR and SEM analysis

FTIR spectrum can provide detailed information of the compounds. Figure 3.9a

shows the spectra of *RA* extracts, retentate and permeate. It revealed that the profiles of each powder were similar but the intensities were different. The spectra showed a broad absorption at 3000 to 3700 cm^{-1}, indicating existence of the stretching of O-H bond in hydroxyl functional groups, and the peak at 2932 cm^{-1} indicated the C-H functional group [16]. There was also a peak at 1053 cm^{-1}, due to C-O bonds in alcohols, ethers and polysaccharides. This peak was attributed to the polysaccharides or polysaccharides-like substances [17]. Two peaks, at 1633 and 1415 cm^{-1}, unique to the protein secondary structure called amides I and II [18], existed in these spectra. Figure 3.9b showed the spectra of foulants after chemical cleaning in or on the membranes rinsed by NaOH solution. Compared with the spectra in Figure 3.9a, the peak at 1053 cm^{-1} disappeared, indicating that polysaccharides did not exist in the membrane foulants after chemical cleaning.

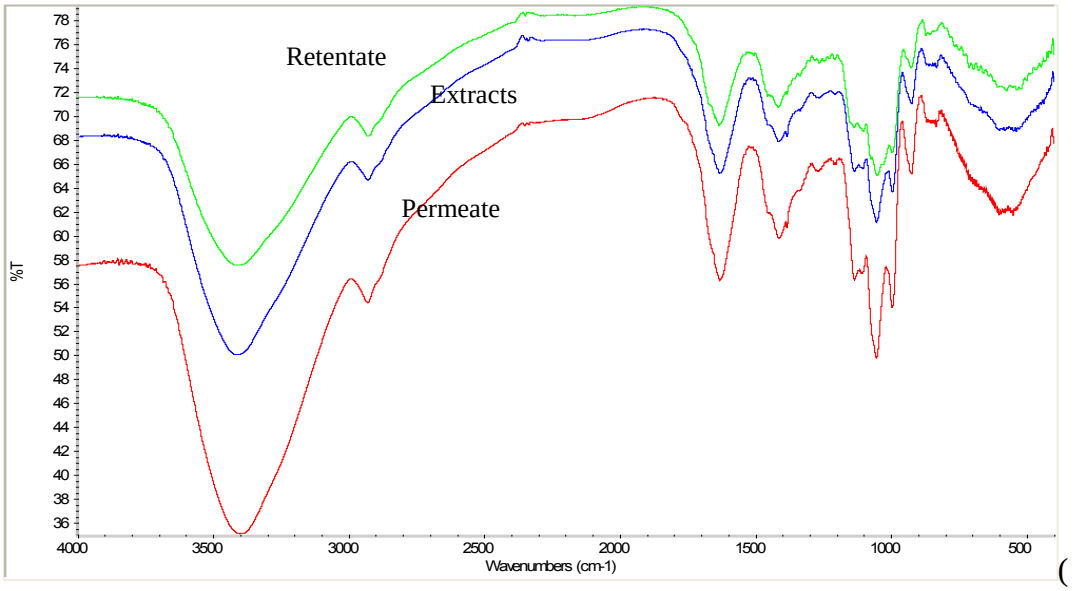

a)

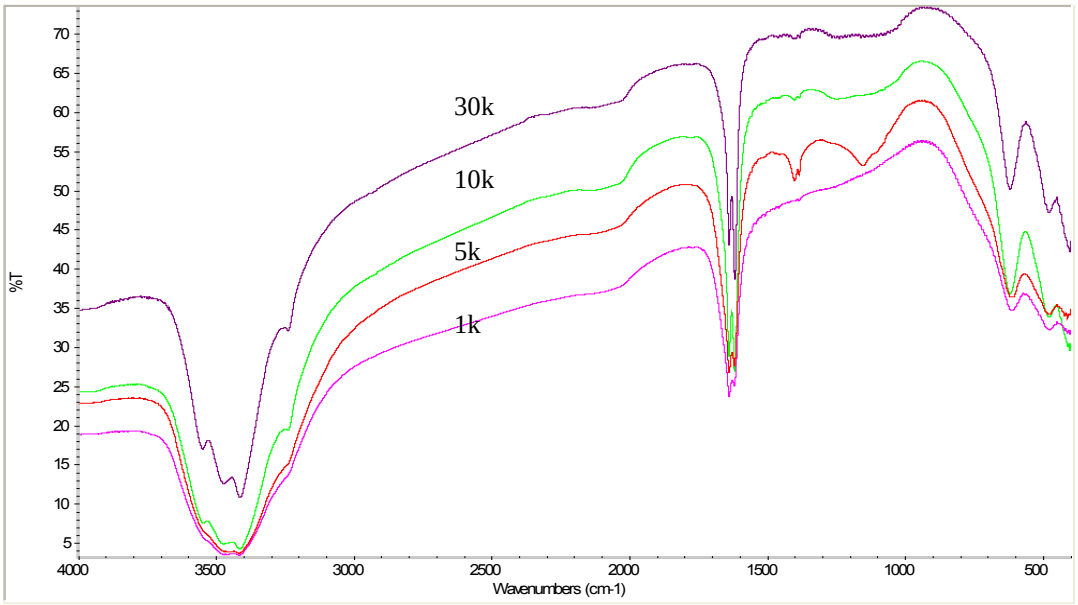

(b)

Figure 3.9 FTIR spectra of extracts, retentate and permeate in UF of *RA* extracts

Figure 3.10 shows the SEM images of the fouled and washed flat sheet and hollow fiber membranes. The surface of membrane looked much cleaner after the foulants were washed away by water, this proved that cake layer was definitely formed on the membranes in the UF process, as shown in Figures 3.10a and 3.10c, and the cake layer as reversible resistance could be removed by the water flushing.

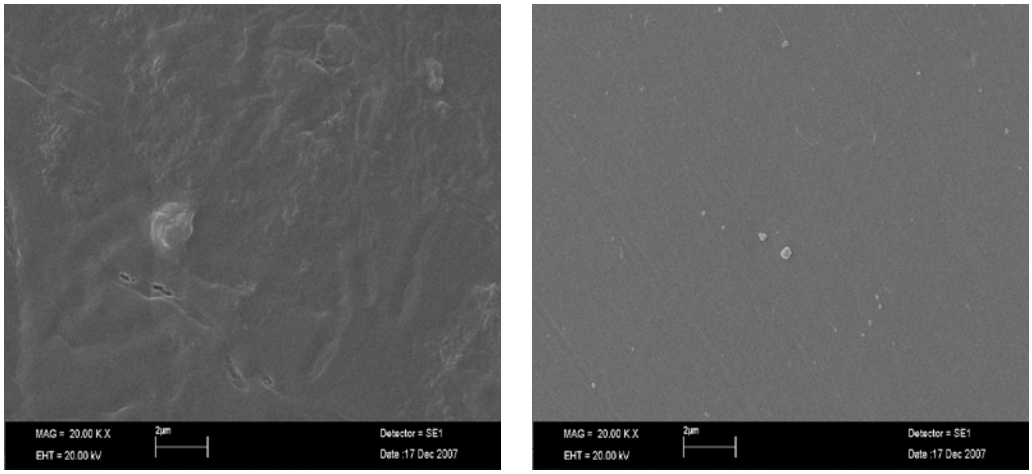

(a) (b)

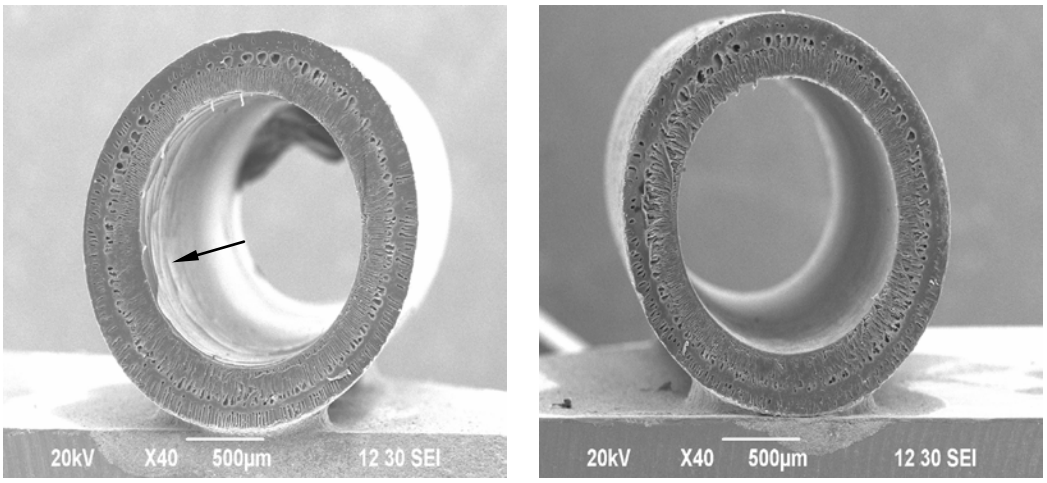

(c) (d)

Figure 3.10 Views of the flat sheet and hollow fiber membranes with 10 k Da MWCO: (a) fouled flat sheet; (b) washed flat sheet; (c) fouled hollow fiber; (c) washed hollow fiber

3.4 Conclusion

In DEFS UF process of *RA* extracts, the effect of temperature, ranging from 20 to 50 ºC, on flux was insignificant, but the effects of TMP and MWCO were significant. Higher TMP could enhance the flux, making the concentration polarization and fouling phenomena more obvious. The contribution of reversible resistance was increased almost to 60% at 1.2 bar TMP. The

contributions of R_{rev} for 100 k, 30 k and 10 k Da membrane were strong, all up to 60%, indicating that the amount of substances with molecular weight between 10 k and 100 k Da in the *RA* extracts was small. Hence, it was appropriate to use 10 k or 30 k Da membrane for UF process of *RA* extracts. In CFHF UF process, temperature and flow rate were not significant, but TMP showed significant effect on the flux and resistance. Flux enhancements were 75%, 123% and 166% at 0.6, 0.8 and 1.0 bar, respectively. Based on these results, it could be concluded that concentration polarization and reversible fouling were two main resistances in the UF process of *RA* extracts. Consequently, effective techniques can be applied to reduce the concentration polarization and cake layer in both DEFS and CFHF UF processes. SEM images revealed the evidence that foulants accumulated readily on the membrane surface as cake layer. Meanwhile, FTIR spectra indicated that protein and polysaccharides definitely existed in the extracts, retentate and permeate, but they could be removed from the membrane after chemical cleaning.

Reference

1. S. Metsamuuronen, M. Nystrom, Evaluation of six flat sheet ultrafiltration membranes for fraction of whey proteins, Desalination 200 (2006) 290-291
2. Z. Borneman, V. Gokmen, H.H. Nijhuis, Selective removal of polyphenols and brown colour in apple juices using PES/PVP membranes in a single ultrafiltration process, Separation and Purification Technology 22-23 (2001) 53-61
3. M. Shahidi, S.M.A. Razavi, Improving thin sugar beet juice quality through ultrafiltration, Desalination 200 (2006) 518-519
4. P.J. Evans, M.R. Bird, Solute-membrane fouling interactions during the ultrafiltration of black tea liquor, Food Bioproduct Process 84 (2006) 292-301
5. T. Kawakatsu, T. Kobayashi, Y. Sano, M. Nakajima, Clarification of green tea extract by microfiltration and ultrafiltration, Bioscience Biotechnology Biochemistry 59 (1995)1016-1020
6. A.W. Zularisam, A.F. Ismail, M.R. Salim, M. Sakinah, O. Hiroaki, Fabrication, fouling and foulant analyses of asymmetric polysulfone (PSF) ultrafiltraion membrane fouled with natural organic matter (NOM) source waters, Journal of Membrane Science 299 (2007) 97-113
7. D. Wu, M.R. Bird, The fouling and cleaning of ultrafiltration membranes during the filtration of model tea component solutions, Journal of Food Process Engneering 30 (2007) 293-323
8. N.K. Saha, M. Balakrishnan, M. Ulbricht, Polymeric membrane fouling in

sugarcane juice ultrafiltration: role of juice polysaccharides, Desalination 189 (2006) 59-70

9. M. Moresi, S. L. Presti, Present and potential application of membrane processing in the food industry, Ital. Journal of Food Science 15 (2003) 3-34
10. Z.F Liu., X.P. Liu, D.P. Liu, J. Chen, R.M. Sun, P. Jiang, Z.R. Huang, F.X. Li, A Novel Method for Extractin and Separation of Total flavones and Total Astragalosides from Radix astragali, Chem. Nat. Compd., 43 (2007) 29-33
11. R. Jiraratananon, A. Chanachai, A study of fouling in the ultrafiltration of passion fruit juice, Journal of Membrane Science 111(1996) 39-48
12. A. Simon, N. Gondrexon, S. Taha, J. Cabon, G. Dorange, Low-frequency ultrasound to improve dead-end ultrafiltration performance, Separation Science and Technology, 35 (2000) 2619-2637
13. A. Cassano, L. Donato, E. Drioli, Ultrafiltration of kiwifruit juice: Operating parameters, juice quality and membrane fouling, Journal of Food Engineering 79(2007) 613-621
14. S. Dharmananda, Astragalus: Practical Aspects of Administering the Herb. http://www.itmonling.org/arts/astragalus/htm
15. Q.J. Yan, L.J. Han, Z.Q. Jiang, C.J. Huang, Molecular Mass Distribution of Astragalus Polysaccharrides. Food Science 25 (2004) 27-30 (in Chinese)
16. J. Zhou, F.L. Yang, F.G. Meng, P. An, D. Wang, Comparison of membrane fouling during short-term filtration of aerobic granular sludge and activated sludge, Journal of Environment Science 19 (2007) 1281-1286
17. F.F. Meng, F.L. Yang, B.Q. Shi, H.M. Zhang, A comprehensive study on

membrane fouling in submerged membrane bioreactors operated under different aeration intensities, Separation and Purification Technology 59 (2008) 91-100

18. T. Maruyama, S. Katoh, M. Nakajima, H. Nabetani, T.P. Abbott, A. Shono, K. Satoh, FT-IR analysis of BSA fouled on ultrafiltration and microfiltration membranes, Journal of Membrane Science 192 (2001) 201-207

Chapter 4

Effects of Ultrasonic Parameters on US-assisted UF of *RA* Extracts in Classic Dead-end Flat Sheet Mode

---

Separation and Purification Technology 68(2009) 351-356

Abstract

The objective of this study was to evaluate the effect of ultrasound (US) on ultrafiltration (UF) of a natural product, *Radix astragalus* (*RA*) aqueous extract, and cleaning processes of fouled membrane. Specifically, the effects of ultrasonic frequency, power and irradiation mode on flux and resistances during the UF process were investigated. Ultrasonic irradiation had a strong impact on the normal UF process of *RA* extracts, especially with low frequency and high output power. An enhancement of 12-15% in flux was observed when US at effective power of 10 W and frequency of 28 or 45 kHz was used. When irradiated with an US power of 120 W, the fluxes increased dramatically with the increased ultrasonic intensity, nearly 70% higher in flux than those with stirring only. The intermittent irradiation mode was desirable not only for its effective flux enhancement, but also for lowering energy consumption. Upon ultrasonic irradiation, the reversible resistance, including concentration polarization and cake layer, was sufficiently reduced as revealed by the quantitative resistance analysis using resistance-in-series model. The employment of US in both mechanical and chemical cleaning processes for fouled membranes resulted in much higher flux recovery, especially at low frequency and high power setups. The application of US is an effective and promising approach to enhance the UF process for natural products, and for both mechanical and chemical cleaning of fouled membranes.

4.1 Introduction

Natural products are the sources of functional foods, drug supplements or medicines for human because of their effective pharmacological or biological activities. Plants, marine organism and microorganism are the main origins of natural products. In the manufacture processes of natural products, these materials are preliminarily extracted by water or organic solvents, followed by separation, isolation or purification using appropriate technologies. Membrane filtration, especially ultrafiltration (UF) and microfiltration (MF), has been accepted as a sophisticated technology to separate or isolate the natural product mixtures in recent years [1-4]. However, rapid flux decline caused by concentration polarization and membrane fouling in the process hinder its further industrial applications. To solve these problems many mechanical approaches, such as vibration [5], gas sparging [6, 7], backflushing [8, 9] and pulsatile flow [10], have been applied to the membrane filtration process itself or to the cleaning of fouled membrane. To improve the efficiency of mechanical cleaning methods, chemicals such as sodium hydroxide, sodium hypochlorite, EDTA or citric acid are often used in further cleaning of fouled membrane [11]. Recently, electrical field [12] and ultrasound (US) [13] have been used as novel techniques in membrane filtration as well as membrane cleaning to improve the permeate flux or the recovery of membrane permeability.

US technique has been proved to be an effective approach to enhance the flux in

UF or MF process and to improve the cleaning of fouled membranes because of its characteristics of cavitations, acoustic streaming and micro streaming, etc. [14]. Significant improvement of flux in dead-end UF cell for dextran solution was obtained with low frequency US irradiation, and the enhancement was attributed to the hydrodynamic motions generated by US [15]. Kobayashi et al. studied the effects of US on cross-flow flat sheet membrane filtration for water treatment [16, 17]. The effects of ultrasonic frequency, power intensity and irradiation direction on membrane filtration were investigated and it was found that all these factors significantly affected the flux enhancement induced by US. Moreover, US has been comprehensively accepted as a powerful method for the cleaning of fouled membrane in water treatment [18] and dairy industry [19]. However, most of these studies on the effects of US on membrane filtration were done with model solutions such as dextran, peptone or BSA solutions. Therefore, it is valuable and necessary to investigate the applicability of US on membrane separation process of real natural products and on the cleaning of fouled membrane caused by the mixed ingredients involved.

In this study, US was applied to the UF process of the real extract of a natural product, *Radix astragalus* (*RA*), and to the cleaning of fouled membrane. *RA* extracts was selected as a target solution because it consists of polysaccharides, saponins and flavonoids which have satisfactory medicinal activities and wide distribution of molecular weight. Amicon type UF cell was modified by introducing mechanical stirring as well as US irradiation, and used to study their

effects on permeate flux and filtration resistances in membrane separation of natural products. Influences of various US parameters in terms of US frequency, power and irradiation mode on permeate flux and filtration resistances in the UF process, and flux recovery in cleaning of fouled membranes were investigated.

4.2 Materials and methods

4.2.1 Materials and experimental set-up

The experimental setup in this study is shown in Figure 4.1. A polyethersulfone (PES) flat sheet UF membrane (Millipore, Bedford, USA) with a molecular weight cut off (MWCO) of 10 k Da and effective membrane area of 41.8 cm^2 was placed into the Amicon type UF cell (Millipore, Bedford, USA). A magnetic plate (Thermolyne Cimarec 1, Dubuque, USA) was used to introduce the necessary stirring at a desired speed. Two ultrasonic systems were employed in the experiments, namely ultrasonic transducer plates (Kamson Ultrasonic Equipment Co., Ltd. China) at frequencies of 28, 45 and 100 kHz, and variable output power ranging 0-200, 0-300 and 0-600 W, respectively; a ultrasonic transducer probe with 12.7 mm^2 flat tip (CPX600, Cole-Parmer, USA) at frequency of 20 kHz and variable output power ranging 0-600 W. When frequency was the key parameter to study, the UF cell was immersed into a water bath with ultrasonic transducer plate; whilst output power was the study parameter, the ultrasonic probe was embedded into the UF cell. Thus the investigation to the effects of various

ultrasonic frequencies and powers on both UF and cleaning processes can be carried out, respectively. The permeate weight was measured by an electronic balance (Ohaus, USA) in an interval of 2-min during the UF process.

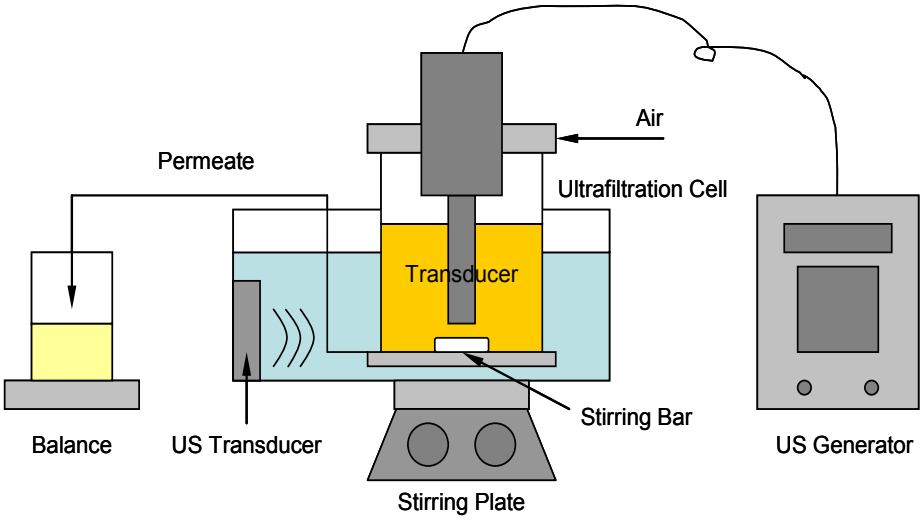

Figure 4.1 Experimental setup for US and stirring assisted UF of *RA* extracts

RA extracts were prepared as described in Section 3.2.1.

Needle hydrophone (Precision Acoustics, UK), power transformer (PAC 300, BIO-RAD, CA) and oscilloscope (TDS 2024B, Tektronix, Japan) were used to determine the US power intensity inside the UF cell when irradiated with ultrasonic transducer plate or ultrasonic transducer probe.

4.2.2 Experimental procedure

4.2.2.1 Ultrafiltration process

150 ml *RA* aqueous extract was transferred into the UF cell and the filtrations were

operated at the constant trans-membrane pressure (TMP) mode by controlling TMP at 0.8 bar. The stirring speed was set at 500 rpm in each run. The permeate fluxes of the *RA* extracts at various experimental conditions, namely frequency of 28, 45 or 100 kHz at a fixed power of 120 W, and output power of 60, 90 or 120 W at 20 kHz, were measured at a 2-min interval by an electronic balance. Resistances were calculated with the resistances-in-series model according to the experimental procedure described in Section 4.2.2.3.

4.2.2.2 Cleaning process of fouled membrane

100 mL *RA* extract was used in each fouling experiment. The fouling process was operated at a constant TMP of 0.8 bar till the accumulated volume of permeate solution reached 80 ml. When the fouling completed, the retentate of the *RA* extracts was emptied out, followed by mechanical cleaning with fresh DI water. 100 mL DI water was put into the cell and filtered at mild flow velocity with US irradiation. Instead of DI water, 100 mL sodium hydroxide of 0.1M solution was used in the chemical cleaning process with or without US after mechanical cleaning. DI water flux was determined right after every on-site cleaning stage. In order to clean the membrane thoroughly, it was taken out and immersed into 0.1 M NaOH solution for 24 h. Flux recovery, used as an index for the efficiency of the cleaning method is defined as follows:

$$\Phi = \frac{J_{ac}}{J_w} \tag{4-1}$$

where Φ is flux recovery, J_{ac} the water flux after cleaning, J_w the water flux of original membrane. The virginal membrane water flux was measured before all the UF experiments. Unless otherwise started, all water flux measurements were carried out under the same conditions.

4.2.2.3 Determination of resistances and US intensity

The different resistances were determined according to the procedures as described in Section 3.2.4.1.

Ultrasonic power in a US-assisted UF system can usually be measured by a calorimetrically method that observes temperature changes with time. In addition to the calorimetrically method, a sonic probe connected to a pulse receiver was used to estimate the US power intensity [16]. It was found the US power intensity inside the filtration cell would be reduced sharply, to about only 10% of the original power. In this study, a needle hydrophone and an oscilloscope were used to measure the power intensity. The needle hydrophone was positioned vertically into the UF cell and its tip was immersed under the water and close to the surface of membrane. As soon as the US power was turned on, the waveform amplitude displayed on the oscilloscope was recorded and converted into acoustic intensity, I, by

$$I = \frac{P^2}{\rho c} \tag{4-2}$$

where P is the acoustic pressure (Pa), ρ the density of the propagating medium

($kg \cdot m^{-3}$), and *c* the velocity of sound in the propagating medium ($m \cdot s^{-1}$).

4.2.2.4 SEM analysis

The fouled, cleaned and US irradiated UF membranes were freeze dried at -60 ^{o}C for 24 h, sputter-coated with gold, and then imaged using a scanning electron microscope (SEM) (Stereoscan 440, Leica, UK).

4.3 Results and Discussion

4.3.1 Ultrasonic power intensity

4.3.1.1 Ultrafiltration cell irradiated with ultrasonic transducer plate

The US wave inside the UF cell detected by the needle hydrophone was basically the latus rectum waveform as shown in Figure 4.2. US waves at all three frequencies were able to propagate into the UF cell without any frequency alteration from the original source. Upon reflection and transmission by the dual interfaces of liquid bath and cell housing, only 8% of the source US at 120 W (or just about 10 W of effective US power) could penetrate the UF cell and reach the membrane inside. When the US output power was kept constant, the detected intensity inside the cell with 100 kHz frequency was much lower than those observed with 45 and 28 kHz. Interestingly, the latter two frequencies generated approximately the same acoustic voltage inside the UF cell. This confirmed that low frequency contributed relatively higher power intensity in ultrasonic field.

Thus low frequency US can make significant effect on UF process.

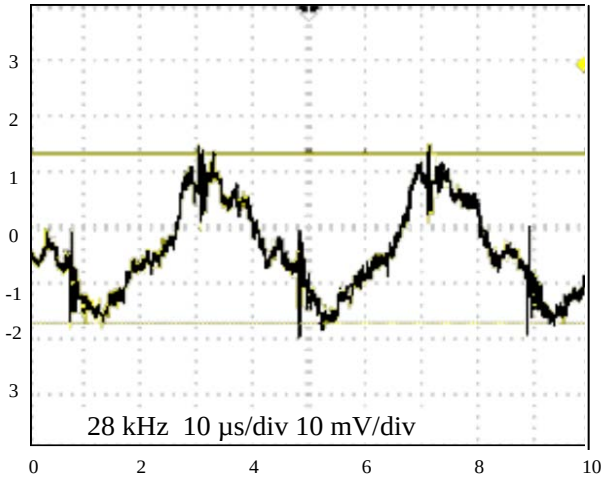

a

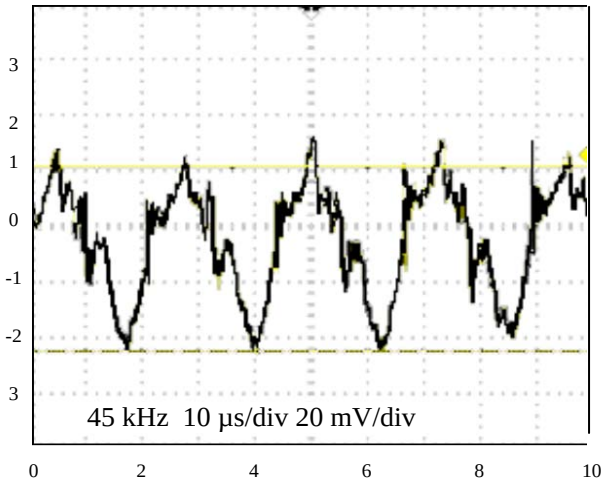

b

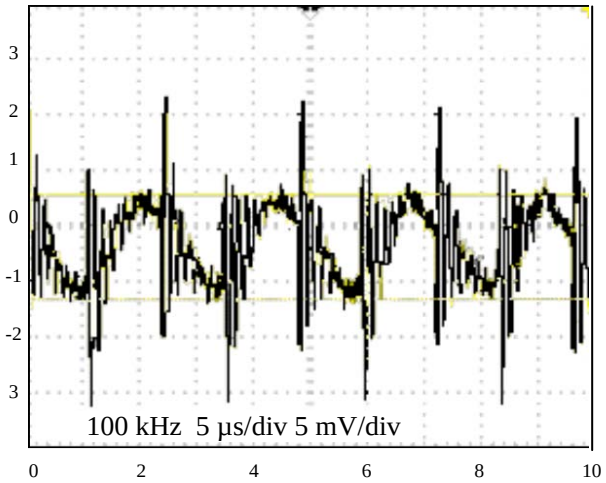

c

Figure 4.2 Waveforms of US detected in UF cell with ultrasonic transducer plate: (a): 28 kHz, 10µs/div, 10mV/div; (b): 45 kHz, 10 µs/div, 20mV/div; (c) 100 kHz, 5µs/div, 5mV/div

4.3.1.2 Irradiated with ultrasonic transducer probe

The output power of the ultrasonic generator was adjusted from 5% to 30% of the total 600 W power. The transducer probe was immersed into the solution and kept at 5 cm from the surface of the membrane sheet. The actual voltages inside ultrasonic field were measured and calculated into the acoustic intensities. The US power intensities generated by output power of 30, 60, 120 and 180 W were found to be 14, 48, 77 and 150 $mV \cdot cm^{-2}$, respectively.

4.3.1.3 Resistibility of membrane to US irradiation

The PES flat sheet UF membrane used in this study is resistant to US irradiation applied, even when the efficient ultrasonic probe at high power level was used. The SEM images shown in Figure 4.3 indicated that no damage was found on the membrane surface after US irradiation. After UF, there was a thick cake layer formed on the surface. After cleaning, the membrane surface looks the same as the original. This result demonstrates that it is feasible to apply US to the PES flat sheet UF membrane.

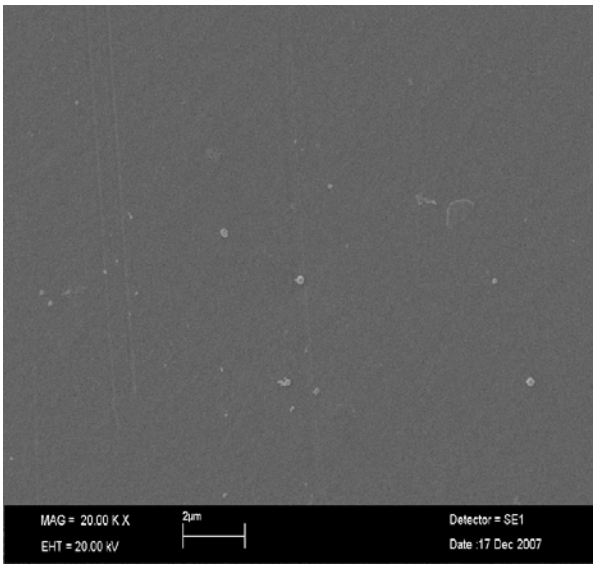

(a)

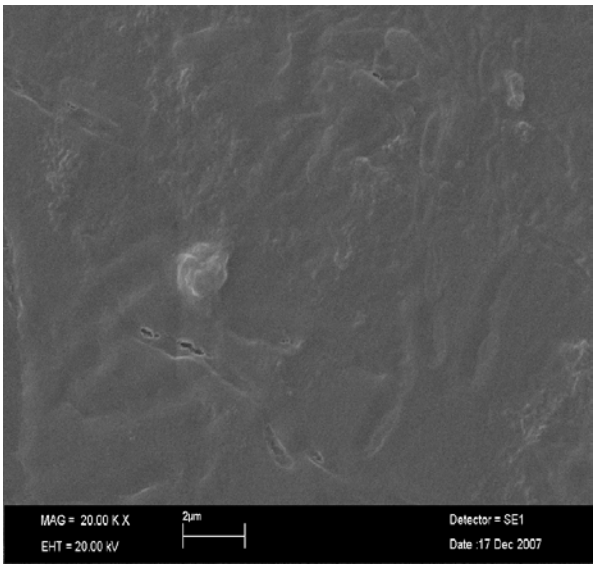

(b)

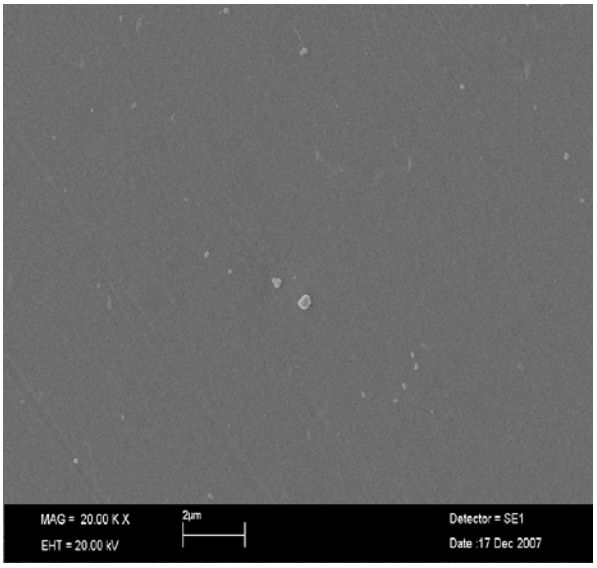

(c)

Figure 4.3 SEM images of original membrane (a), fouled membrane (b) cleaned membrane (c) after US irradiation, used in UF process of *RA* extracts

4.3.2 Effect of ultrasound on ultrafiltration process

4.3.2.1 Effect of ultrasonic frequency

The effects of US frequencies of 28, 45 and 100 kHz on the permeate flux and filtration resistances in UF process of *RA* extracts are shown in Figure 4.4. The flux decline profiles at the initial stage of US irradiation at various frequencies are the same. As filtration continued, differences in flux attributed to the difference of frequencies gradually appeared. At the first 20 minutes, all the fluxes decreased rapidly despite the frequencies used, then came the relative steady stages. This trend was different from that obtained by the model solutions such as dextran and peptone. In Kobayashi's studies, the flux with 45 or 28 kHz US irradiation increased continually during the whole filtration process when 1 wt% dextran solution was used, and the flux of both dextran and peptone solution could be enhanced by US irradiation at the very beginning of filtration [16, 17]. This flux declined was caused by fouling, indicating the UF process could be affected by the complexity of real natural products, which may result in severe accumulation of foulants on to the membranes. The flux enhancements with 28 and 45 kHz US irradiation were almost the same, almost up to 12-15% higher than that with stirring only. The effect of US on reversible and irreversible fouling with respect to total resistance was plotted in Figure 4b. Reversible fouling was dominant in the UF process of *RA* extract as versatile components of the extracts were able to build up a cake layer very quickly. US can reduce the total resistance, especially the reversible resistance, to a nearly 40% reduction with 28

or 45 kHz US. However, irreversible fouling with low frequency became more serious than that without US irradiation. This phenomenon indicated that lower frequency US may generate stronger vibration which is one of the mechanisms for US enhancement. The substances in extracts suspension having similar molecular size with the pore size of membranes had stronger tendency trapping into the pores and irradiation force could accelerate this irreversible pore blocking in consequence.

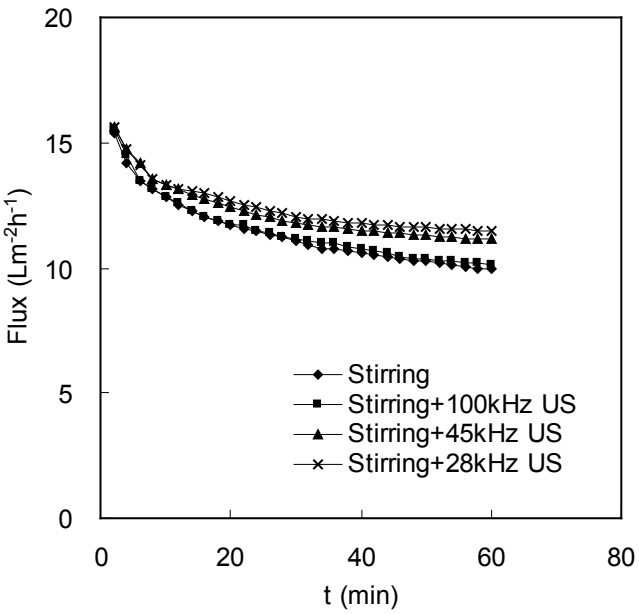

(a)

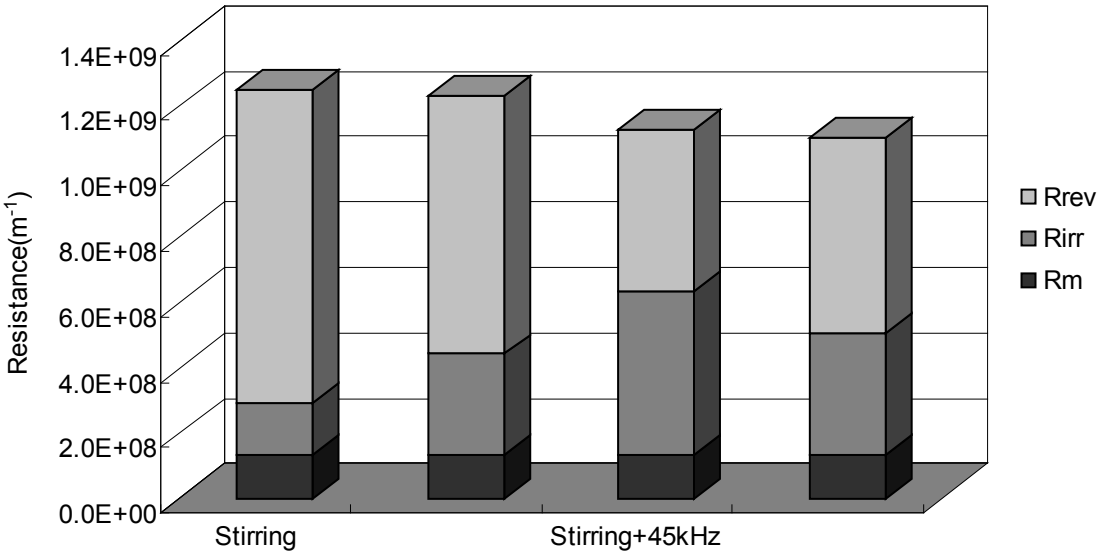

(b)

Figure 4.4 Effect of US frequencies on (a) flux and (b) resistances in UF of *RA* extracts with stirring at 500 rpm, MWCO of 10 kDa, TMP of 0.8 bar, 120 W US output power

4.3.2.2 Effect of Ultrasonic power

The ultrasonic transducer probe was embedded into the UF cell and directly immersed into the extracts. A cooling system was used to control the temperature

of the extracts to prevent its rise due to US irradiation. Figure 4.5 illustrates the flux performances over time with or without US irradiation. The permeate flux increased significantly with US irradiation and the enhancement was proportional to the increase of US power. With US irradiation of 60, 90 and 120 W, fluxes were respectively 35%, 57% and 68% higher than that with stirring only. At US irradiation of 180W, the heat generated was faster than what the cooling system could removed, resulted in a temperature raise up to 55 ºC, which might contribute greatly to the flux enhancement. Higher power US has stronger effects of cavitation, acoustic streaming, vibration and heating, which have been confirmed to be the dominant mechanisms affecting the UF performance in US field. However, higher output power is not always favorable in industrial applications due to massive energy consumption. Moreover, higher power might induce unexpected physicochemical changes to the natural products.

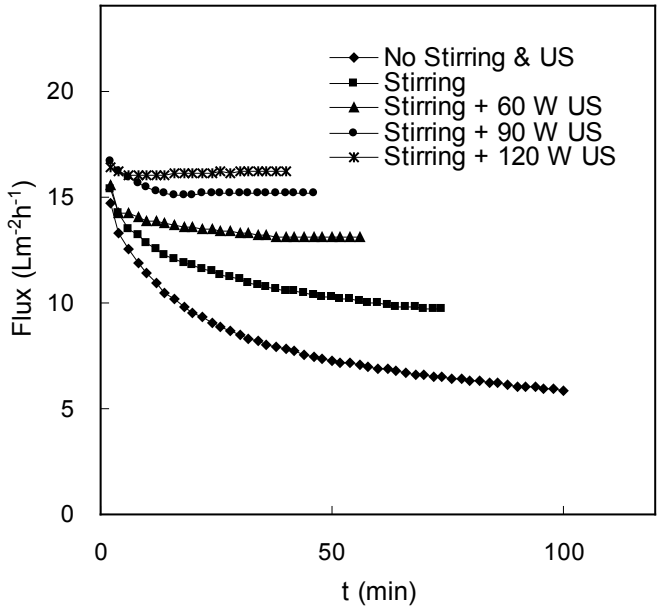

Figure 4.5 Effect of US power on flux performance in UF of *RA* extracts process with stirring at 500 rpm, MWCO of 10 kDa, TMP of 0.8 bar, 20 kHz US

4.3.2.3 Effect of Ultrasound irradiation mode

The effects of various intermittent modes of US irradiation (1-1 s on-off (A), 1-5 s on-off (B), 1-9.9 s on-off (B)) on the permeate flux and filtration resistances in UF process are shown in Figure 4.6. The “B” and “C” modes exhibited almost the same trends in their flux performances, and the flux at the “A” mode was about 40% higher than those at “B” and “C” modes. Without running of the cooling system, the flux with continued US irradiation increased dramatically due to the rise of temperature induced by US irradiation, which rose up to almost 70 ºC in 30 min. Obviously, even though consistent with the results reported by by Simon et al. [15] and Muthukumaran et al. [19] that intermittent mode appears to be not as effective as continued US, the former is still a preferable as long as energy efficiency is taken into consideration. In terms of resistance analysis, the reversible resistance strongly affected the performance of UF as discussed before. The longer the US irradiation time, the more effective the US on reversible fouling resistance. However, the energy cost and the potential damage on the active components are the major drawbacks for continued mode to become a good practice. Therefore, it is more convenient and economic to use the “1-1 s on-off” intermittent mode of US irradiation.

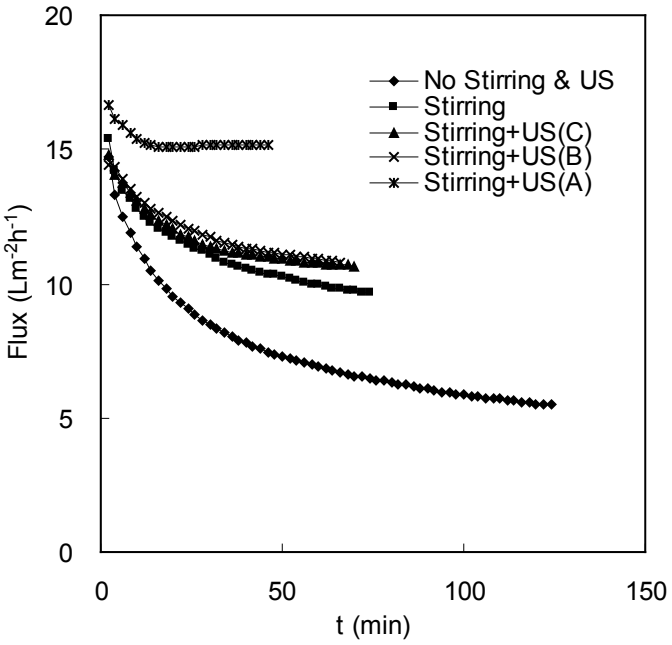

(a)

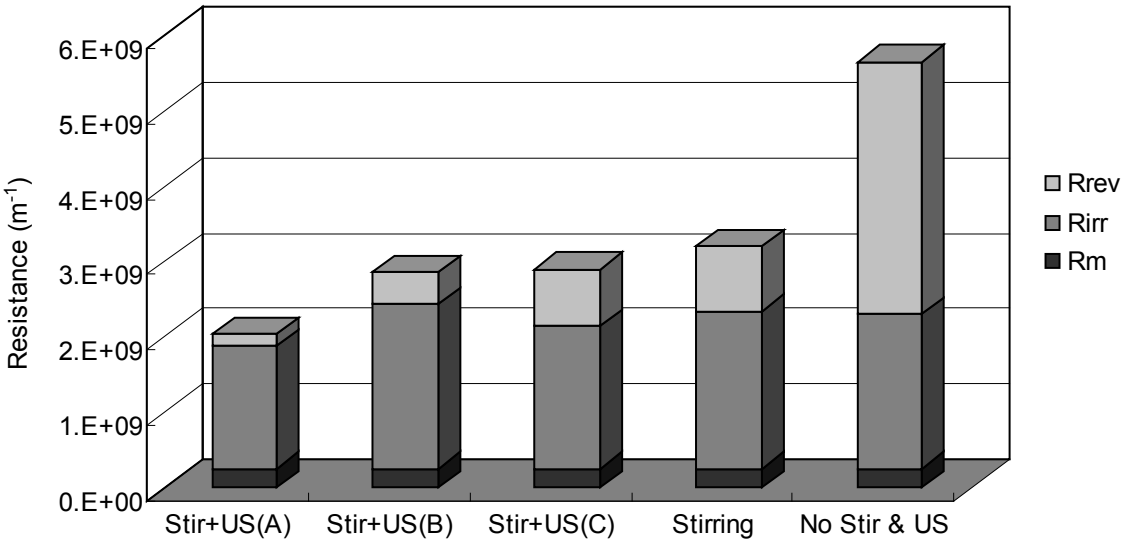

(b)

Figure 4.6 Effect of US irradiation modes (A: 1-1 s on-off; B: 1-5 s on-off; C: 1-9.9 s on-off) on (a) flux performance and (b) resistances in UF of *RA* extracts with stirring at 500 rpm, MWCO of 10 kDa, TMP of 0.8 bar, US at 120 W and 20 kHz

4.3.3 Effect of ultrasound on the cleaning of fouled membrane

4.3.3.1 Effect of ultrasound on mechanical cleaning

Figure 4.3a shows the membrane surface was fouled by accumulated foulant in UF of *RA* extracts. Mechanical cleaning was operated right after the UF process by running fresh DI water through the fouled membrane, which resulted in a 20% flux recovery. In order to boost the insufficient flux recovery, US was applied to the mechanical cleaning process. US irradiation improved the flux recovery more effectively and the improvement is almost linearly with the increased of US power. As shown in Figure 4.7, about 26%, 30%, 34% and 35% flux recovery were achieved at the US power of 30, 60, 120 and 180 W, respectively. Muthukumaran et al. who found that the cleaning efficiency increased linearly with ultrasonic power in dairy industry [20].

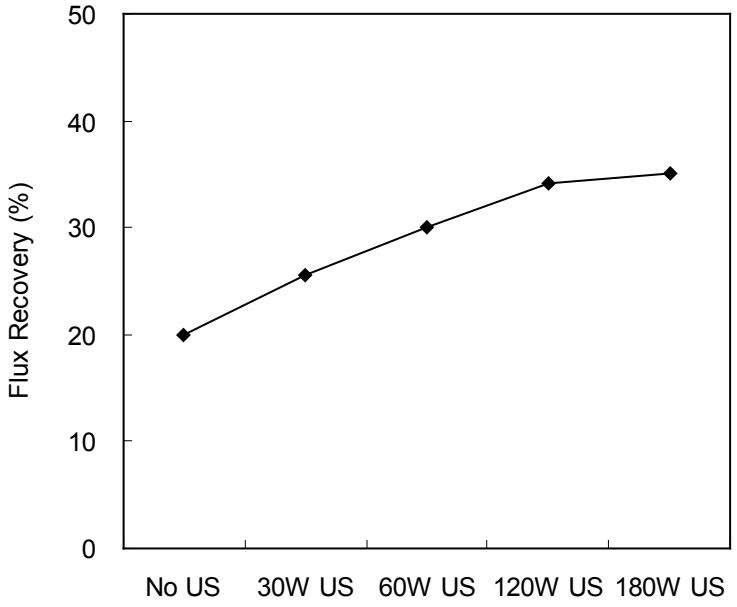

Figure 4.7 Flux recovery after mechanical cleaning assisted with different power US irradiation, 20 kHz US frequency

4.3.3.2 Effect of ultrasound on chemical cleaning

Though flux recovery by mechanical cleaning with US irradiation could be up to 35%, it was still not satisfactory. The foulants, which were primarily polysaccharides and proteins in our study, on or inside the membrane could be permanently removed by sodium hydroxide solution [13]. The SEM image shown in Figure 4.3b evidently presented the effect of chemical cleaning on the fouled membrane. The effects of ultrasonic power, ultrasonic frequency and temperature on US-assisted chemical cleaning were demonstrated in Figure 4.8. Flux recovery at 28 kHz US irradiation was up to 60%, almost 30% higher than that without US; whereas 100 kHz US had almost no effect on the chemical cleaning as the flux recovery was the same as that without US. This result indicated that a lower frequency US was more effective in enhancing the chemical cleaning process. The effect of low frequency US on cleaning is consistent with its effect on UF process: low frequency US generates high US intensity. The flux recovery was about 63% with US of 20 kHz and 30 W, and could be up to 80% with US of 120 W. The effect of temperature on the chemical cleaning efficiency was also shown in Figure 4.8. The temperature of the system was well controlled by the cooling system to remain at constant 40-50 ºC in various setting conditions during the US-assisted chemical cleaning process. Figure 4.8 clearly shows that the improvement in flux recovery caused by US irradiation was much greater than those induced by temperature rise. Undoubtedly, significant flux recovery would be expected in the chemical cleaning assisted by low frequency and high power ultrasonic irradiation.

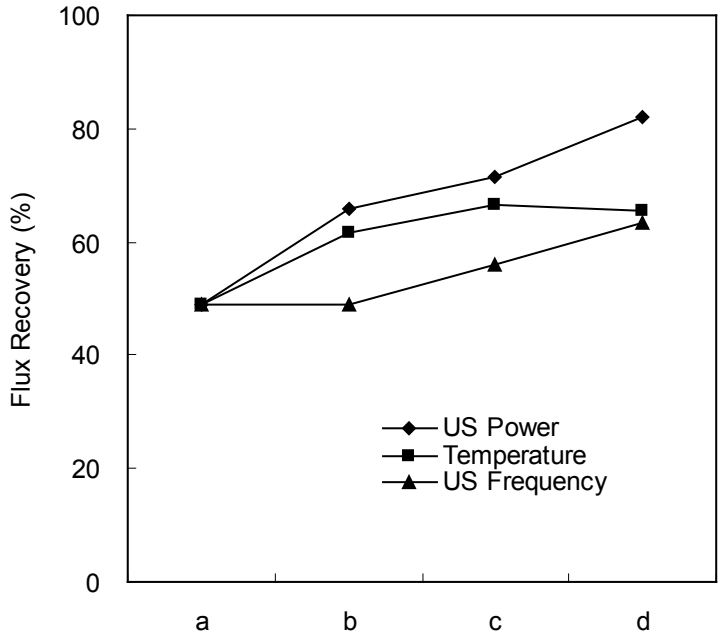

Figure 4.8 Effects of operating parameters on chemical cleaning (a. No US at room temperature; b. US of 100 kHz and 30 W, at 40 ºC; c. US of 45 kHz and 60 W at 50 ºC; d. US of 28 kHz and 120 W at 60 ºC)

4.4 Conclusions

Systematic experiments were carried out in this work to study the effects of US on the stirred dead-end UF process and the cleaning of fouled membrane using *RA* extract as the feed solution. US irradiation can efficiently enhance the permeate flux, reduce the filtration resistances in UF process, and improve the flux recovery in fouled membrane cleaning. Ultrasonic frequency, ultrasonic power and irradiation mode are all significant factors which can affect the outcomes of both UF and cleaning processes. Low frequency and high power US is more effective in enhancing flux and improving flux recovery. It is believed that both cavitation and US induced vibration on top of the mechanical shear are the two possible mechanisms for the enhancements of permeate flux and permeability recovery by

US irradiation. Intermittent US irradiation is a more favorable operation mode for its reasonable flux enhancement as well as low energy consumption. US can reduce the reversible resistance attributed by concentration polarization and cake layer, thus result in higher permeate flux. However, US may accelerate the blocking of solute particles into the membrane pores and lead to even more serious irreversible resistance. To distinguish the tradeoff between the decrease in reversible resistance and the increase in irreversible fouling caused by ultrasonic irradiation, extensive optimization experiments should be carried out. This study suggests that US at low frequency and intermittent mode is a promising approach that can be applied in both UF and fouled membrane cleaning processes for natural product separation.

References

1. T. Kawakatsu, T. Kobayashi, Y. Sano, M. Nakajima, Clarification of green tea extract by microfiltration and ultrafiltration, Bioscience, Biotechnology and Biochemistry 59 (1995) 1016-1020
2. H. Nawaz, J. Shi, G.S. Mittal, Y. Kakuda, Extraction of polyphenols from grape seeds and concentration by ultrafiltration, Separation and Purification Technology 48 (2006) 176-181
3. W.X. Li, W.H. Xing, W.Q. Jing, N.P. Xu, Effect of pH on microfiltration of Chinese herb aqueous extract by zirconia membrane, Separation and Purification Technology 50 (2006) 92-96
4. X.L. Qiao, Z.J. Zhang, Z.H. P, Hydrophilic modification of ultrafiltration membranes and their application in Salvia Miltiorrhiza decoction, Separation and Purification Technology 56 (2007) 265-269
5. F. Vigo, C. Uliana, Ravinae, A. Lucifredi, M. Gandoglia, The vibrating ultrafiltration module performance in the 50-1000 Hz frequency-range, Separation Science and Technology 28 (1993) 1063-1076
6. Z.F. Cui, T. Taha, Enhancement of ultrafiltration using gas sparging: a comparison of different membrane modules, Journal of Chemical Technology and Biotechnology 78 (2003) 249- 253
7. Z.F. Cui, K.I.T. Wright, Flux enhancements with gas sparging in downwards crossflow ultrafiltration: performance and mechanism, Journal of Membrane Science 117 (1996) 109-116

8. M.Y. Jaffrin, B.B. Gupta, P. Blanpain, Membrane fouling control by backflushing in microfiltration with mineral membranes, Proceedings of the Fifth World Filtration Congress, Nice, France, 1990, pp. 479-483
9. P. Srijaroonrat, E. Julien, Y. Aurelle, Unstable secondary oil/water emulsion treatment using ultrafiltration: fouling control by backflushing, Journal of Membrane Science 159 (1999) 11-20
10. S.M. Finngan, J.A. Howell, The effect of pulsatile flow on ultrafiltration fluxes in a baffled tubular membrane system, Chemical Engineering Research & Design 67 (1989) 278-282
11. N. Hilal, O.O. Ogunbiyi, N.J. Miles, R. Nigmatullin, Methods employed for control of fouling in MF and UF membranes: a comprehensive review, Separation Science and Technology, 40 (2005) 1957-2005
12. J. Jurado, B.J. Bellhouse, Application of electric fields and Vortex mixing for enhanced ultrafiltration, Filtration & Separation 31 (1994) 273-281
13. H. M. Kyllonen, P. Pirkonen, M. Nystrom, Membran filtration enhanced by ultrasound: a review, Desalination 181 (2005) 319-335
14. M.O. Lamminen, H.W. Walker, L.K. Weavers, Mechanisms and factors influencing the ultrasonic cleaning of particle-fouled ceramic membranes, Journal of Membrane Science 237 (2004) 213-223
15. A. Simon, N. Gondrexon, S. Taha, J. Cabon, G. Dorange, Low-frequency ultrasound to improve dead-end ultrafiltration performance, Separation Science and Technology 35 (2000) 2619-2637
16. T. Kobayashi, T. Kobayashi, Y. Hosaka, N. Fujii, Ultrasound-enhanced

membrane-cleaning processes applied water treatments: influence of sonic frequency on filtration treatments, Ultrasonics 41 (2003) 185-190

17. T. Kobayashi, X. Chai, N. Fujii, Ultrasound enhanced cross-flow membrane filtration, Separation and Purification Technology 17 (1999) 31-40
18. X. Chai, T. Kobayashi, N. Fujii, Ultrasound-assisted cleaning of polymeric membranes for water treatment, Separation and Purification Technology 15 (1999) 139-146
19. S. Muthukumaran, K. Yang, A. Seuren, S. Kentish, M. Ashokkumar, G. W. Stevens, F. Grieser, The use of ultrasonic cleaning for ultrafiltration membranes in the dairy industry, Separation and Purification Technology 39 (2004) 99-107
20. S. Muthukumaran, S. Kenthish, S. Lalchandani, M. Ashokkumar, R. Mawson, G.W. Stevens, F. Grieser, The optimization of ultrasonic cleaning producedures for dairy fouled ultrafiltration membranes, Ultrasonics Sonochemistry 12 (2005) 29-35

Chapter 5

Effects of Ultrasonic Parameters on US-assisted UF of *RA* Extracts with Cross-flow Hollow Fiber Module

Abstract

Effects of ultrasonic parameters, including frequency, power and irradiation mode, on permeate flux and fouling resistances in the US-assisted UF process of *RA* extracts with hollow fiber membrane were investigated. The ultrasonic intensity inside the hollow fiber module was attenuated to only about 10% of the original ultrasonic power. Results showed that all these ultrasonic parameters could significantly affect the UF process performance. It demonstrated that US at 45 kHz frequency and high output power was more effective on enhancing the flux and reducing the fouling resistances. The flux enhancement could be up to 42% at the US of 45 kHz and 120 W, but it was 29% only at the US of 100 kHz and 600 W. Concentration polarization and cake layer resistances could be effectively decreased by US irradiation, which led to high flux performance. US of continued irradiation was more effective than that of intermittent irradiation on the UF process. Though satisfactory enhancement results were obtained, hollow fiber UF membrane was more susceptible to high power and low frequency US irradiation than the flat sheet membrane. US irradiation could not only enhance the permeate flux in the UF process but also caused destruction in the hollow fiber membrane if the US power was too high. US can be applied to the UF process with hollow fiber membrane with an appropriate output power.

5.1 Introduction

Natural products, including those of plants, marine organism and microorganism, are used as medicines or food complements because of their active components. The active components in these sources are usually extracted, followed by separation, isolation or purification processes. In recent decades, ultrafiltration (UF) and microfiltration (MF) technologies have been used to clarify or separate the natural product mixtures in the manufacture processes [1-4]. However, the membrane filtration is not widely applied to the industries as expected. Membrane fouling is the critical problems, which brings on the rapid flux decline and hinders their application. Thus, it is necessary to apply or develop novel techniques to reduce the membrane fouling during the filtration process. In recent years, some additional techniques have been used to the UF or MF processes, such as vibration [5], gas sparging [6, 7], backflushing [8, 9], pulsatile flow [10], electrical field [11] and ultrasound (US) [12].

US technique has been used to enhance the permeate flux in UF or MF processes, and also to improve the cleaning efficiency of fouled membrane. Significant improvement of permeate flux in dead-end UF of dextran solution was obtained at low frequency US irradiation, and the enhancement was attributed to the hydrodynamic motions generated by US [13]. US was also applied to the cross-flow flat sheet membrane filtration for water treatment by Kobayashi and his group [14, 15]. It was found that all the factors, including ultrasonic frequency,

power intensity and irradiation direction, have significant effects on the filtration process. These effects of US on membrane filtration process were mainly ascribed to its characteristics of cavitations, acoustic streaming, micro streaming, etc. [16]. However, most of these studies focused on the dead-end or cross-flow flat sheet membrane filtration mode, and only model solutions, such as dextran and BSA, were used. In our previous studies, US was applied to a stirred dead-end flat sheet UF process for a natural product [17]. Results showed that it was feasibility to apply US technique to the UF process for natural products. Though cross-flow hollow fiber UF was wildly used in the industry, few studies were carried out to introduce US technique to this process. Therefore, it is necessary to investigate the applicability and feasibility of US on the hollow fiber UF process for natural products.

The purpose of this work was to study the effects of ultrasonic parameters on the cross-flow hollow fiber UF of *Radix astragalus* (*RA*) extracts. Effects of ultrasonic frequency, power and irradiation mode on the permeate flux and fouling resistances were investigated. US power intensity inside the hollow fiber module was measured. Feasibility of US technique introduced to the process and the hollow fiber membrane were studied.

5.2 Materials and methods

5.2.1 Materials

RA extracts were prepared as described in Section 3.2.1.

5.2.2 Ultrasound-assisted ultrafiltration process

The hollow fiber UF module (Microza, Pall Co. USA) was immersed in a water bath with an ultrasonic transducer plate (Kamson Ultrasonic Equipment Co., Ltd. China), as shown in Figure 5.1. The hollow fiber module has a bundle of polysulfone (PS) membranes with 10 k Da molecular weight cut-off (MWCO) and total effective area of 0.015 m^2. The ultrasonic plate works at frequency of 45 kHz or 100 kHz, and has output power of 300 W with an interval of 30 W or 600 W with an interval of 60 W, respectively. *RA* extracts were fed by a peristaltic pump (Masterflex, Cole-Parmer Ins. Co., USA) at a fixed flow rate of 40 $mL \cdot min^{-1}$. The system transmembrane pressure (TMP) was adjusted at 0.8 bar. The feed container with a stirring bar inside was put on a heat plate with magnetic stirring function (Thermolyne Cimarec 1, Dubuque, USA). Permeate solution was collected and its weight was measured by an electronic balance (Ohaus, USA). All experiments were operated in constant pressure and total recycle mode.

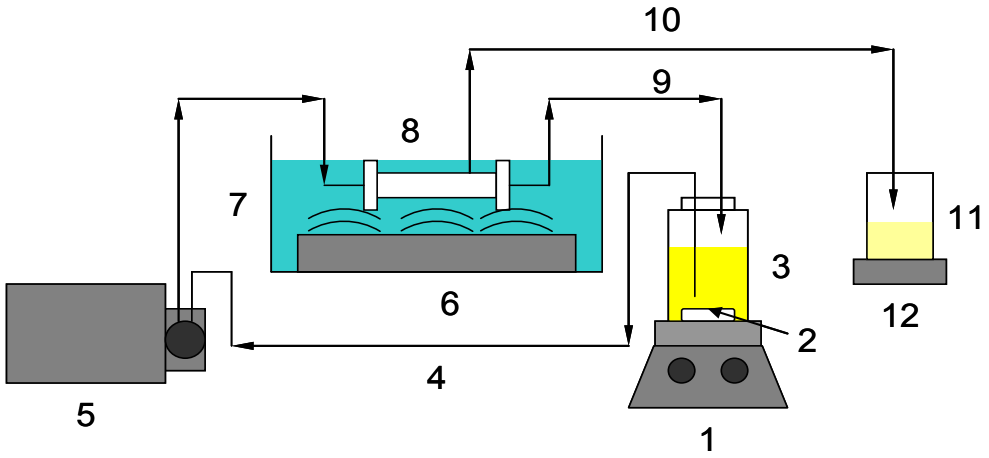

Figure 5.1 Experimental set-up of US-assisted hollow fiber UF process. 1) magnetic stirring and heat plate; 2) stirring bar; 3) feed container; 4) feed; 5) peristaltic pump; 6) ultrasonic transducer plate; 7) water bath; 8) hollow fiber module; 9) retentate; 10) permeate; 11) permeate container; 12) balance.

Flux reduction and flux enhancement are two indexes used to express the effects of US on UF process in this study. These two indexes are defined as follows:

$$Flux \quad reduction = (1 - \frac{Flux_{i-end}}{Flux_{initial}}) \times 100\% \tag{5-1}$$

$$Flux \quad enhancement = (\frac{Flux_{i-end}}{Flux_{without}} - 1) \times 100\% \tag{5-2}$$

where the $Flux_{initial}$ is the flux at the initial 2 minutes, $Flux_{i\text{-}end}$ the flux at the end of process at different US power irradiation and $Flux_{without}$ the flux of process without US irradiation.

5.2.3 Determination of resistances and US intensity

The different resistances in the CFHF UF process were determined according to

the procedures described in Section 3.2.4.2.

Ultrasonic power intensity can be measured by a calorimetric method which observes the temperature changes with time. Besides the calorimetric method, a sonic probe connected to a pulse receiver was used to estimate the US power intensity in US-assisted filtration system [14]. It was found US power intensity inside the membrane unit attenuated sharply, to only about 10% of the original power. In this study, a needle hydrophone and oscilloscope were used to determine the power intensity inside or outside the hollow fiber membrane module. The needle hydrophone was positioned vertically into the module and its tip was immersed under the water and close to the membrane. The waveform amplitude displayed on the oscilloscope was recorded and converted into the acoustic intensity, *I*, by the following equation:

$$I = \frac{P^2}{\rho c} \tag{5-3}$$

where P is the acoustic pressure (Pa), ρ the density of the propagating medium ($kg \cdot m^{-3}$), and c the velocity of sound in the propagating medium ($m \cdot s^{-1}$).

5.2.4 SEM analysis

The hollow fiber UF membranes after different conditional experiments were freeze-dried at -60 ^{o}C for 24 hours, sputter-coated with gold, and then imaged

using a scanning electron microscope (SEM) (JSM-6490, JEOL, USA).

5.3 Results and discussion

5.3.1 Ultrasonic power intensity

Figure 5.2 shows the US waves at 45 kHz detected by a needle hydrophone in the bath or inside the UF module. US waves could propagate into the UF module without any changes in waveform, which indicated that there was no any alteration in frequency. There were some noises occurred in the US waveforms detected inside the module, but not in that of water bath. Compared with the waveforms inside and outside of the module, the voltages inside the hollow fiber module were lower. It demonstrated that the power intensity attenuated when the US transmitted through the wall of UF module. The inside US power intensity was only 10% left from the US source.

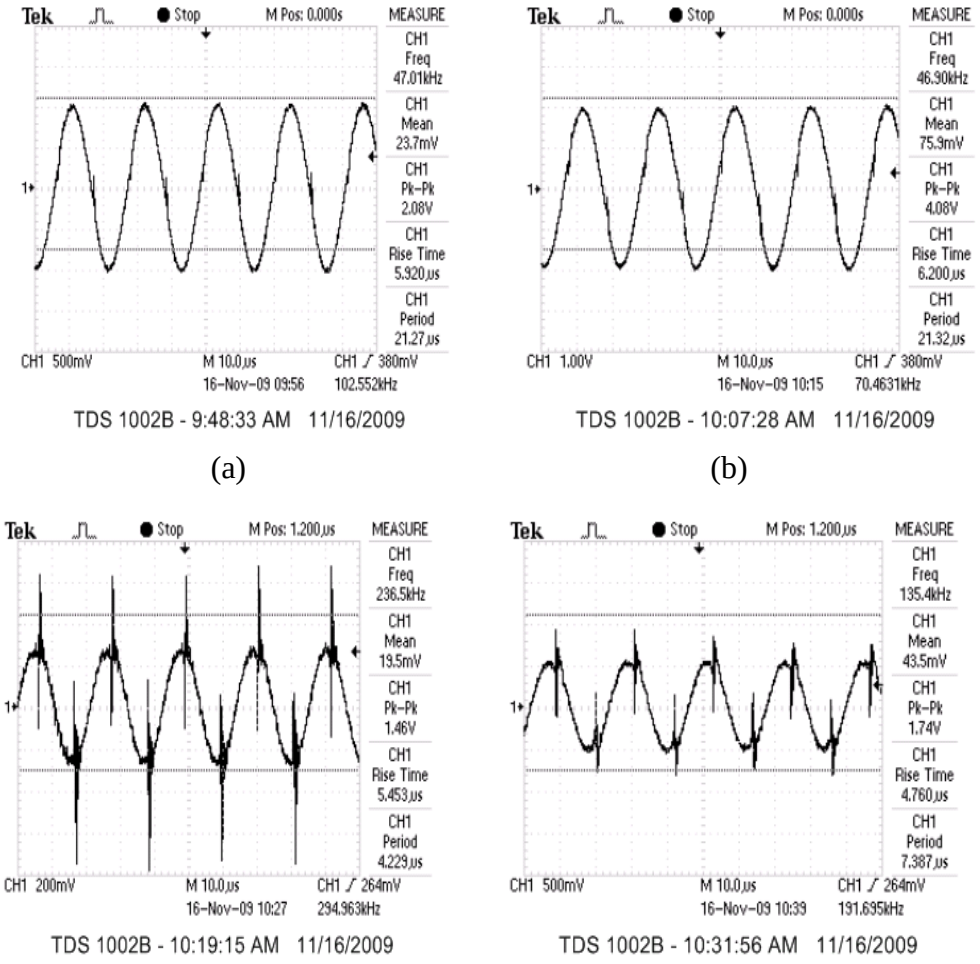

Figure 5.2 Ultrasonic waveforms at 45 frequency in bath and inside hollow fiber module: (a) 30 W in the bath; (b) 180 W in the bath; (c) 30 W inside the module; (d) 180 W inside the module

5.3.2 Effect of ultrasonic frequency

The effects of US at frequencies of 45 kHz and 100 kHz on the flux performance were investigated in the cross-flow hollow fiber UF process. Figure 5.3 shows flux reduction and flux enhancement at different US irradiations. By comparing Figure 5.3a and 5.3b, it was found that both flux reduction and flux enhancement at 45 kHz US irradiation were more significant than that at 100 kHz. The flux enhancements under 100 kHz US irradiation at 360 W and 600 W, which were

10% and 27% respectively, were similar to that under 45 kHz US irradiation at 30 W and 90 W, which were 11% and 28% respectively. This indicated that US at low frequency was more effective on enhancing the flux at a fixed output power; or lower power at low frequency was needed to achieve the same flux enhancement. Thus, low frequency US irradiation could not only obtain higher flux enhancement, but also save the energy. These trends were consistent with our previous studies in the dead-end flat sheet UF [17].

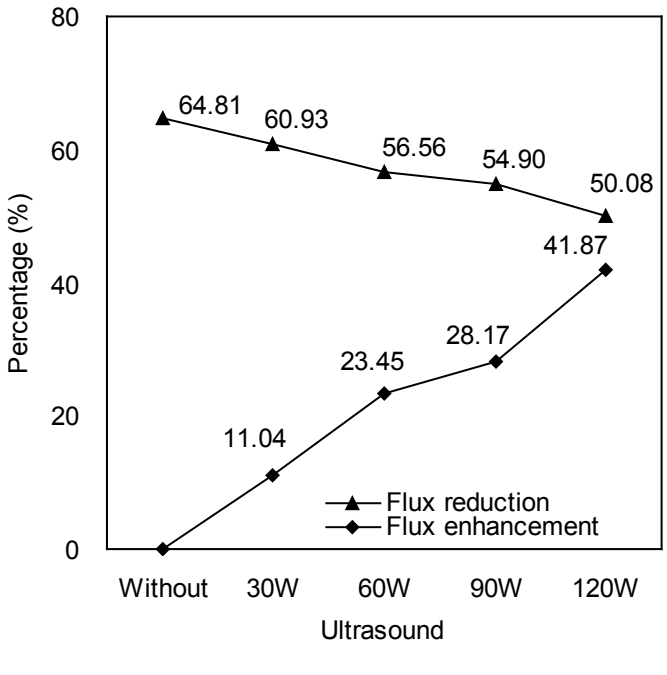

(a)

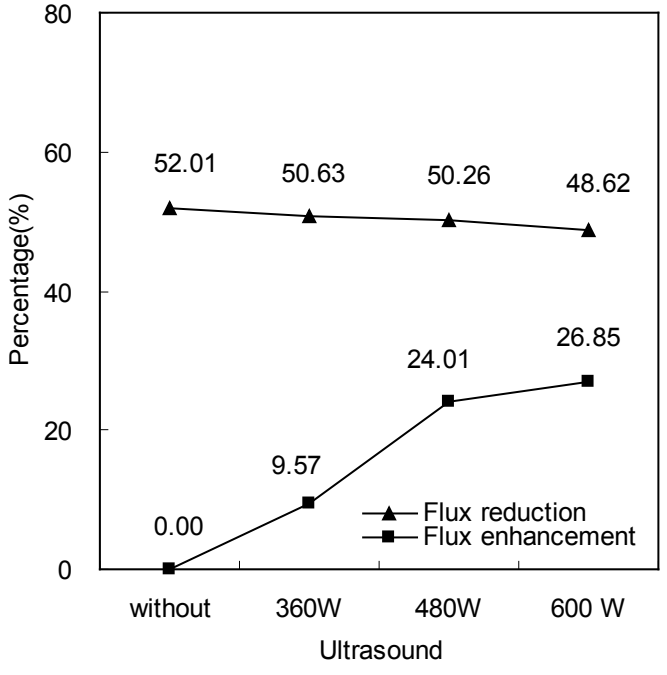

(b)

Figure 5.3 Flux reduction and flux enhancement in the US-assisted hollow fiber UF process of *RA* extracts: (a) 45 kHz; (b) 100 kHz.

Figure 5.4 shows the cross-section view of PS hollow fiber membrane irradiated at a constant power and ultrasonic frequencies of 100 and 45 kHz for 10 minutes. Significant differences were observed on the membrane after US treatment.

Compared with the virgin membrane (Figure 5.4a), the change of cross-section membrane was slight at 100 kHz US irradiation (Figure 5.4b). However, there were some breakages occurred on the membrane after 45 kHz US irradiation (Figure 5.4c). This phenomenon can demonstrated the mechanisms of US irradiation on membrane process. At the same output power, the number of cavitation bubble increases as the ultrasonic frequency increased, but the radius of bubbles decreases [18]. Acoustic pressure becomes weaker with the radius of bubble decreasing. It revealed that acoustic pressure could be a reason for reducing the resistances of concentration polarization and cake layer in UF process.

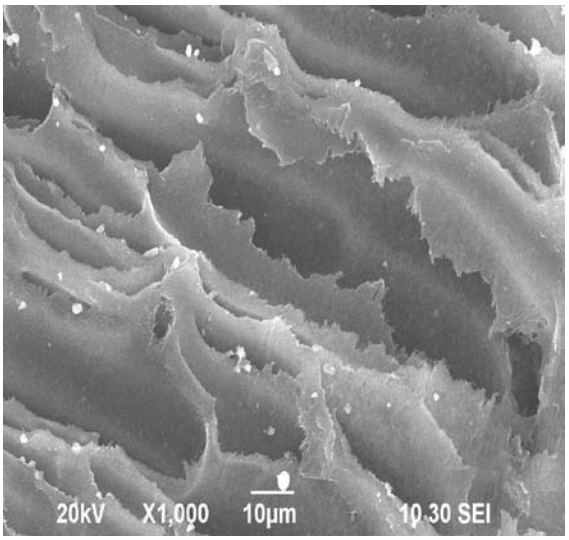

(a)

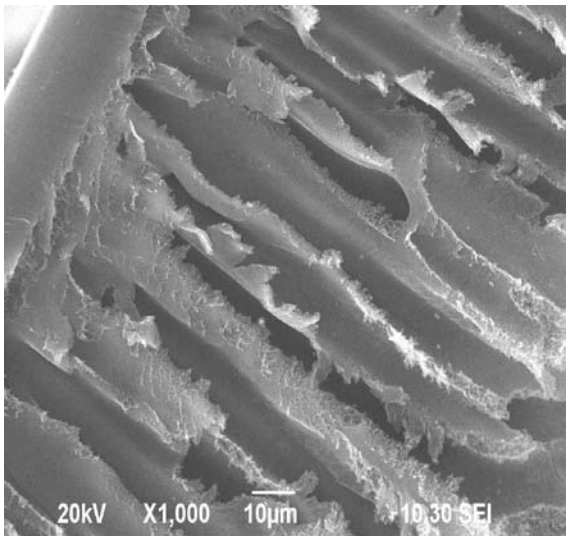

(b)

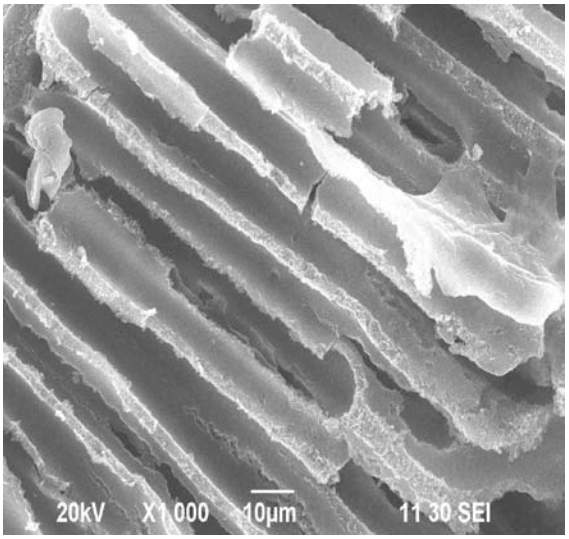

(c)

Figure 5.4 Images of PS hollow fiber UF membranes irradiated with different US frequencies and 100 W power for 10 min. (a) membrane without US irradiation, (b) membrane irradiated at 100 kHz, (c) membrane irradiated at 45 kHz

5.3.3 Effect of ultrasonic power

The effects of ultrasonic power on permeate flux and filtration resistances at 45 kHz and 100 kHz frequencies were investigated, as shown in Figures 5.5 and 5.6, respectively. With 45 kHz US irradiation, the difference of flux enhancement at different powers was slight at the initial stage, but it became more obvious when the process continued. The flux enhancement gradually improved as the power increased, up to 42% at 120 W. In resistance analysis, as shown in Figure 5.5b, the fouling resistances were decreased as the ultrasonic power increased, especially those of concentration polarization and cake layer. The same trends were also observed at the 100 kHz US irradiation, as shown in Figures 5.3b and 5.6. But the enhancements at 100 kHz US were not as significant as that at 45 kHz US, only 27% higher enhancement was obtained at 100 kHz US of 600 W, compared to 28% at 45 kHz US of 90 W. These results indicated that ultrasonic power could significantly affect the flux performance and fouling resistances; higher power led higher permeate flux and lower fouling resistance. It was also proved that US at low frequency was more effective on flux enhancement than that at high frequency. Thus relative less power was needed at low frequency US than that at high frequency US if the same flux enhancement was desired.

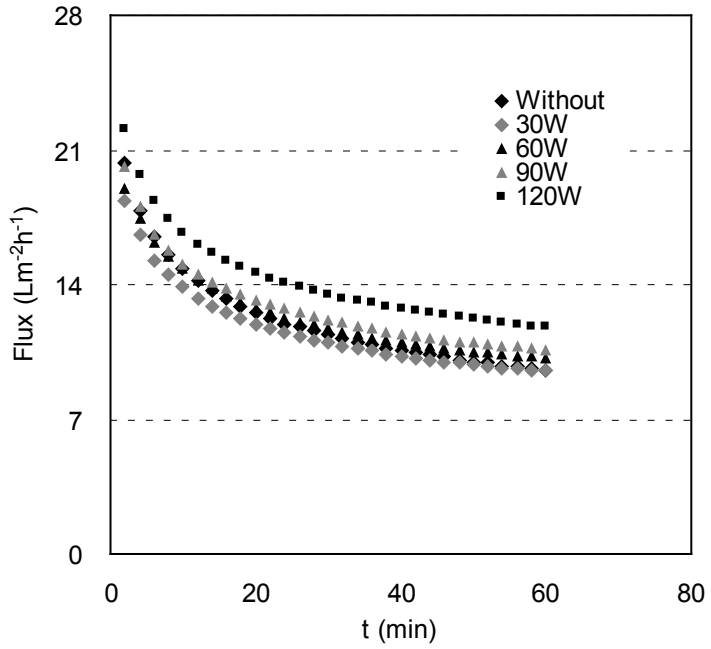

(a)

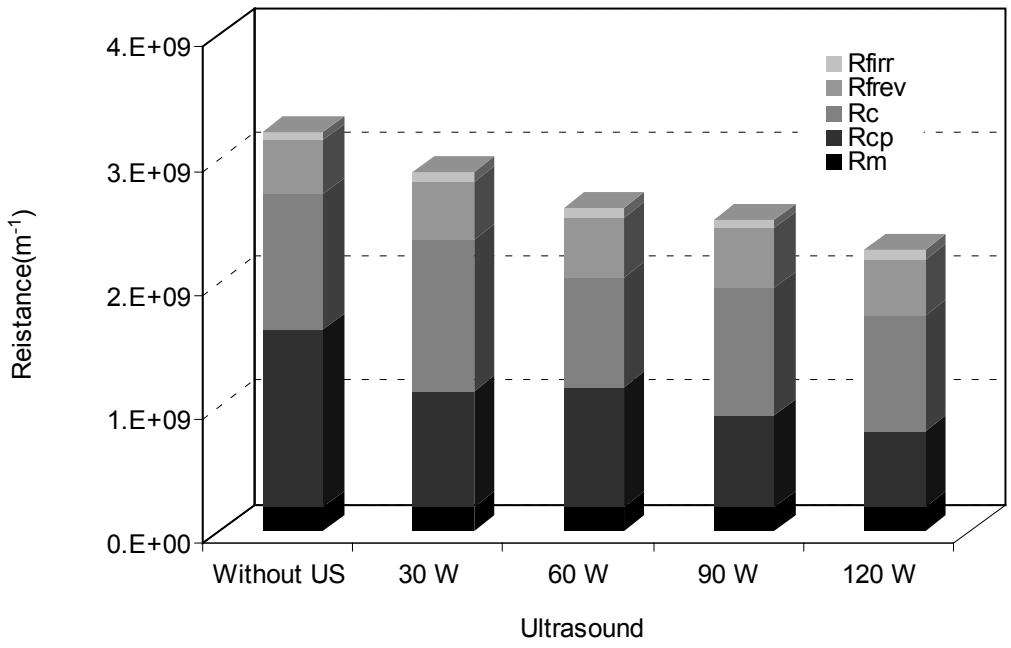

(b)

Figure 5.5 Effects of ultrasonic power on flux (a) and resistances (b) during hollow fiber UF of *RA* extracts (45 kHz)

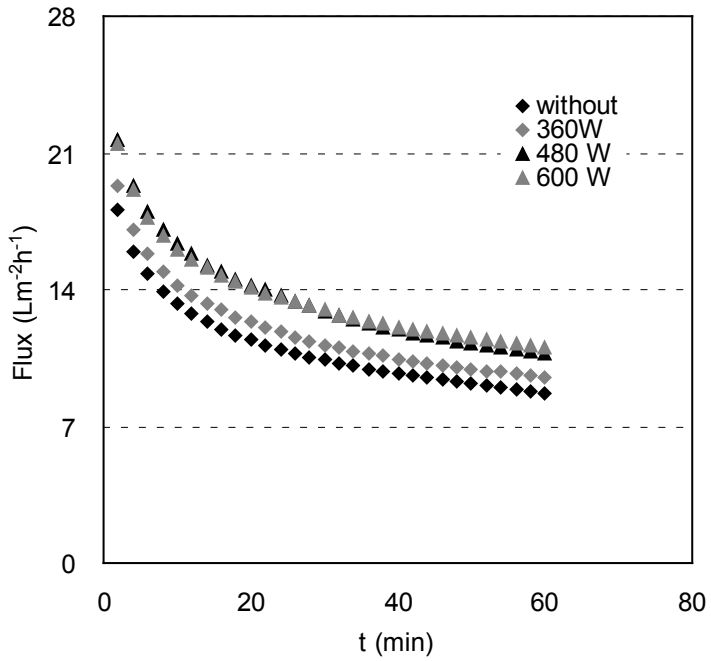

(a)

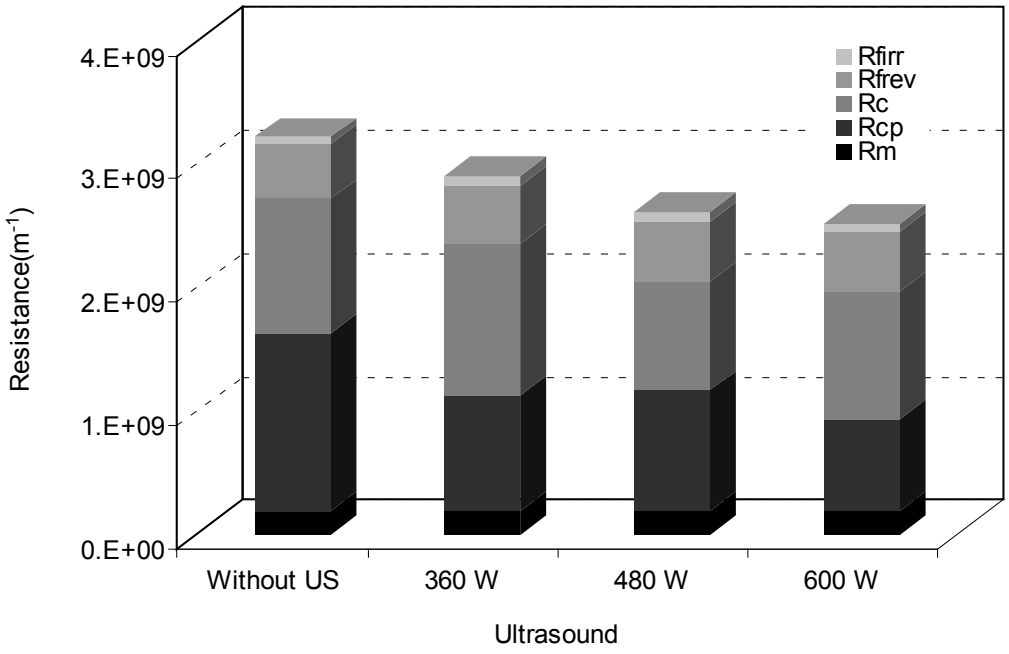

(b)

Figure 5.6 Effects of ultrasonic power on flux (a) and resistances (b) during hollow fiber UF of *RA* extracts (100 kHz)

5.3.4 Effect of ultrasonic irradiation mode

Effects of continued and various intermittent US irradiation modes on permeate flux and fouling resistances in the UF process were investigated. The results are shown in Figures 5.7 and 5.8. In Figure 5.7, the flux was gradually decreased at the US irradiation modes with the sequence of “continued on”, “40s off/60s on”, “60s off/60s on”, “120s off/60s on” and “continued off”. It indicated that the longer US irradiation time on filtration, the higher of flux could be obtained. In resistance analysis, the same trend was obtained. The continued US irradiation made the total resistance the smallest, almost half of that without US irradiation. In Figure 5.8, it showed obviously that the flux enhancement increased with more US irradiation, particularly about 63% enhancement was obtained at the continued US irradiation. Accordingly, the continued US irradiation was more appropriate and effective for applying to the UF process.

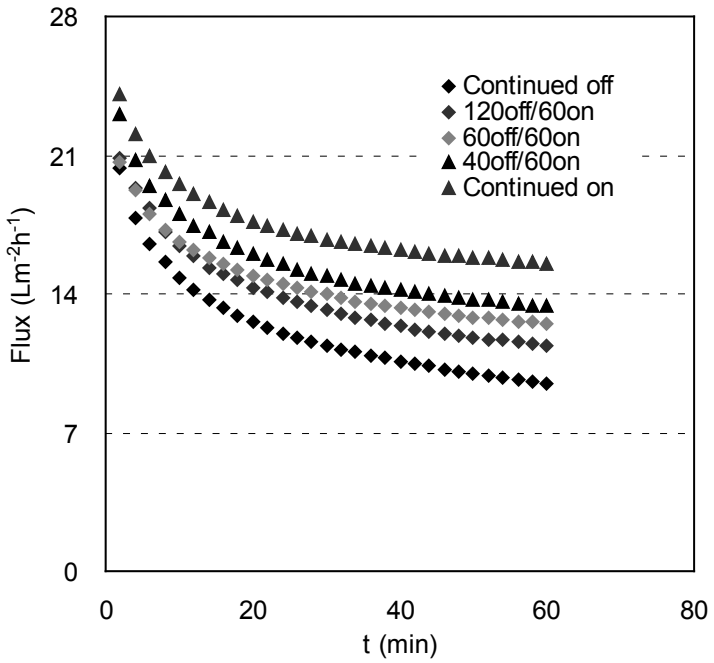

(a)

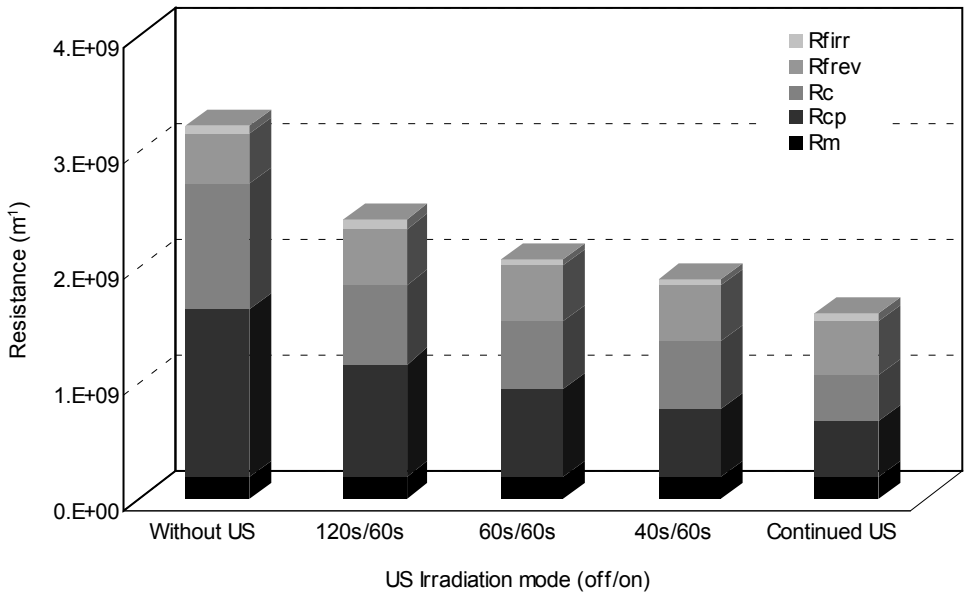

(b)

Figure 5.7 Effects of ultrasonic irradiation modes on permeate flux (a) and filtration resistances (b) during hollow fiber UF of *RA* extracts (45 kHz)

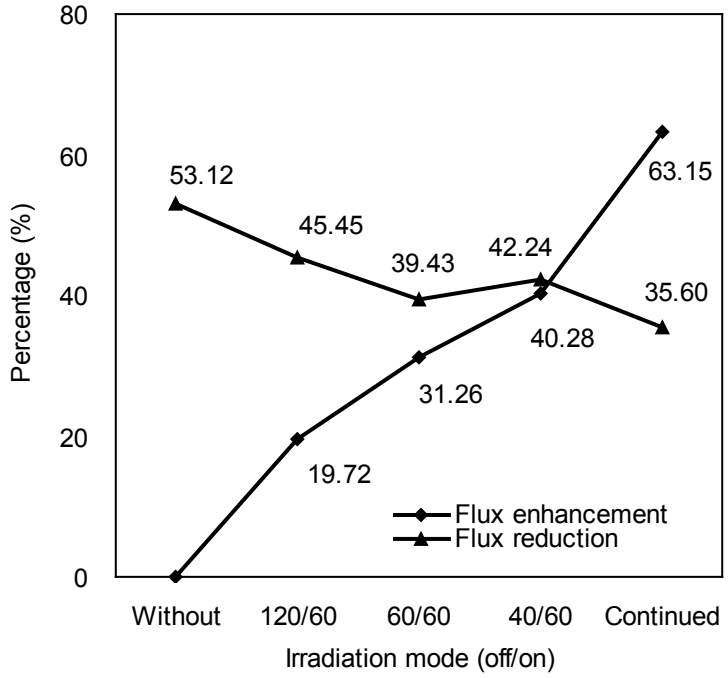

Figure 5.8 Flux reduction and enhancement at different ultrasonic irradiation modes during hollow fiber UF of *RA* extracts (45 kHz)

5.3.5 Effect of US irradiation on hollow fiber membrane

Different from the flat sheet membranes, the hollow fiber membrane is softer and weaker in mechanic strength without the support layer. Thus, it is more susceptible to the US irradiation. Polysulfone (PS) hollow fiber UF membrane was put in a glass beaker with water and the beaker was immersed into the ultrasonic bath. Figure 5.9 shows the SEM images of the hollow fiber membranes before and after US irradiation. After 30 minutes irradiation at 45 kHz US, polymeric material fragmentized from the hollow fiber body (Figure 5.9c), as well as from the inside and outside layers. After 90 minutes irradiation, some holes occurred in the body of hollow fiber membrane (Figure 5.9d), and both inside and outside layer were dramatically broken. Hollow fiber membrane can

be easily broken at high power US irradiation. Accordingly, it should be operated at conditions at which US power intensity is not very high.

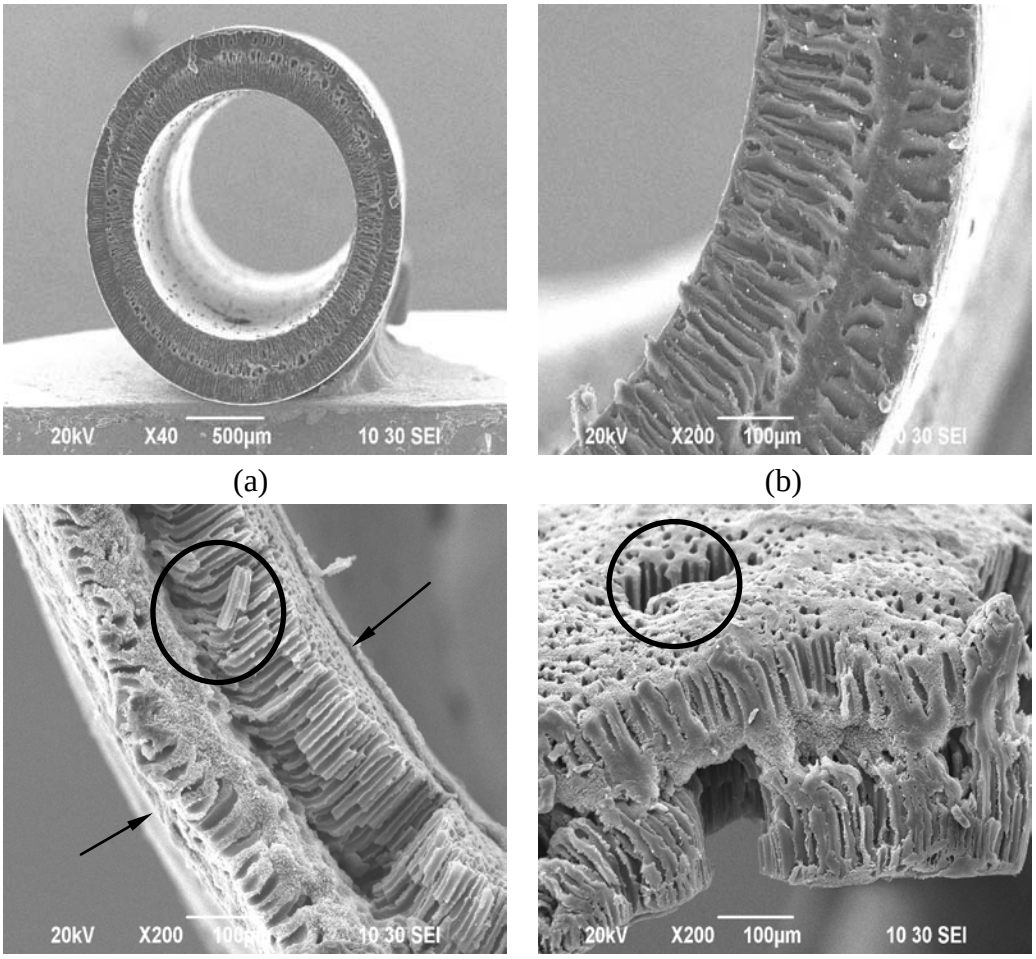

Figure 5.9 Images of PS hollow fiber UF membrane before or after US irradiation: (a) full membrane without US irradiation; (b) partial membrane without US irradiation; (c) fragments on the membrane irradiated at 45 kHz and 100 W US for 30 min, (d) holes in the membrane after irradiating with 45 kHz and 100 W US for 90 min.

5.4 Conclusion

Effects of various ultrasonic parameters on US-assisted UF process of *RA* extracts with hollow fiber membranes have been investigated. Ultrasonic frequency, power and irradiation mode can significantly affect the permeate flux and filtration resistances in the UF process. Low frequency US is more effective on enhancing

the permeate flux and reducing the filtration resistances. As the US power increases, the flux enhancement become more significant both in 45 kHz and 100 kHz US. The effect of intermittent US irradiation on flux is not as significant as the continued US. Different from the flat sheet UF membrane, the hollow fiber membrane is more susceptible to US irradiation. It is breakable at a US irradiation of high power and low frequency. Thus, the US power applied to hollow fiber membranes should not as strong as that used in the flat sheet membranes. Accordingly, the flux enhancement induced by US irradiation in hollow fiber membrane UF process may be not as significant as that in flat sheet membrane UF process. In conclusion, US can be applied to hollow fiber UF process, and enhance flux and reduce fouling, if the applied US power was carefully controlled.

Reference

1. T. Kawakatsu, T. Kobayashi, Y. Sano, M. Nakajima, Clarification of green tea extract by microfiltration and ultrafiltration, Bioscience, Biotechnology and Biochemistry 59 (1995) 1016-1020
2. H. Nawaz, J. Shi, G.S. Mittal, Y. Kakuda, Extraction of polyphenols from grape seeds and concentration by ultrafiltration, Separation and Purification Technology 48 (2006) 176-181
3. W.X. Li, W.H. Xing, W.Q. Jing, N.P. Xu, Effect of pH on microfiltration of Chinese herb aqueous extract by zirconia membrane, Separation and Purification Technology 50 (2006) 92-96
4. X.L. Qiao, Z.J. Zhang, Z.H. P, Hydrophilic modification of ultrafiltration membranes and their application in Salvia Miltiorrhiza decoction, Separation and Purification Technology 56 (2007) 265-269
5. F. Vigo, C. Uliana, Ravinae, A. Lucifredi, M. Gandoglia, The vibrating ultrafiltration module performance in the 50-1000 Hz frequency-range, Separation Science and Technology 28 (1993) 1063-1076
6. Z.F. Cui, T. Taha, Enhancement of ultrafiltration using gas sparging: a comparison of different membrane modules, Journal of Chemical Technology and Biotechnology 78 (2003) 249- 253
7. Z.F. Cui, K.I.T. Wright, Flux enhancements with gas sparging in downwards crossflow ultrafiltration: performance and mechanism, Journal of Membrane Science 117 (1996) 109-116

8. M.Y. Jaffrin, B.B. Gupta, P. Blanpain, Membrane fouling control by backflushing in microfiltration with mineral membranes, Proceedings of the Fifth World Filtration Congress, Nice, France, 1990, pp. 479-483
9. P. Srijaroonrat, E. Julien, Y. Aurelle, Unstable secondary oil/water emulsion treatment using ultrafiltration: fouling control by backflushing, Journal of Membrane Science 159 (1999) 11-20
10. S.M. Finngan, J.A. Howell, The effect of pulsatile flow on ultrafiltration fluxes in a baffled tubular membrane system, Chemical Engineering Research & Design 67 (1989) 278-282
11. J. Jurado, B.J. Bellhouse, Application of electric fields and Vortex mixing for enhanced ultrafiltration, Filtration & Separation 31 (1994) 273-281
12. H. M. Kyllonen, P. Pirkonen, M. Nystrom, Membran filtration enhanced by ultrasound: a review, Desalination 181 (2005) 319-335
13. A. Simon, N. Gondrexon, S. Taha, J. Cabon, G. Dorange, Low-frequency ultrasound to improve dead-end ultrafiltration performance, Separation Science and Technology 35 (2000) 2619-2637
14. T. Kobayashi, T. Kobayashi, Y. Hosaka, N. Fujii, Ultrasound-enhanced membrane-cleaning processes applied water treatments: influence of sonic frequency on filtration treatments, Ultrasonics 41 (2003) 185-190
15. T. Kobayashi, X. Chai, N. Fujii, Ultrasound enhanced cross-flow membrane filtration, Separation and Purification Technology 17 (1999) 31-40
16. M.O. Lamminen, H.W. Walker, L.K. Weavers, Mechanisms and factors influencing the ultrasonic cleaning of particle-fouled ceramic membranes,

Journal of Membrane Science 237 (2004) 213-223

17. M. Cai, S.J. Wang, Y.P. Zheng, H.H. Liang, Effects of ultrasound on ultrafitration of *Radix astragalus* extract and cleaning of fouled membrane, Separation and Purification Technology 68 (2009) 351-356
18. T.J. Mason, J.P. Lorimer, Applied Sonochemistry: The uses of power ultrasound in chemistry and processing, WILEY-VCH, Weinheim, 2002

Chapter 6

Optimization of Ultrasound-assisted UF of *RA* Extracts with Hollow Fiber Membrane using Response Surface Methodology

---

Journal of Membrane Science (submitted)

Abstract

Response surface methodology (RSM) with a central composite rotatable design (CCRD) was employed to optimize the process of ultrasound-assisted ultrafiltration (USUF) of *Radix astragalus* mixtures with hollow fiber membrane. The effects and mutual interaction of various parameters, namely ultrasonic power, ultrasonic irradiation mode, transmembrane pressure (TMP) and temperature, on flux reduction (Y_1) and process duration (Y_2) were investigated simultaneously. The analysis of variance (ANOVA) demonstrated that the second order polynominal regression models were appropriate and significant, with R^2 of 0.9927 and 0.9615 for Y_1 and Y_2, respectively. The study also showed that TMP was the most significant parameter, followed by the temperature, ultrasonic power and irradiation mode in decreasing levels of significance. The global criterion and desirability function approaches were used to obtain the optimal conditions to minimize Y_1 and Y_2 simultaneously. The optimum conditions were found to be ultrasonic power of 120 W, continued ultrasonic irradiation mode, TMP of 0.64 bar and temperature of 20℃. The two predicted response values were 55.3% and 53 minutes for Y_1 and Y_2, respectively, which were in good agreement with the results from the confirmation experiments, about 57.0-60.3% and 53-58 minutes. These results indicated that the regression models were adequate and RSM was an efficient statistical tool to be used to investigate the USUF process.

6.1 Introduction

Natural products are the most healthy food or medicine for people in the 21st century, because of their effective pharmacological or biological activities. *Radix astragalus* (*RA*), which consists of various satisfactory active components, such as polysaccharides, saponins and flavonoids, is a widely used natural product [1]. In most manufacture processes, natural products are preliminarily extracted, followed by separation or purification using various appropriate technologies. In recent years, ultrafiltration (UF) and microfiltration (MF) have been acknowledged as promising technologies to clarify or separate the natural product mixtures [2-5]. However, flux decline is the most critical problems in the processes, which is mainly caused by concentration polarization and membrane fouling. In order to solve this problem, some additional techniques have been employed to the processes, such as vibration [6], gas sparging [7, 8], electrical field [9] and ultrasound (US) [10].

In recent years, US has been employed in the membrane filtration process and proved to have the effects of enhancing the permeate flux and improving the cleaning of fouled membrane [11-15]. The effects of ultrasonic frequency, power intensity and irradiation direction on cross-flow flat sheet membrane filtration were investigated by Kobayashi et al. [13-15]. It was found all these factors can significantly affect the flux enhancement and flux recovery induced by US. However, all of these studies used one-variable-at-a-time approach only, which

was time consuming and could not show the interaction effects among these factors. According to our knowledge, there is no study on optimizing the US-assisted membrane filtration process. Therefore, it is necessary to use a systematic experimental design to investigate the effects and mutual interaction of parameters, and to find the optimum conditions for the process of USUF of *RA* mixtures.

Response surface methodology (RSM) is an efficient statistical tool used to solve multi-variable problems and to optimize one or several responses. It has been used in many manufacture processes besides the membrane filtration process. Optimum conditions of UF and nanofiltration were investigated for separation and concentration of isoflavones and oligosaccharides from Sunmul using RSM by Kim et al. [16]. Cheison et al. [17] used RSM to optimize the hydrolysis of whey protein isolate in a tangential flow filter membrane reactor. The effects of some factors were investigated and optimum conditions were obtained. Sivakumar, Malaisamy and their group [18, 19] investigated the effects of some factors in UF process for BSA or riboflavin separation. Zakrzewska-Trznadel et al. [20-22] used response surface to model and optimize some membrane processes. In their studies, one or several responses were investigated and optimized by superimposition or some mathematical methods such as desirability function and Lagrange multipliers method. Accordingly, RSM is an appropriate and promising tool to optimize a membrane filtration process with one or several responses.

The objectives of this study are to investigate the effects and mutual interaction of some operational parameters, namely ultrasonic power, ultrasonic irradiation mode, TMP and temperature, on the USUF of *RA* mixtures process, and to obtain the optimum conditions of the process for minimizing both flux reduction and process duration, using RSM with a central composite rotatable design (CCRD).

6.2 Materials and methods

6.2.1 Materials

RA extracts were prepared as described in Section 3.2.1.

6.2.2 Ultrasound-assisted ultrafiltration

All experiments were carried out in a water bath with an ultrasonic transducer plate (Kamson Ultrasonic Equipment Co., Ltd. China) and a hollow fiber UF module (Microza, Pall Co. USA) immersed, as shown in Figure 5.1, Chapter 5. The ultrasonic plate has 45 kHz frequency and power output ranged 0-300 W with a 30 W interval. The hollow fiber module has a bundle of 10 k Da molecular weight cut-off (MWCO) polysulfone membrane with an effective area of 0.015 m^2. *RA* extracts were transmitted into the system by a peristaltic pump (Masterflex, Cole-Parmer Ins. Co., USA) at a fixed flow rate of 40 $mL \cdot min^{-1}$. The system transmembrane pressure (TMP) was adjusted at 0.2, 0.4, 0.6, 0.8 and 1.0 bar by a valve on the side of retentate tube. The feed container with a stirring bar inside

was put on a magnetic and heat plate (Thermolyne Cimarec 1, Dubuque, USA). The feed solutions were kept at 20, 30, 40, 50 and 60 ℃ by the heat plate. Permeate solution was weighed by an electronic balance (Ohaus, USA). All the optimization trials were operated in the constant pressure and diafiltration mode.

The flux reduction and process duration were chose as the two objectives of the optimization study. The flux reduction was calculated as follows:

$$Flux \quad reduction = (1 - \frac{Flux_{end}}{Flux_{initial}}) \times 100\% \qquad (6\text{-}1)$$

where $Flux_{end}$ is the flux obtained at the end of UF process when 140 mL permeate solution is collected from the total 200 mL feed. This operational time in each run was considered as the process duration.

6.2.3 Experimental design

Based on the results of our previous studies, a CCRD with four variables and five levels (i.e. -2.0, -1.0, 0, 1.0, 2.0) was employed. The four independent variables were ultrasonic power (X_1), ultrasonic irradiation mode (X_2), TMP (X_3) and feed temperature (X_4). The dependent variables were flux reduction (Y_1) and process duration (Y_2), which could express the membrane fouling phenomenon and the efficiency of UF process, respectively. The experimental design as well as the obtained two responses is shown in Table 6.1.

Table 6.1 The central composite rotatable design and two responses

Run	X_1 US Power (W)	X_2 US mode	X_3 TMP (bar)	X_4 Temp (℃)	Y_1 Flux Reduction (%)	Y_2 Process Duration (min)
1	-1 (30)	-1 (0.5)	-1 (0.4)	-1 (30)	55.05	80
2	-1 (30)	-1 (0.5)	-1 (0.4)	1 (50)	58.58	69.5
3	-1 (30)	-1 (0.5)	1 (0.8)	-1 (30)	70.72	50
4	-1 (30)	-1 (0.5)	1 (0.8)	1 (50)	72.23	42
5	-1 (30)	1 (1.5)	-1 (0.4)	-1 (30)	53.51	93
6	-1 (30)	1 (1.5)	-1 (0.4)	1 (50)	55.17	74.5
7	-1 (30)	1 (1.5)	1 (0.8)	-1 (30)	70.64	54.5
8	-1 (30)	1 (1.5)	1 (0.8)	1 (50)	70.47	43.5
9	1 (90)	-1 (0.5)	-1 (0.4)	-1 (30)	47.29	83
10	1 (90)	-1 (0.5)	-1 (0.4)	1 (50)	56.40	66
11	1 (90)	-1 (0.5)	1 (0.8)	-1 (30)	67.05	47
12	1 (90)	-1 (0.5)	1 (0.8)	1 (50)	68.26	35
13	1 (90)	1 (1.5)	-1 (0.4)	-1 (30)	53.25	90
14	1 (90)	1 (1.5)	-1 (0.4)	1 (50)	56.60	73
15	1 (90)	1 (1.5)	1 (0.8)	-1 (30)	69.58	51.5
16	1 (90)	1 (1.5)	1 (0.8)	1 (50)	71.10	35.5
17	-2 (0)	0 (1.0)	0 (0.6)	0 (40)	68.66	60
18	2 (120)	0 (1.0)	0 (0.6)	0 (40)	64.41	49
19	0 (60)	-2 (0)	0 (0.6)	0 (40)	67.60	46.5
20	0 (60)	2 (2)	0 (0.6)	0 (40)	67.14	53
21	0 (60)	0 (1.0)	-2 (0.2)	0 (40)	35.65	145
22	0 (60)	0 (1.0)	2 (1.0)	0 (40)	70.41	38.5
23	0 (60)	0 (1.0)	0 (0.6)	-2 (20)	60.17	63
24	0 (60)	0 (1.0)	0 (0.6)	2 (60)	64.04	41.5
25	0 (60)	0 (1.0)	0 (0.6)	0 (40)	64.36	52.75
26	0 (60)	0 (1.0)	0 (0.6)	0 (40)	64.51	52

Note: X_2, irradiation mode: 0 (continued), 0.5 (30 sec off/ 60 sec on), 1 (60 sec off/60 sec on), 1.5 (90 sec off/ 60 sec on), 2 (120 sec off/ 60 sec on).

6.2.4 Statistical analysis and optimization

A second order polynominal model, shown as follows, was used for regression with the experimental results using the software of Statistica 6.0 (StatSoft, USA).

$$Y_k = b_{k0} + \sum_{i=1}^{4} b_{ki} X_i + \sum_{i=1}^{4} b_{kii} X_i^2 + \sum_{i=1}^{3} \sum_{j=i+1}^{4} b_{kij} X_i X_j \qquad (6\text{-}2)$$

where Y_k are the responses, namely Y_1 for the flux reduction and Y_2 for the process duration; b_{k0}, b_{ki}, b_{kii} and b_{kij} are the regression coefficients; and Xs are the coded independent variables. The R^2 and the lack-of-fit are evaluated for the fitness of the model.

Both the responses, flux reduction and process duration, are the smaller the better. Therefore, in order to obtain the optimum results, the global criterion method and the desirability function approach were used.

The global criterion method is an additive method, combining the individual responses as follows [23]:

$$F = \sum_{i=1}^{k} \left[\frac{Y_i - Y_{i\min}}{Y_{i\max} - Y_{i\min}} \right]^{p_i} \qquad (6\text{-}3)$$

where F is the global criterion, $0 \le F \le 1$, p_i the response weight used to determine scale of importance, Y_{imin} the minimum acceptable value, Y_{imax} the maximum value.

The desirability function is a multiplicative model as follows [24]:

$$D = (d_1^{w_1} \times d_2^{w_2} \times \cdots \times d_k^{w_k})^{1/\sum w_i} \quad (6\text{-}4)$$

where D is the overall desirability, $0 \le D \le 1$, w_i defined as a response weight, d_k the individual desirability, $0 \le d_k \le 1$:

$$d_k = \begin{cases} 0, & if \quad Y_k \le Y_{k\min} \\ \left(\dfrac{Y_k - Y_{k\min}}{Y_{k\max} - Y_{k\min}} \right)^r, & if \quad Y_{k\min} \le Y_k \le Y_{k\max} \\ 1, & if \quad Y_k \ge Y_{k\max} \end{cases} \quad (6\text{-}5)$$

where $Y_{k\min}$ is the minimum acceptable value of Y_k, Y_{kmax} is the maximum value that is considered desirable and r is a positive constant. If r<1, the d_k changes less rapidly towards the Y_{kmax}; If r=1, the d_k increases linearly as Y_k increases; if r>1, the d_k changes more rapidly towards the Y_{kmax}.

6.3 Results and Discussion

6.3.1 Modeling the response and ANOVA

The experimental design and obtained two responses (Y_1 and Y_2) data are shown in Table 6.1. Two second order polynominal regression models were established and tested for adequacy and fitness by the analysis of variance (ANOVA). The regression coefficients (coded factors) of the models for Y_1 and Y_2 are listed in Table 6.2. The significance of each coefficient was tested by the *p*-value, at 0.05, 0.01 and 0.001 levels. All the coefficients, which are significant at p<0.05 level, were remained in the models, as follows:

$$Y_1 = 0.6444 - 0.0106X_1 + 0.0052X_1^2 + 0.0073X_2^2 + 0.0802X_3 - 0.0285X_3^2 + 0.0123X_4 - 0.0059X_4^2 + 0.0115X_1X_2 + 0.0054X_1X_4 - 0.0056X_2X_4 - 0.0085X_3X_4 \quad (6\text{-}6)$$

$$Y_2 = 52.3750 - 2.0X_1 + 2.3333X_2 - 20.125X_3 + 9.7917X_3^2 - 6.375X_4 \quad (6\text{-}7)$$

where X_1, X_2, X_3 and X_4 are the coded values of the independent variables.

Table 6.2 Coefficients of the fitted polynominal models for responses

	Y_1 (Flux Reduction)		Y_2 (Process Duration)	
	Coefficient	*p*-Value	Coefficient	*p*-Value
b_0	0.644350***	0.000741	52.3750**	0.004558
b_1 (X_1, US Power)	-0.010558*	0.013053	-2.0000*	0.034424
b_{11}	0.005223*	0.030921	0.4792	0.164863
b_2 (X_2, US mode)	0.001592	0.086068	2.3333*	0.029514
b_{22}	0.007310*	0.022100	-0.7083	0.112888
b_3 (X_3, TMP)	0.0801717**	0.001708	-20.1250**	0.003424
b_{33}	-0.028540**	0.005663	9.7917**	0.008253
b_4 (X_4, Temp)	0.012275*	0.011228	-6.3750*	0.010809
b_{44}	-0.005852*	0.027601	-0.0833	0.630173
b_{12}	0.011450*	0.014741	-0.3125	0.255442
b_{13}	0.000437	0.346886	-1.0000	0.083915
b_{14}	0.005412*	0.031164	-0.8750	0.095734
b_{23}	0.0001450	0.115148	-1.3125	0.064091
b_{24}	-0.005625*	0.029988	-0.9375	0.089439
b_{34}	-0.008487*	0.019883	1.0000	0.083915

*p<0.05, **p<0.01, ***p<0.001

According to the ANOVA, the linear terms are all significant for both Y_1 and Y_2, except X_2 for Y_1; the quadratic terms are all significant for Y_1, but not significant

for Y_2 except X_3^2; the cross terms are all not significant for Y_2, but X_1X_2, X_1X_4, X_2X_4 and X_3X_4 are significant for Y_1.

The results of ANOVA are shown in Table 6.3. The R^2s for Y_1 and Y_2 models are 0.9927 and 0.9615, which are in good agreement with the adjusted R^2_{adj}, 0.9834 and 0.9125, respectively. Also, both the lack-of-fits are not significant, at p>0.05 level. It indicates that both established models are goodness of fit and appropriate for representing the relationship between independent variables and dependents. Figure 6.1 shows the observed values compared with the predicated values by the models, which are good fit. Therefore, these models are adequate for prediction and optimization.

Table 6.3 Analysis of variance (ANOVA) for the polynominal models

Response	Source	Degrees of freedom	Sum of Square	*F*-value	*p*-value
Y_1	Model	14	0.1924		
	Residual	11	0.001426		
	Lack of fit	10	0.001425	126.7	0.06905
	Pure error	1	0.000001		
	R^2	0.9927			
Y_2	Model	14	13548.59		
	Residual	11	542.32		
	Lack of fit	10	542.04	192.73	0.0560
	Pure error	1	0.28		
	R^2	0.9615			

*p<0.05, **p<0.01, ***p<0.001

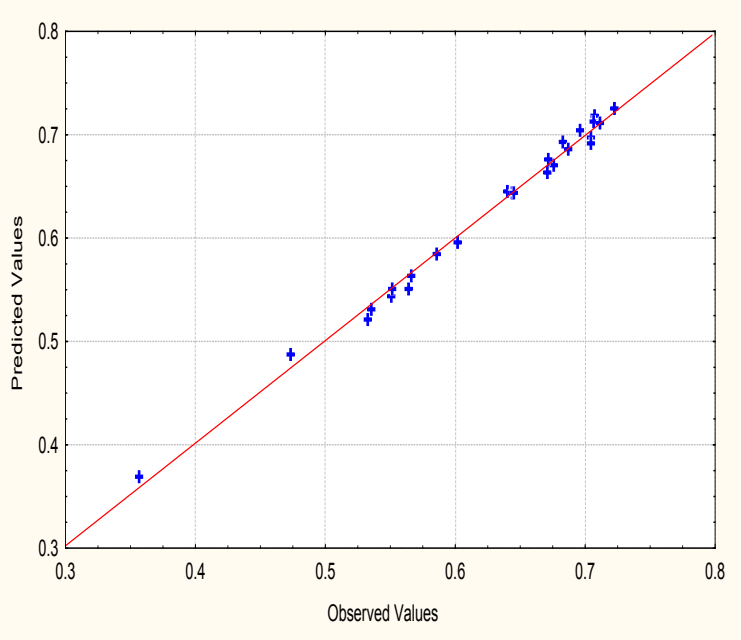

(a)

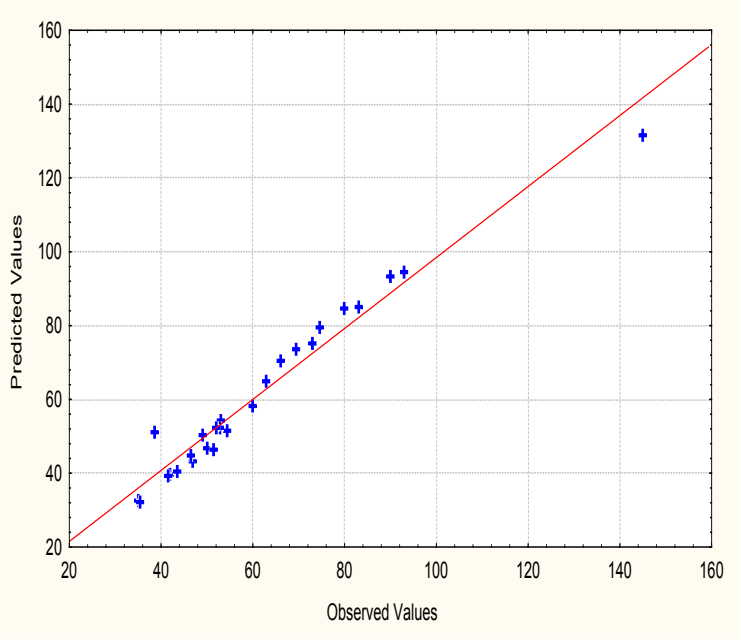

(b)

Figure 6.1 Experimental observed values compared to the predicted values obtained from the regression models: a) Y_1; b) Y_2.

6.3.2 Effect and interaction of variables

Figure 6.2 shows the linear, quadratic and cross effects of each independent variable, the bar lengths indicate the absolute values of the effects. A vertical line is marked to reveal the significance variables at the p=0.05 level.

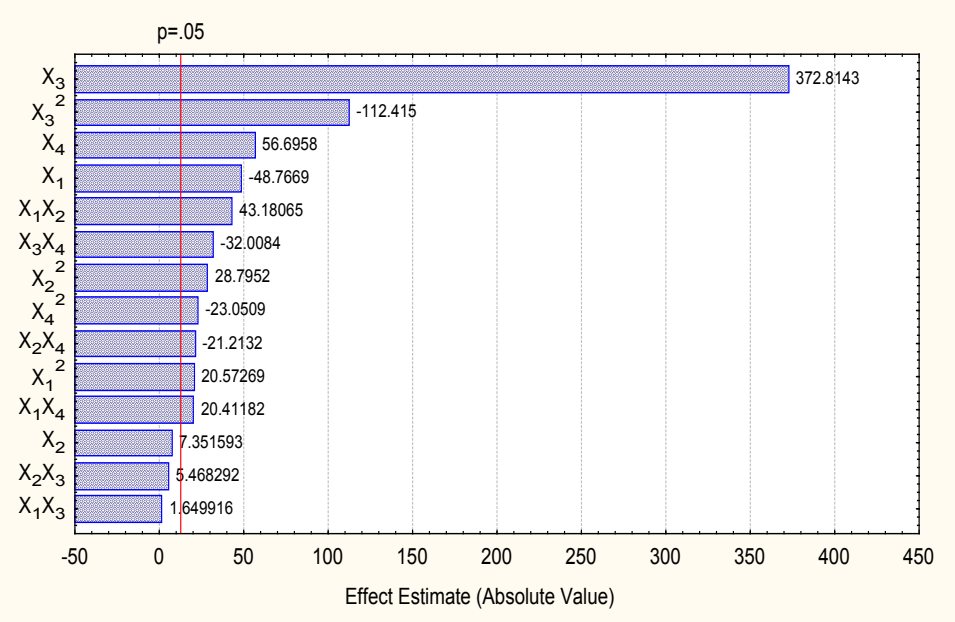

(a)

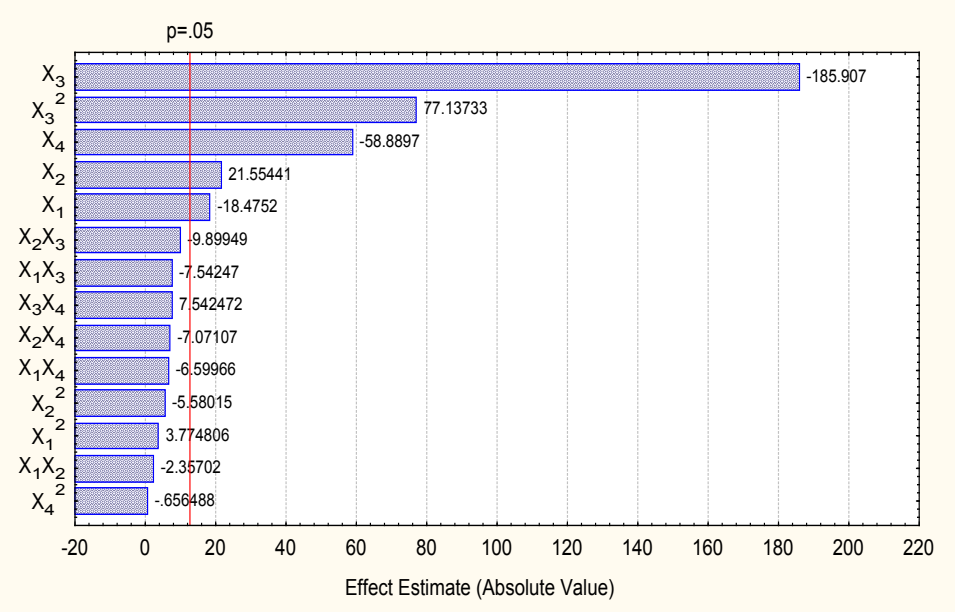

(b)

Figure 6.2 Pareto charts of standardized effects for the responses. (a) Flux reduction, Y_1; (b) Process duration, Y_2.

In Figure 6.2a, among the linear terms, TMP (X_3) shows the most significant effect on Y_1. Temperature (X_4) is the second significant factor, followed by the ultrasonic power (X_1). Ultrasonic irradiation mode (X_2) is not a significant factor for Y_1. The quadratic terms, X_3^2, X_2^2, X_4^2 are significant on Y_1, decreasingly.

Cross terms of X_1X_2, X_3X_4, X_2X_4 and X_1X_4 on Y_1 are all significant, indicating the interaction among these variables on Y_1 is complicated. The number of significant factors is much less for Y_2 than for Y_1 as shown in Figure 6.2b. For Y_2, the linear terms, X_3, X_4, X_2 and X_1, all are significant, decreasingly, and all the other terms, quadratic and cross terms, are not significant except X_3^2. Accordingly, the two most significant parameters in this process are TMP and temperature, and the two ultrasonic parameters, ultrasonic power and irradiation mode are not as significant as expected. These results demonstrate that US is an additional technique which can effectively affect the fouling in UF process, but it may not be as significant as TMP.

The effects of the independent variables and their interaction on Y_1 and Y_2 are illustrated as response surface and contour plots in Figures 6.3 and 6.4. As discussed above, TMP is the most significant parameter for both Y_1 and Y_2. As shown in Figure 6.3, the flux reduction becomes more serious with the increased TMP from 0.2 to 1.0 bar, indicating that higher TMP can make dramatic fouling leading to a sharp flux decline. The effect of temperature on flux reduction was not as significant as TMP, increased slightly as temperature increased. It indicates that higher temperature makes flux decline more dramatically. Generally, higher ultrasonic power decreases flux reduction as shown in the plots. In other words, higher ultrasonic power reduces the concentration polarization and fouling phenomena in the process, leading to higher flux performance. This result is consistent with that of the previous studies [11, 14]. Ultrasonic

irradiation mode shows little effect on flux reduction, which is also proved in the pareto chart.

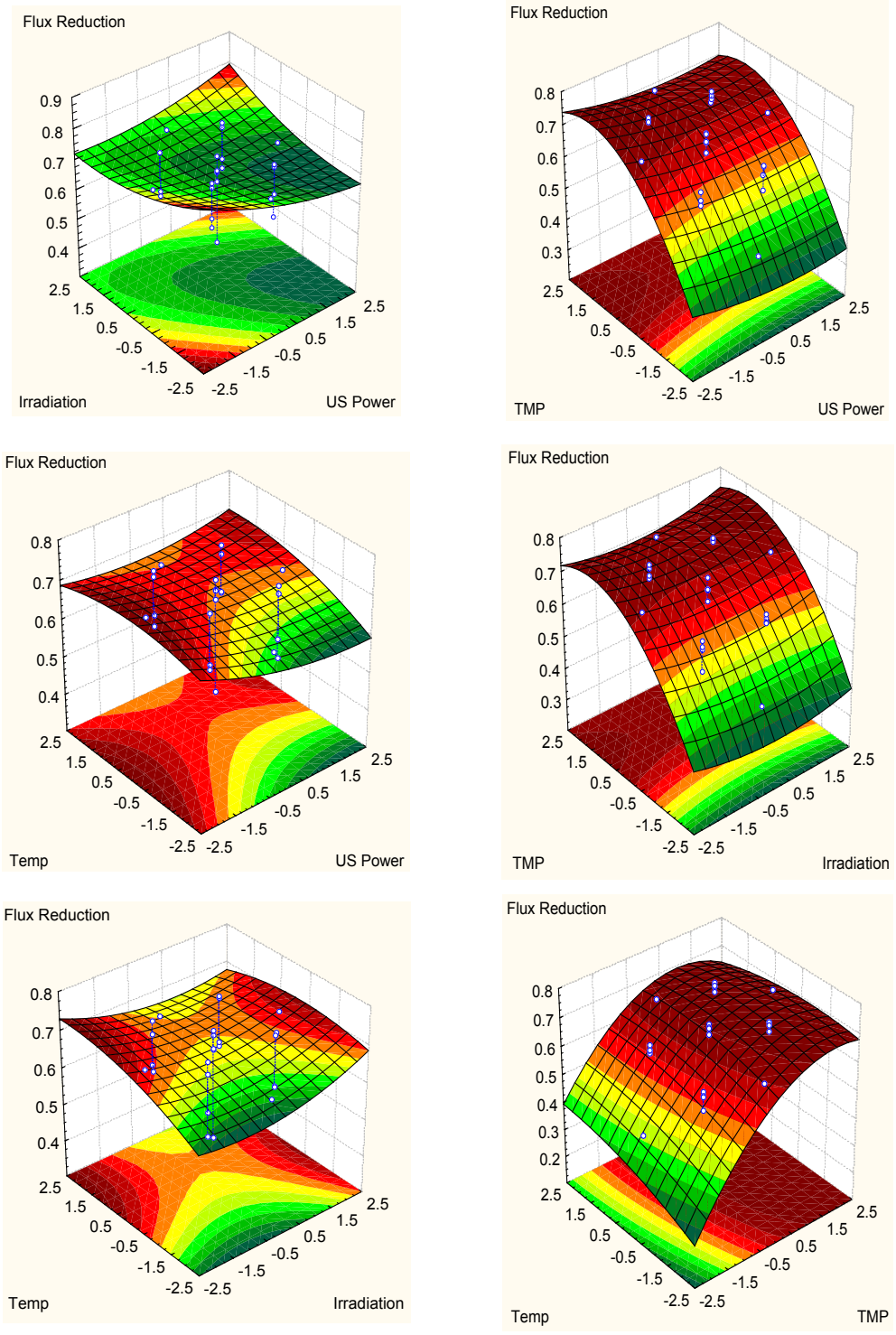

Figure 6.3 Response surface and contour plots of the effects of four independent variables for flux reduction, Y_1. The other variable is at zero level in each plot. z: the flux reduction; x, y: two variables.

For Y_2, TMP is also the most significant factor. As shown in Figure 6.4, the response surfaces with the variable of TMP are sharp. With increased TMP, the process duration becomes shorter. It indicates the UF technology is a pressure-driven force process. The effect of temperature on process duration is also significant, the higher the temperature, the faster the process. It may be caused by the diffusion coefficient and viscosity changes induced by the temperature rise. Higher ultrasonic power and continued US make the UF process faster, because the fouling is reduced by US irradiation as proved in Figure 7.3.

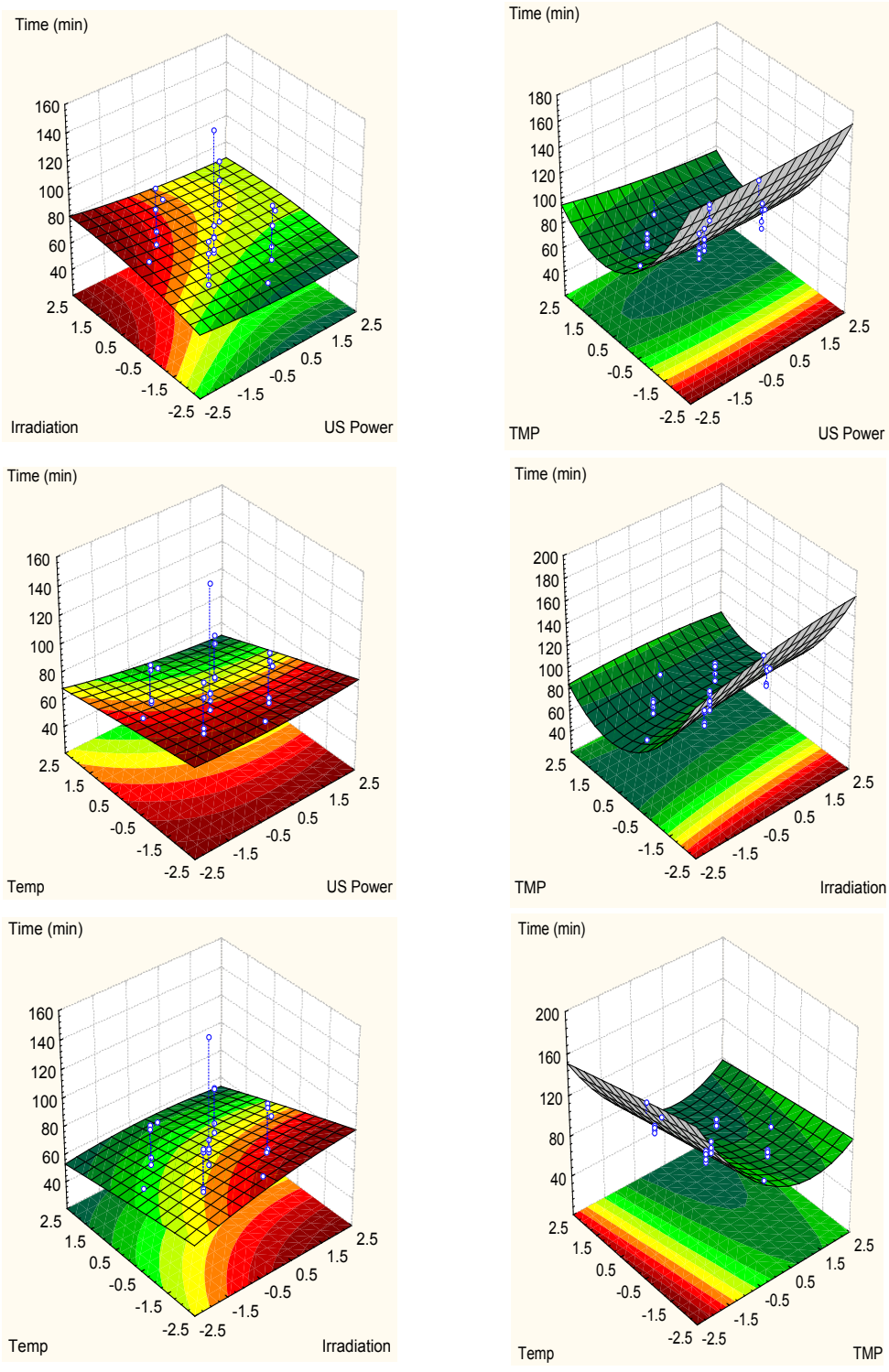

Figure 6.4 Response surface and contour plots of the effects of four independent variables for process duration, Y_2. The other variable is at zero level in each plot. z: the process duration; x, y: two variables.

6.3.3 Optimization and confirmation

The objective of optimizing the process is to find the operational conditions which lead to a minimum flux reduction and process duration, simultaneously. The global criterion and desirability function approaches both were employed for optimization. For the two responses, Y_{1min}=35%, Y_{1max}=75%, Y_{2min}=35 minutes and Y_{2max}=145 minutes were selected as the minimum and maximum acceptable values, respectively. In both optimization methods, it is important to find an appropriate response weight value, p_1, p_2, w_1 and w_2, for each response. According to our experiences, in the global criterion method, p_1=0.4 and p_2=1 were used in practice. In the desirability function approach, the response weights, w_1, w_2, and r were specified at 1, 3 and 1, respectively.

For each response, the four independent variables are coded from -2.0 to 2.0 with a 0.1 interval. Computer programs were written to obtain the maximum F and D values by these two approaches, respectively. The results are shown in Table 6.4. The optimum responses and conditions are the same using these two methods, the independent variables of which are 2.0 for ultrasonic power (120 W), -2.0 for ultrasonic irradiation mode (continued), 0.2 for TMP (0.64 bar), -2.0 for temperature (20℃), and responses are 55.3% for Y_1 and 53 minutes for Y_2.

The confirmation experiments were carried out at the optimum conditions to check the optimum results in Table 6.4. The experimental results at the optimum

conditions are about 57.0-60.3% and 53-58 minutes. The deviations between the confirmation and predicted values are within 10%. Therefore, it indicates that the second order polynominal regression models are appropriate.

Table 6.4 The optimum conditions and predicted responses

Objective	Optimized condition (coded level)				Response	
	X_1,Power	X_2,Irradiation	X_3,TMP	X_4,Temp	Y_1 (%)	Y_2 (min)
F=1.5722	2.0 (120)	-2.0 (0)	-0.2 (0.64)	-2.0 (20)	55.33	53
D=0.7221	2.0 (120)	-2.0 (0)	-0.2 (0.64)	-2.0 (20)	55.33	53

6.4 Conclusions

The effects and mutual interaction of operational parameters on USUF process of *RA* mixtures have been investigated. The results show that TMP is the most significant factor for the process, followed by temperature, ultrasonic power and irradiation mode in decreasing level of significant. US can affect the flux reduction and process duration by reducing the concentration polarization and fouling. The optimum conditions for the process have been obtained to be ultrasonic power of 120 W, ultrasonic irradiation mode of continued, TMP of 0.64 bar and temperature of 20 ℃ with flux reduction of 57.0-60.3% and process duration of 53-58 minutes. These experimental results have been found to be in good agreement with the predicted values obtained by the regression models. RSM is a good statistic tool to investigate the effects of parameters and optimize the process of USUF process.

Nomenclature

b_{k0}	coefficient of constant term in the regression model
b_{ki}	coefficient of linear term in the regression model
b_{kii}	coefficient of quadratic term in the regression model
b_{kij}	coefficient of cross term in the regression model
d_k	the individual desirability
D	the overall desirability
F	the global criterion
F-value	Fisher's test, ratio of variances
k	total number of parameters in the regression model
p_i	response weight
p-value	the probability under the null hypothesis
r	positive constant
R^2	coefficient of multiple determination
R_{adj}^2	adjust coefficient of multiple determination
w_i	the response weight
X_1, X_2, X_3, X_4	the coded levels of the factors (independent variables)
Y_k	the dependent responses
Y_1	flux reduction
Y_2	process duration

References

1. Roy Upton Herbalist, *Astragalus* Root, American Herbal Pharmacopoeia and Therapeutic Compendium, August 1999
2. T. Kawakatsu, T. Kobayashi, Y. Sano, M. Nakajima, Clarification of green tea extract by microfiltration and ultrafiltration, Bioscience Biotechnology Biochemistry 59 (1995) 1016-1020
3. H. Nawaz, J. Shi, G.S. Mittal, Y. Kakuda, Extraction of polyphenols from grape seeds and concentration by ultrafiltration, Separation and Purification Technology 48 (2006) 176-181
4. W.X. Li, W.H. Xing, W.Q. Jing, N.P. Xu, Effect of pH on microfiltration of Chinese herb aqueous extract by zirconia membrane, Separation and Purification Technology 50 (2006) 92-96
5. X.L. Qiao, Z.J. Zhang, Z.H. Ping, Hydrophilic modification of ultrafiltration membranes and their application in Salvia Miltiorrhiza decoction, Separation and Purification Technology 56 (2007) 265-269
6. F. Vigo, C. Uliana, Ravinae, A. Lucifredi, M. Gandoglia, The vibrating ultrafiltration module performance in the 50-1000 Hz frequency-range, Separation. Science and Technology 28 (1993) 1063-1076
7. Z.F. Cui, T. Taha, Enhancement of ultrafiltration using gas sparging: a comparison of different membrane modules, Journal of Chemical Technology & Biotechnology 78 (2003) 249- 253
8. Z.F. Cui, K.I.T. Wright, Flux enhancements with gas sparging in downwards

crossflow ultrafiltration: performance and mechanism, Journal Membrane Science 117 (1996) 109-116

9. J. Jurado, B.J. Bellhouse, Application of electric fields and Vortex mixing for enhanced ultrafiltration, Filtration and Separation 31 (1994) 273-281
10. H. M. Kyllonen, P. Pirkonen, M. Nystrom, Membrane filtration enhanced by ultrasound: a review, Desalination 181 (2005) 319-335
11. A. Simon, N. Gondrexon, S. Taha, J. Cabon, G. Dorange, Low-frequency ultrasound to improve dead-end ultrafiltration performance, Separation Science and Technology 35 (2000) 2619-2637
12. M.O. Lamminen, H.W. Walker, L.K. Weavers, Mechanisms and factors influencing the ultrasonic cleaning of particle-fouled ceramic membranes, Journal of Membrane Science 237 (2004) 213-223
13. T. Kobayashi, T. Kobayashi, Y. Hosaka, N. Fujii, Ultrasound-enhanced membrane-cleaning processes applied water treatments: influence of sonic frequency on filtration treatments, Ultrasonics 41 (2003) 185-190
14. T. Kobayashi, X. Chai, N. Fujii, Ultrasound enhanced cross-flow membrane filtration, Separation and Purification Technology 17 (1999) 31-40
15. A. Maskooki, T. Kobayashi, S.A. Mortazavi, A. Maskooki, Effect of low frequencies and mixed wave of ultrasound and EDTA on flux recovery and cleaning of microfiltration membranes, Separation and Purification Technology 59 (2008) 67-73
16. W.J. Kim, H.H. Kim, S.H. Yoo, Ultra- and Nano-Filtration process optimization of isoflavones and oligosaccharides from Sunmul, Food Science

and Biotechnology 14 (2005) 380-386

17. S.C. Cheison, Z. Wang, S.Y. Xu, Use of response surface methodology to optimize the hydrolysis of whey protein isolate in a tangential flow filter membrane reactor, Journal of Food Engineering 80 (2007) 1134-1145
18. M. Sivakumar, G. Annadurai, D. Mohan, Studies on Box-Behnken design experiments: cellulose acetate-polyurethane ultrafiltration membranes for BSA separation, Bioprocess Engineering 21 (1999) 65-68
19. R. Malaisamy, G. Annadurai, D. Mohan, Perfrmance optimization of polysulfone ultrafiltration membranes for riboflavin separation using design experiments, Bioprocess Engineering 22 (2000) 227-232
20. C. Cojocaru, G. Zakrzewska-Trznadel, Response surface modeling and optimization of copper removal from aqua solution using polymer assisted ultrafiltration, Journal Membrane Science 298 (2007) 56-70
21. I. Xiarchos, A. Jaworska, G. Zakrzewska-Trznadel, Response surface methodology for the modeling of copper removal from aqueous solution using micellar-enhanced ultrafiltration, Journal Membrane Science 321 (2008) 222-231
22. M. Khayet, C. Cojocaru, G. Zakrzewska-Trznadel, Response surface modeling and optimization in pervaporation, Journal Membrane Science 321 (2008) 272-283
23. J. Kros, C.M. Masterangelo, Comparing methods for the multi-response design problem, Quality and Reliability Engineering International 17 (2001) 323-331
24. G. Derringer, R. Suich, Simultaneous optimization of several response

variables, Journal of Quality Technology 21(1980) 214-219

Chapter 7

Modeling and Mechanisms of US-assisted UF process of *RA* Extracts with Hollow Fiber Membrane

Abstract

The kinetics of various resistances, including adsorption, pore blocking and cake layer resistances, were quantified as time or time and TMP dependent equations. Mechanisms for the effects of US irradiation on membrane fouling were demonstrated by comparing with the dynamics of these different resistances in UF and US-assisted UF (USUF) processes. Furthermore, the changes of membrane structure after US irradiation were used to help the reveal of the mechanisms of US effects. The degree of adsorption gradually increased with time in both processes. The degree of pore blocking increased as the pressure increased, but did not change with time in the UF process. However, in the USUF process, the pore blocking resistance was affected by pressure and increased with time at a constant pressure. The cake layer resistance contributed more significantly as TMP increased and it was the crucial resistance in the UF processes. US irradiation could reduce the cake layer, cutting its contribution from 75% to 50%. The developed semi-empirical models could be successfully applied to UF and USUF processes for predicting the flux performance with deviations about 5% and 10%, respectively. According to the resistance analysis and the phenomena of US irradiated hollow fiber membranes, acoustic cavitation, bubble collapse and micro-jet could be the main factors leading to membrane fouling reduction and permeate flux improvement.

7.1 Introduction

Flux decline is one of the main problems in the application of ultrafiltration (UF) which is mainly caused by membrane fouling. A number of models have been developed to investigate and predict the flux decline during the membrane filtration process. These models can be classified as (a) gel polarization model, (b) osmotic pressure model and (c) resistance-in-series model [1, 2]. In the resistance-in-series model, the mechanisms for membrane fouling are usually divided into several resistances, such as adsorption, pore blocking, concentration polarization and cake layer formation. Solutes in solution such as protein and polysaccharides can be easily adsorbed on the membrane surface by membrane-solute interactions [3, 4], called adsorption. Pore blocking is the phenomenon that membrane pores are plugged by some solutes or particles if they are similar in shape or size [5, 6]. These two resistances are usually called irreversible fouling as they cannot be removed by water flushing and need further chemical cleaning. Concentration polarization is that the solutes accumulate near the membrane surface and bring on arising of the concentration. It leads to the subsequent formation of cake layer which takes the most responsible for the membrane fouling [7, 8]. Cake layer occurs when the solutes gradually accumulate on the membrane surface at a critical concentration to form a thin additional resistance. Its structure depends on the solute particle size, electrostatic, TMP, etc [6, 9]. These two fouling resistances are considered as reversible since they can be removed by water flushing. All the resistances can

be determined by experiments independently so that the contributions of each resistance can be obtained. Comprehensively understanding of the contributions of each resistance provides basic reasons to use effective methods for improving flux.

In recent years, some modified models have been developed based on the resistance-in-series model. Zydney's group developed a filtration model combined the pore blockage and the cake for protein and humic acid fouling during microfiltration [10, 11]. They divided the fouling resistances into initial pore blockage and subsequent growth of a protein cake. Purkait et al. found that the membrane permeability decreased rapidly due to reversible pore blocking and further flux decline was caused by the growth of a gel-type layer over the membrane surface [12]. In Choi's study, the total resistance in biological suspension filtration was composed of intrinsic membrane, adsorption, concentration polarization and fouling resistances [13]. The fouling resistance was subdivided into reversible and irreversible, which characterizes the fouling being removed by flushing or not. The irreversible fouling consists of pore blocking, strong cake, gel and biofilm. Though most of these previous studies divided the total resistance into several resistances, few of them provide the kinetic change of each resistance during the process. Furthermore, their filtration solutions are not as complex as the natural product mixtures, such as *Radix astragalus* (*RA*) extracts, which may result in different contributions of each resistance.

The purpose of this study is to develop semi-empirical models to describe the UF and US-assisted UF (USUF) processes of *RA* extracts with hollow fiber modules. Each resistance in the models, including adsorption, pore blocking and cake layer, will be quantified and provided their time-dependant kinetics in the process. Finally, flux decline performance with time can be simulated and predicted, and be compared with the experimental data. Accordingly, the fouling mechanisms for such complicated solution in the USUF process will be demonstrated. By analyzing the kinetics of each resistance and the structural changes of US irradiated membranes, mechanisms for US induced fouling reduction and flux enhancement in USUF process will be demonstrated.

7.2 Theory

The flux decline profile can be different due to the different characteristics of filtered solution and the operational conditions. The kinetics and contribution of each resistance are affected by the constituents in filtration solution. In *RA* extracts, components in the solution are complex and the distribution of their molecular weights is wide. Proteins and polysaccharides in the extracts can be easily adsorbed on the membrane surface by the membrane-solutes interaction, especially on the hydrophobic membranes [14]. Solutes having relatively smaller size than the membrane pores may go inside the pores and be adsorbed on the inside surface of membrane. The pores can be plugged by the components or particles with similar size in the extracts. Fouling caused by adsorption or pore

blocking is mostly irreversible and need further chemical cleaning. These two resistances usually occur at the initial stage during the membrane filtration processes [12, 15]. When the process goes on, solutes gradually accumulate on the membrane surface leading to the formation and growth of a cake layer. Cake layer resistance usually contributes the most of total resistances, but it can be removed by flushing with water. Figure 7.1 illustrates the different types of fouling in the UF process.

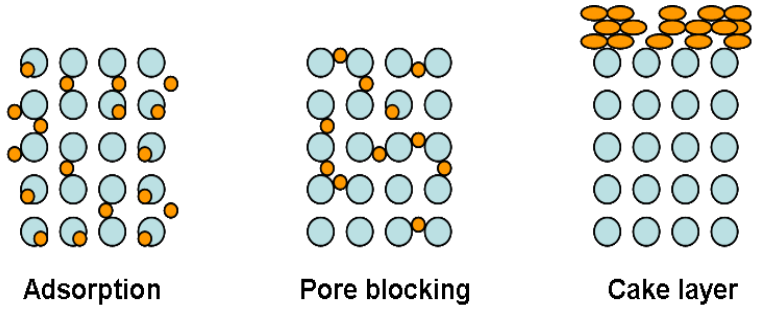

Figure 7.1 Different types of fouling in the UF process

According to Darcy's law, the resistance-in-series model can be written as follows:

$$J = \frac{1}{A}\frac{dV}{dt} = \frac{\Delta P}{\mu(R_m + R_{ad} + R_p + R_c)} \tag{7-1}$$

where J is the permeate flux ($L \cdot m^{-2} \cdot h^{-1}$), A the effective area of membrane (m^2), R_m the intrinsic membrane resistance (m^{-1}), R_{ad} the adsorption resistance (m^{-1}), R_p the pore blocking resistance (m^{-1}), R_c the cake layer resistance (m^{-1}), ΔP the TMP (bar) and μ the viscosity of solution (bar·h).

The water flux can be written as:

$$J_0 = \frac{\Delta P}{\mu_w R_m} \tag{7-2}$$

Combining Equations (7-1) and (7-2) gives the following dimensionless equation by assuming that the viscosity of solution is similar to the water due to its dilute concentration:

$$\frac{J_t}{J_0} = \frac{1}{1 + \frac{R_{ad}}{R_m} + \frac{R_p}{R_m} + \frac{R_c}{R_m}} \tag{7-3}$$

The kinetics of $\frac{R_{ad}}{R_m}$, $\frac{R_p}{R_m}$, $\frac{R_c}{R_m}$ will be developed according to the experimental data.

7.3 Materials and methods

7.3.1 Materials

RA extracts were prepared as described in Section 3.2.1.

7.3.2 Experimental apparatus

All experiments were carried out with a hollow fiber UF module (Microza, Pall Co. USA) which has a bundle of 10 k Da MWCO polysulfone membranes and total effective area of 0.015 m^2. The module was immersed in a water bath with an

ultrasonic transducer plate (Kamson Ultrasonic Equipment Co., Ltd. China). The ultrasonic plate works at 45 kHz frequency and has the power output ranged 0-300 W with an interval of 30 W. The *RA* extracts were fed by a peristaltic pump (Masterflex, Cole-Parmer Ins. Co., USA) at a fixed flow rate of 40 mL·min^{-1}. The system TMP was adjusted to 0.4, 0.6 or 0.8 bar by a valve on the side of retentate tube. The feed container with a stirring bar inside was put on a magnetic and heat plate (Thermolyne Cimarec 1, Dubuque, USA). The schematic of the USUF setup is shown in Figure 5.1, Chapter 5.

7.3.3 Determination of various resistances

7.3.3.1 Intrinsic membrane resistance

The permeate flux was determined at different TMPs by DI water. The plot of fluxes at different pressures against TMP shows a straight line. Hence, the intrinsic membrane resistance can be calculated by the following equation transformed from the Equation (7-2):

$$R_m = \frac{\Delta P}{\mu_w J_0} \tag{7-4}$$

The water fluxes are 36.70, 100.69 and 160.80 L·m^{-2}·h^{-1} at the TMPs of 0.4, 0.6 and 0.8 bar, respectively.

7.3.3.2 Adsorption resistance

RA extracts was pumped through the hollow fiber membrane without pressure at the feed velocity of 40 mL·min^{-1} for various durations of 5, 15, 30, 60 and 120 minutes. After a particular time, the membrane was rinsed by DI water for 10 minutes so as to wash the loosely adsorbed solutes off the membrane surface. Then, water fluxes were determined by DI water at various pressures. The adsorption resistance at given time can be calculated by:

$$J' = \frac{\Delta P}{\mu(R_{ad} + R_m)} \tag{7-5}$$

Combining Equations (7-4) and (7-5), gives the following equation:

$$\frac{R_{ad}}{R_m} = \frac{J_0}{J'} - 1 \tag{7-6}$$

After all the values of adsorption resistance at different times were calculated, a kinetic curve of $\frac{R_{ad}}{R_m}$ against time could be plotted.

7.3.3.3 Pore blocking resistance

UF experiment was carried out with *RA* extracts at particular operating conditions: TMP of 0.4, 0.6 or 0.8 bar at different durations of 5, 15, 30, 60 and 120 minutes, respectively. After each run, the membrane was flushed by DI water thoroughly so that any deposits on the membrane surface, or the reversible fouling, can be washed off. Then, the water flux was determined with DI water at the same

operating condition. Thus, $\frac{R_p}{R_m}$ can be obtained by the following Equation (7-7), based on the already calculated value of $\frac{R_{ad}}{R_m}$.

$$\frac{R_p}{R_m} = \frac{J_0}{J_w} - \frac{R_{ad}}{R_m} - 1 \tag{7-7}$$

Similar procedure was followed at other times to calculate the $\frac{R_p}{R_m}$.

After all values of pore blocking resistance at different times and pressures were obtained, the kinetic curves of $\frac{R_p}{R_m}$ at different pressures can be plotted.

7.3.3.4 Cake layer resistance

UF processes of *RA* extracts were run for 120 minutes at different TMPs. Since the kinetics of $\frac{R_{ad}}{R_m}$ and $\frac{R_p}{R_m}$ have already obtained, the dynamic growth of cake layer resistance can be calculated by the following equation.

$$\frac{R_c}{R_m} = \frac{J_0}{J_t} - \frac{R_{ad}}{R_m} - \frac{R_p}{R_m} - 1 \tag{7-8}$$

7.4 Results and discussion

7.4.1 Modeling of UF process of *RA* extracts

7.4.1.1 Analysis of various resistances

The adsorption resistances at 5, 15, 30, 60 and 120 minutes were obtained and plotted in Figure 7.2. The adsorption resistance increased rapidly at the initial 15 minutes in the UF process. Proteins and polysaccharides in the extracts were adsorbed immediately when they contacted with the surface of polysulfone membrane because of the physical or chemical interactions. The growth kinetics of adsorption resistance can be fitted by the following equation:

$$\frac{R_{ad}}{R_m} = a_1 Ln(t) + b_1 \tag{7-9}$$

where the coefficients a_1=0.52 and b_1=0.35 in this study.

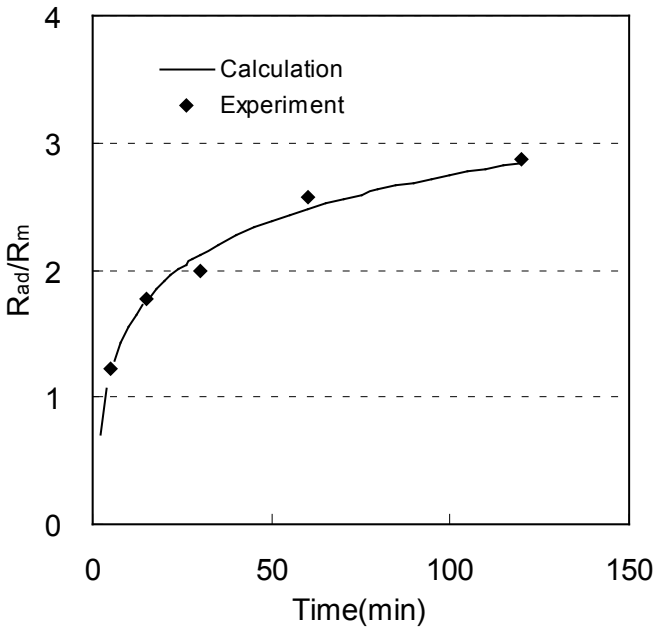

Figure 7.2 Growth kinetic of adsorption resistance with time in UF of *RA* extracts.

The pore blocking resistances were measured at different pressures and the results are shown in the Figure 7.3a. It can be seen that the pore blocking resistance kept almost the same level at constant pressure during the filtration process. The value increased linearly with the increased pressure, as shown in the Figure 7.3b. This phenomenon indicated that the pore blocking happened immediately when the process started and the degree kept almost the same level subsequently. The degree of pore blocking was mainly affected by the driving force, TMP. Accordingly, a linear equation can be developed to describe the pore blocking resistance:

$$\frac{R_p}{R_m} = a_2 \Delta P + b_2 \qquad (7\text{-}10)$$

where the coefficients a_1=2.78 and b_1=0.17 in this study.

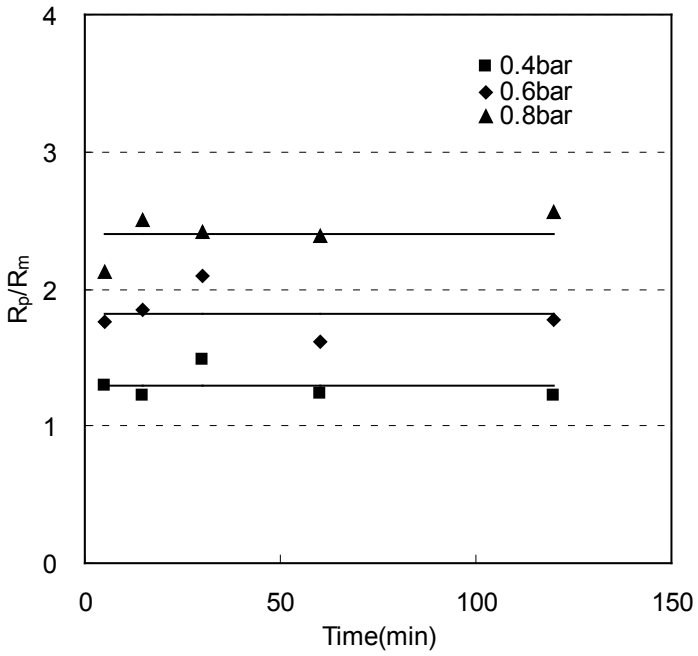

(a)

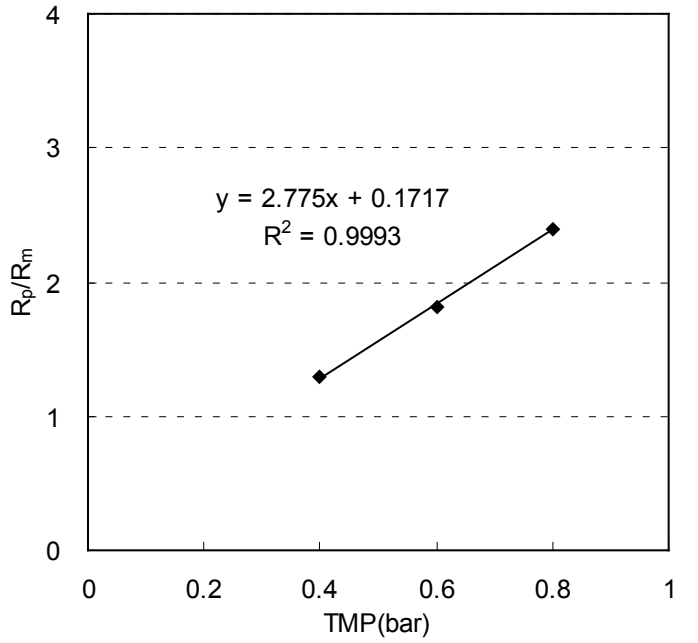

(b)

Figure 7.3 Characteristic of pore blocking with time at different TMPs in UF of *RA* extracts.

Cake layer usually occurs after adsorption and pore blocking. The growth kinetics of cake layer resistance against time at different pressures is shown in Figure 7.4. The cake layer increased almost linearly at low pressure and rapidly

increased as the pressure increased. According to the growth kinetics of cake layer resistance at different pressures, an equation expressing the function of TMP and time could be written as follows:

$$\frac{R_c}{R_m} = (a_3 \Delta P + b_3) t^c \tag{7-11}$$

where the coefficients a_3=8.31, b_3=-2.80 and c=0.28 in this study.

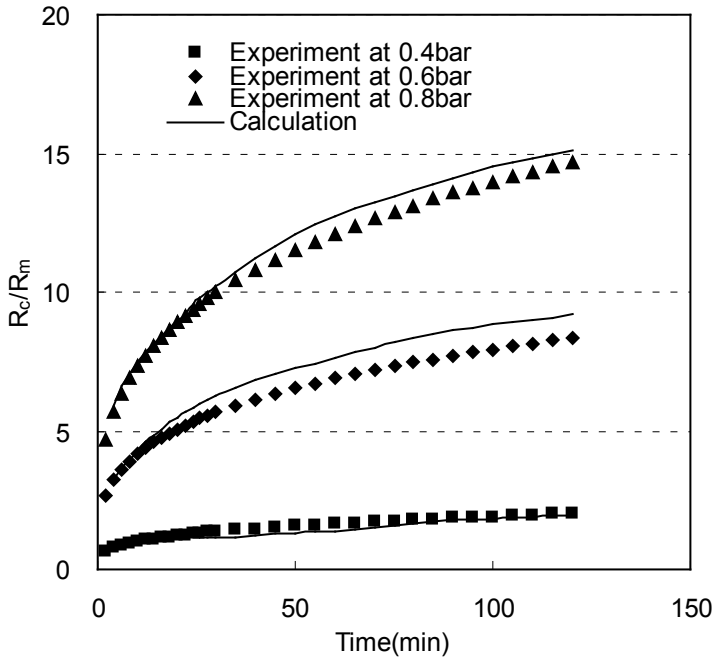

Figure 7.4 Growth kinetics of cake layer resistance with time at different TMPs in UF of *RA* extracts.

7.4.1.2 Model verification

After obtained the kinetic models of each resistance, the flux decline performance could be simulated by combining all the equations together. Figure 7.5 shows the flux decline profiles from modeling simulation and experiments. The curves of model fitted quite well with the experimental data, and the deviations between

calculation and experiments are 4.1%, 4.5% and 4.0% at 0.4. 0.6 and 0.8 bar, respectively, all of which are below 5%.

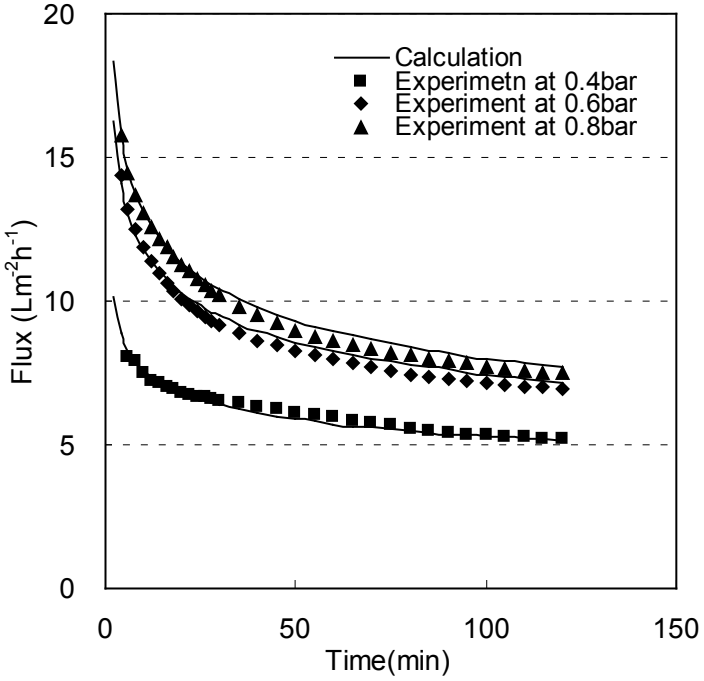

Figure 7.5 Flux decline profiles in UF of *RA* extracts at different TMPs. .

7.4.2 Modeling of US-assisted UF process of *RA* extracts

7.4.2.1 Analysis of various resistances

The adsorption resistances at 5, 15, 30, 60 and 120 minutes were obtained and plotted in Figure 7.6. The adsorption resistance increased gradually during the USUF process. The values and trends were almost identical with that in the UF process without US. It indicated that the US irradiation affected the interaction of solutes and membrane slightly. The growth kinetics of adsorption resistance can be fitted by the Equation (7-9), in which the coefficients a_1=0.21 and b_1=1.38 for this study.

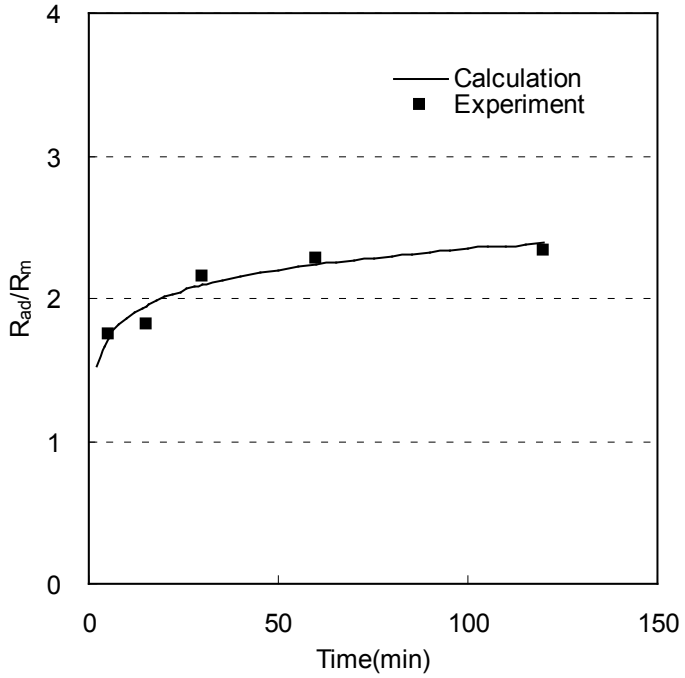

Figure 7.6 Growth kinetics of adsorption resistance with time in UF of *RA* extracts.

Pore blocking resistances were measured at different pressures against time and the results were shown in Figure 7.7. It shows that the pore blocking resistance gradually increased at a constant pressure in the filtration process, and the value increased with the increased pressure. This phenomenon was different from that in the UF process without US irradiation. At low TMP, e.g. at 0.4 bar, the pore blocking resistance was very small, but it became significant at high TMP, indicating that the US irradiation could affect the degree of pore blocking and this effect was also jointly affected by the applied pressure. At low pressure, the solutes may just block the pores near the membrane surface, which can be removed by US irradiation more easily. Under high pressure, the solutes can be pushed deeper in the pores of membrane by both US irradiation and strong driven force; therefore, the degree of pore blocking becomes significant in the process.

Accordingly, an equation expressing the function of TMP and time was developed to describe the pore blocking resistance:

$$\frac{R_p}{R_m} = (a_2 \Delta P + b_2) t^{c_2} \tag{7-12}$$

where the coefficients a_2=2.38, b_2=0.72 and c_2=0.21 in this study.

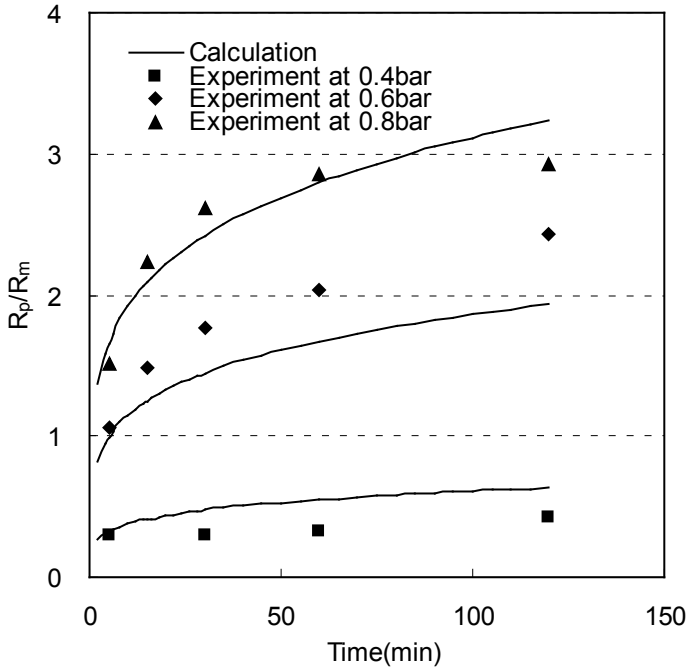

Figure 7.7 Growth kinetics of pore blocking resistance with time at different pressures in UF of *RA* extracts.

The growth kinetics of cake layer at different pressures was determined as shown in Figure 7.8. The cake layer increased slowly and almost linearly at low pressure but rapidly increased as the pressure increased. Be compared the values with that in the UF process without US, cake layer were much lower after US irradiation. It demonstrates that the US irradiation mainly reduce the thickness of cake layer. Consequently, the flux can be enhanced. According to the growth

kinetics of cake layer resistance at different pressures, an equation could be given:

$$\frac{R_c}{R_m} = (a_3 \Delta P + b_3) t^{c_3} \tag{7-13}$$

where the coefficients a_3=6.54, b_3=-1.68 and c_3=0.18 in this study.

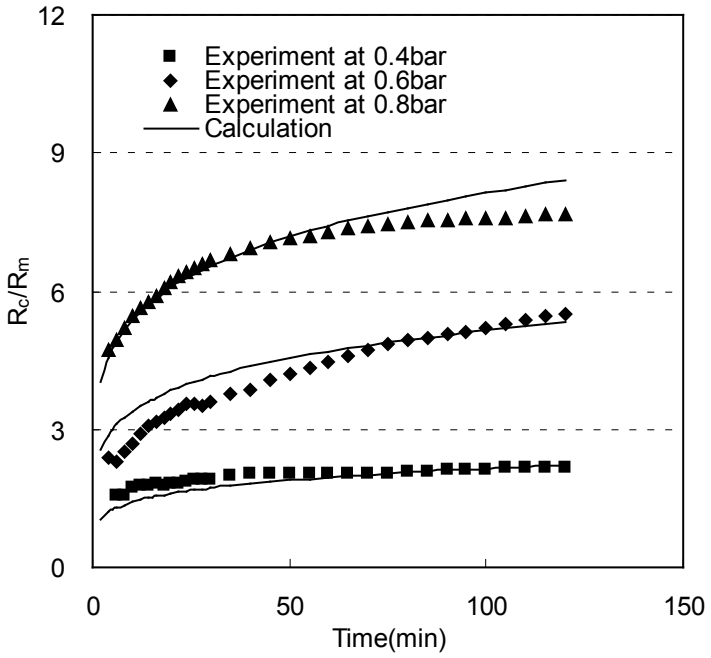

Figure 7.8 Growth kinetics of cake layer resistance against time at different TMPs in UF of *RA* extracts.

7.4.2.2 Model verification

Flux decline performance can be simulated by the established model after obtaining the kinetic models of each resistance. Figure 7.9(a) shows the flux decline profiles from simulation and experiments. The curves of model fitted well with the experimental data, and the deviations between calculation and experiments were 5.6%, 9.3% and 6.9% at 0.4, 0.6 and 0.8 bar, respectively.

In order to represent the ultrasonic effect in the model, ultrasonic parameters γ and λ , which considered as a function of ultrasonic power, were introduced to the Equations (7-14) and (7-15). γ and λ are ranged from 0 to 1, and both are decreased as the ultrasonic power increased in the range of 0-120 W.

$$\frac{R_p}{R_m} = \gamma(a_2\Delta P + b_2)t^{(1-\lambda)} \tag{7-14}$$

$$\frac{R_c}{R_m} = \gamma(a_3\Delta P + b_3)t^{\lambda c_3} \tag{7-15}$$

where a_2=2.78, b_2=0.17, a_3=8.33, b_3=-2.81, c_3=0.28, γ=0.65 and λ=0.85.

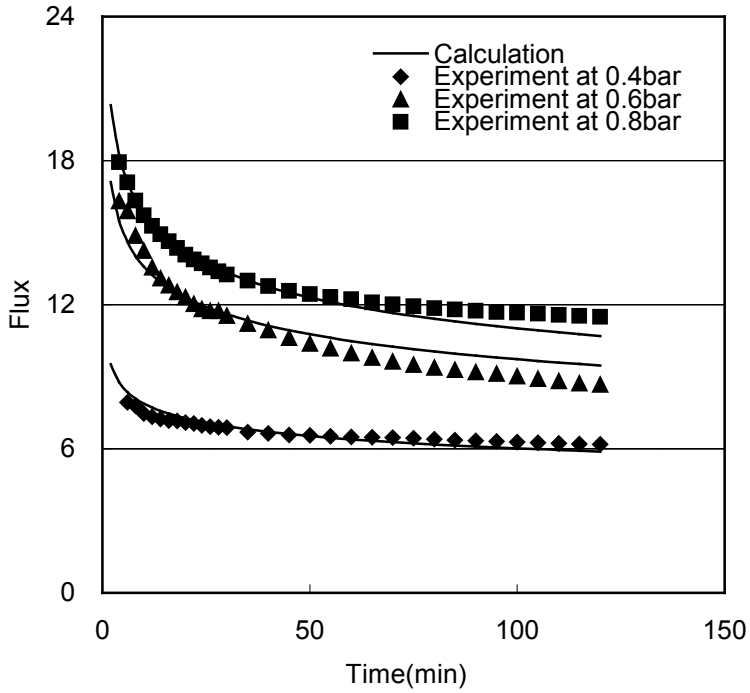

(a)

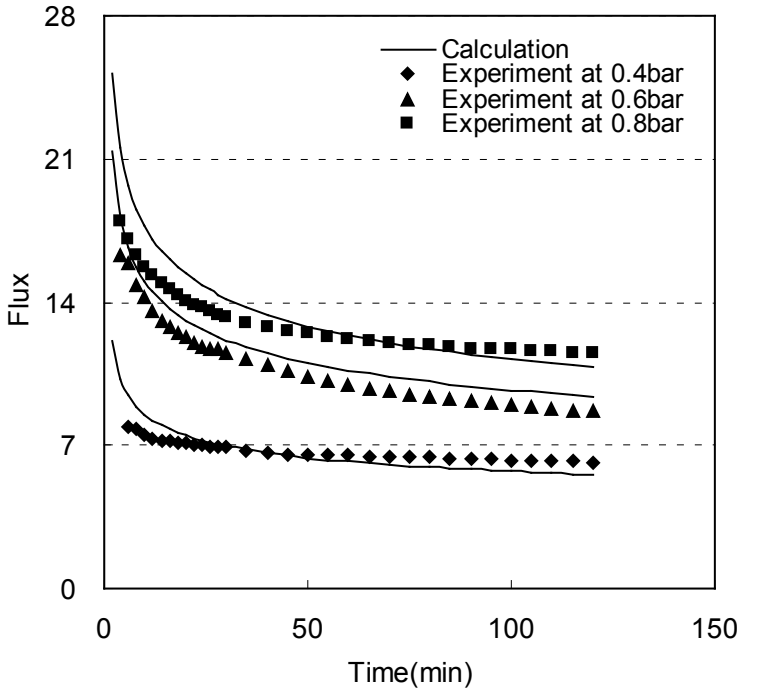

(b)

Figure 7.9 Flux decline profiles in US-assisted UF of *RA* extracts at different TMPs, (a) model without γ and λ; (b) model with γ and λ.

7.4.3 Mechanisms of US irradiation on flux enhancement

7.4.3.1 Contributions of each resistance

Figures 7.11 and 7.12 show the increase of total resistances, including adsorption, pore blocking and cake layer, during UF and USUF processes of *RA* extracts, respectively. Figure 7.10 indicated that at low TMP, i.e. 0.4 bar, the adsorption resistance contributed nearly 50% of the total resistance, more significant than the others at higher TMPs. The US irradiation did not affect the adsorption resistance, as shown in Figure 7.11. Compared with the pore blocking resistances in these processes, it was evident that US could affect the degree of pore blocking during the UF process. This could attribute to the vibration characteristic of US. As the TMP increased, the contribution of cake layer resistance became significant in both processes, almost 75% at 0.8 bar in the UF process and over 50% in the USUF process. It demonstrated that TMP was the dominating driving force for cake formation and membrane fouling during the UF process [6]. This phenomenon also gave the evidence that the most effective method to reduce membrane fouling was to decrease the cake layer, which US technique could successfully achieve, decreasing the contribution of cake layer from 75% to 50%.

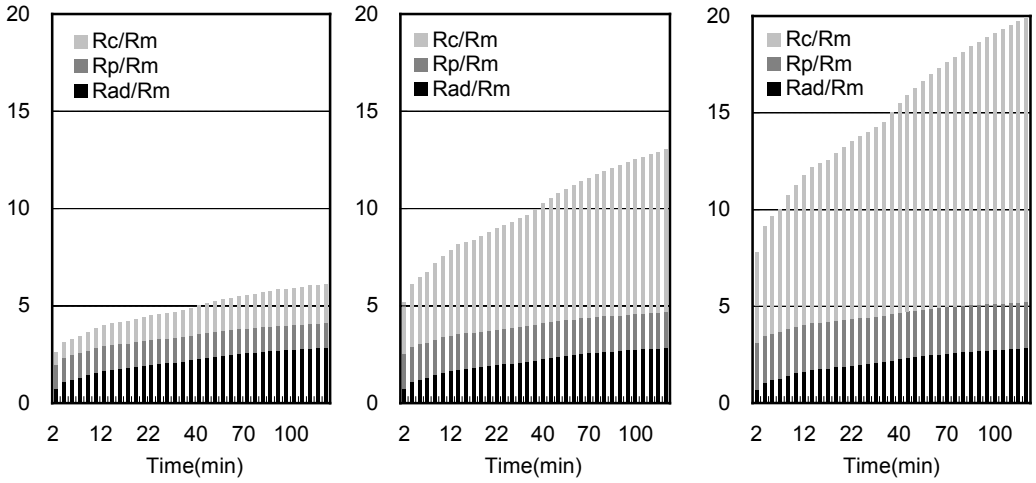

(a) (b) (c)

Figure 7.10 Changes of contributions of three different resistances during UF process at TMPs of 0.4 (a), 0.6 (b) and 0.8 (c) bar.

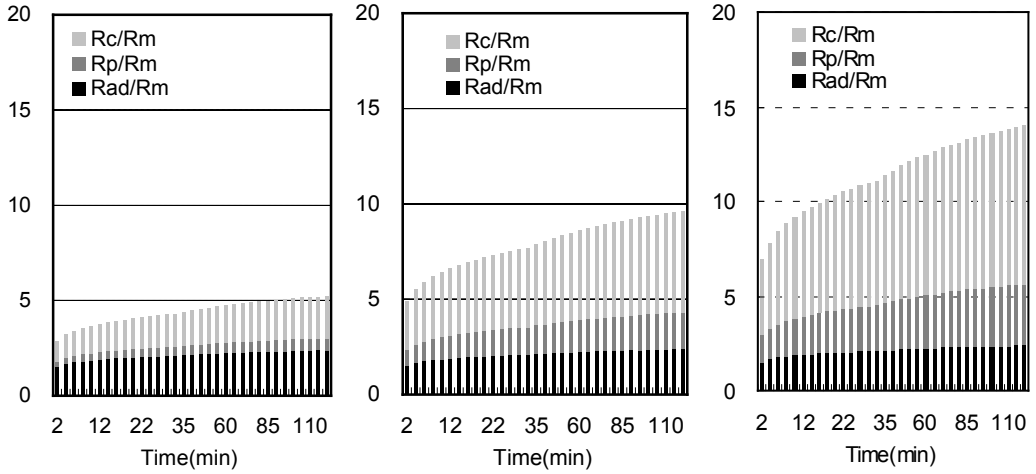

(a) (b) (c)

Figure 7.11 Changes of contributions of three different resistances during US-assisted UF process at TMP of 0.4 (a), 0.6 (b) and 0.8 (c) bar.

7.4.3.2 Mechanisms of US irradiation on hollow fiber UF membrane

Cavitation, acoustic streaming, microstreaming, liquid micro-jet, radiation force are considered as the main effects induced by US irradiation in water [16]. Cavitation bubble collapses when the pressure reaches a high value, even up to

2000 atm. Localized hot temperature can also be produced by US, up to 5000 K. When acoustic bubble collapses near a solid surface, powerful micro-jet of liquid occurs, with an estimated velocity of 100-200 ms^{-1} [17].

Figure 7.12 shows the cross section view of PS hollow fiber membrane irradiated at ultrasonic frequencies of 100, 45 and 28 kHz for 10 minutes. Significant differences were observed on the membrane structure after US treatment. The change of cross section view of membrane was slight with 100 kHz ultrasonic irradiation (Fig.7.12b); however, it became significant under irradiation of 45 kHz and 28 kHz (Fig.7.12c, 7.12d). The explanation can be that the number of cavitation bubble increases with the increased ultrasonic frequency at the same output power, but the radius of bubbles decreases [18]. Acoustic pressure becomes weaker with the decreasing of bubble radius. This phenomenon reveals that acoustic pressure can be the major factor leading to damages of hollow fiber membrane under ultrasonic irradiation.

Figure 7.13 shows the damages on the membrane after ultrasonic irradiation. A great number of small holes existed inside the surface of hollow fiber membrane under ultrasonic irradiation (Figure 7.13a). A concavity was found (Figure 7.13b) on the membrane surface which supposed to be smooth without ultrasonic irradiation. These images demonstrated that acoustic cavitation could be the main factor causing the membrane change or damage. Bubble collapse and micro-jet produced strong pressure and force leading to the damages. It was also

supported by the evidences from the effect of ultrasonic frequency on membrane mentioned before. With the US irradiating for a longer time, cracks occurred on the membrane surface, which led to fatal damage of the hollow fiber (Figure 7.13c, 7.13d). These cracks might be caused by the micro-jet which can produce strong force.

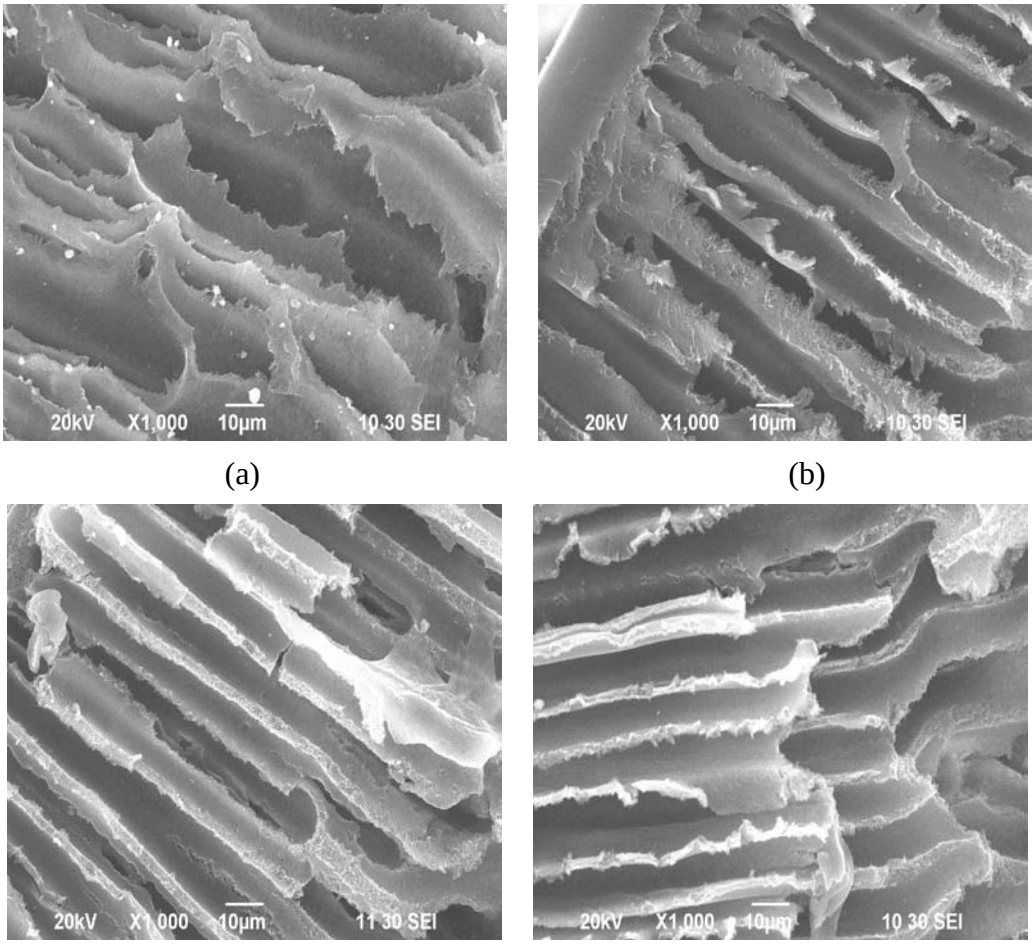

Figure 7.12 Images of PS hollow fiber UF membranes irradiated with different US frequencies and 100 W power for 10 min. (a) membrane without US irradiation, (b) membrane irradiated at 100 kHz, (c) membrane irradiated at 45 kHz, (d) membrane irradiated at 28 kHz.

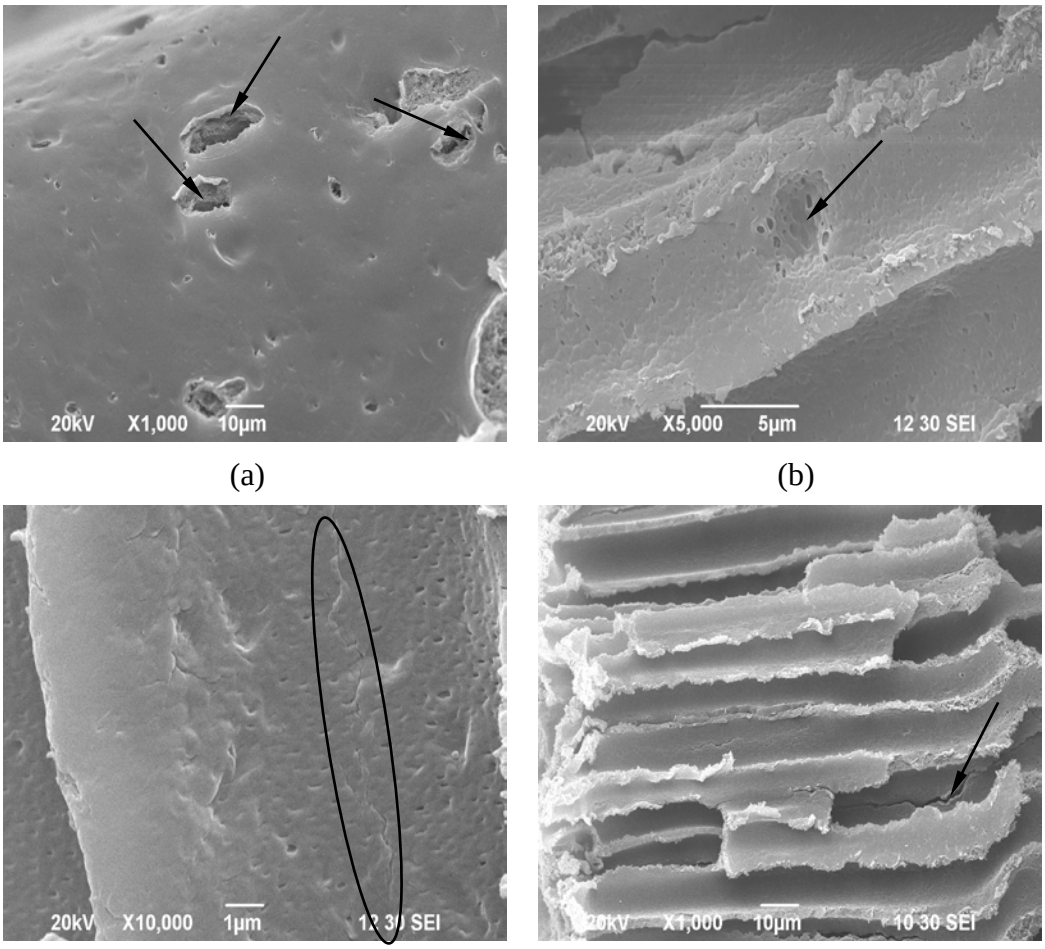

(a) (b)

(c) (d)

Figure 7.13 Images of PS hollow fiber membrane after 45 kHz US irradiation. (a) inside surface of hollow fiber, (b) concavity on the membrane surface, (c), (d) cracks on the membrane surface.

7.5 Conclusion

Semi-empirical models were developed for predicting flux decline in UF and USUF processes of *RA* extracts. The kinetics of various resistances, including adsorption, pore blocking and cake layer resistances, were quantified as functions of time or time and TMP. These models were in good agreement with the experimental data and the predicting deviations were within 5% and 10%, respectively. The mechanisms of US irradiation on membrane fouling were

demonstrated by analyzing the dynamics of different resistances in UF and USUF processes. The adsorption resistance increased gradually in these two processes with no significant differences. With the US irradiation, pore blocking resistance gradually increased under a constant pressure in the filtration process, which was different from that in the UF process without US. The degree of blocking increased with the pressure increasing. The dominated cake layer resistance could be reduced from 75% to 50% by US irradiation. The models developed could be successfully applied to UF and USUF processes for predicting flux. By analyzing the effects of US irradiation on hollow fiber membrane, acoustic cavitation, bubble collapse and micro-jet were believed to be the main mechanisms for membrane fouling reduction and flux improvement.

Reference

1. P. Rai, C. Rai, G.C. Majumdar, S. DasGupta, S. De, Resistance in series model for ultrafiltration of mosambi (Citrus sinensis (L.) Osbeck) juice in a stirred continuous mode, Journal of Membrane Science 283 (2006) 116-122
2. W.R. Bowen, F. Jenner, Theoretical descriptions of membrane filtration of colloids and fine particles an assessment and review, Advances in Colloid and Interface Science, 56 (1995) 141-200
3. A.G. Fane, C.J.D. Fell, A.G. Waters, Ultrafiltration of protein solutions through partially permeable membranes-the effect of adsorption and solution environment, Journal of Membrane Science, 16 (1983) 211-224
4. M. Ulbricht, W. Ansorge, I. Danielzik, M. König, O. Schuster, Fouling in microfiltration of wine: The influence of the membrane polymer on adsorption of polyphenols and polysaccharides, Separation and Purification Technology, 68 (2009) 335-342
5. G. Belfort, R.H. Davis, A.L. Zydney, The behavior of suspensions and macromolecular solutions in crossflow microfiltration, Journal of Membrane Science, 96 (1994) 1-58
6. L. Song, Flux decline in crossflow microfiltration and ultrafiltration: mechanisms and modeling of membrane fouling, Journal of Membrane Science, 139 (1998) 183-200
7. S.K. Hong, R.S. Faibish, M. Elimelech, Kinetics of permeate flux decline in crossflow membrane filtration of colloidal suspensions, Journal of Colloid and

Interface Science, 196 (1997) 267-277

8. J. Kim, F.A. DiGiano, Fouling models for low-pressure membrane systems, Separation and Purification Technology, 68 (2009) 293-304
9. P. Le-Clech, V. Chen, T.A.G. Fane, Fouling in membrane bioreactors used in wastewater treatment, Journal of Membrane Science, 284 (2006) 17-53
10. C.C Ho, A.L. Zydney, A combined pore blockage and cake filtration model for protein fouling during microfiltration, Journal of Colloid and Interface Science 232 (2000) 389-399
11. W. Yuan, A. Kocic, A.L. Zydney, Analysis of humic acid fouling during microfiltration using a pore blockage-cake filtration model, Journal of Membrane Science 198 (2002) 51-62
12. M.K. Purkait, S. DasGupta, S.De, Resistance in series model for micellar enhanced ultrafiltration of eosin dye, Journal of Colloid and Interface Science 270 (2004) 496-506
13. H. Choi, K. Zhang, D.D. Dionysiou, D.B. Oerther, G.A. Sorial, Influence of cross-flow velocity on membrane performance during filtration of biological suspension, Journal of Membrane Science 248 (2005) 189-199
14. L.C. Koh, W.Y. Ahn, M.M. Clark, Selective adsorption of natural organic foulants by polysulfone colloids: Effect on ultrafiltration fouling, Journal of Membrane Science, 281 (2006) 472-479
15. T. Mohammadi, A. Kohpeyma, M. Sadrzadeh, Mathematical modeling of flux decline in ultrafiltrtion, Desalination, 184 (2005) 367-375
16. K.S. Suslick, Ultrasound: Its Chemical, Physical, and Biological Effects, VCH,

New York, 1988

17. T.G. Leighton, The Acoustic Bubble, Academic Press, London, 1994
18. T.J. Mason, J.P. Lorimer, Applied Sonochemistry: The uses of power ultrasound in chemistry and processing, WILEY-VCH, Weinheim, 2002

Chapter 8

Conclusions

The objectives of this study is to apply the US technique to the UF of *RA* extracts in both dead-end flat sheet (DEFS) and cross-flow hollow fiber (CFHF), and to investigate the effects of various ultrasonic parameters, including ultrasonic frequency, power and irradiation mode, on the US-assisted UF processes. Permeate flux and filtration fouling resistances have been studied at different conditions in the processes. Optimum conditions of US-assisted CFHF UF process have been obtained by using response surface methodology. Semi-empirical dynamic models have been developed to study the fouling mechanisms and to predict the flux declines in the processes.

The major findings and significant conclusions are as follows:

(1) Effects of operational parameters on permeate flux and fouling resistances have been studied in both DEFS and CFHF UF processes of *RA* extracts. In DEFS, the effect of temperature on flux is small, and the effects of TMP and MWCO are significant. Higher TMP can enhance the flux but made the concentration polarization and fouling phenomena more serious. It is appropriate to use 10 k or 30 k Da membrane for the UF process of *RA* extracts. In CFHF, the effects of temperature and flow rate are not significant, but TMP shows a strong effect on the flux and resistances. Concentration polarization and reversible fouling are two main resistances in the UF process of *RA* extracts. Consequently, effective techniques can be applied to reduce the concentration polarization and cake layer in both DEFS and CFHF UF processes.

(2) Effects of ultrasonic factors on the permeate flux and fouling resistances have been investigated in the US-assisted DEFS UF process of *RA* extracts. US irradiation can efficiently enhance the permeate flux, reduce the fouling resistances in the UF process, and improve the flux recovery in cleaning of fouled membrane. US of low frequency and high power is the most effective in enhancing flux and improving flux recovery. US at low frequency and intermittent mode is a promising approach that can be applied to both DEFS UF and cleaning processes of fouled membrane for natural product separation.

(3) Effects of ultrasonic factors on permeate flux and fouling resistances have been investigated in the US-assisted CFHF UF process of *RA* extracts. The hollow fiber membrane is more susceptible to the US irradiation at high power and low frequency. Thus, the ultrasonic power applied should not be as strong as that used in the flat sheet membranes. Ultrasonic frequency, power and irradiation mode can significantly affect the permeate flux and fouling resistances in the UF process. Consequently, US can be applied to the hollow fiber UF process for flux enhancement and fouling reduction, but the applied US power should be carefully controlled.

(4) US-assisted CFHF UF process of *RA* extracts has been optimized by using response surface methodology (RSM). TMP is the most significant factor in the process, followed by temperature, ultrasonic power and irradiation mode.

The optimum conditions of the process were obtained at ultrasonic power of 120 W, ultrasonic irradiation mode of continued, TMP of 0.64 bar and temperature of 20 ℃ with flux reduction of 57.0-60.3% and process duration of 53-58 minutes. RSM is proven to be a good statistic tool to investigate the effects of parameters and to optimize the US-assisted UF process.

(5) Semi-empirical models are developed for predicting the flux decline in UF and US-assisted UF processes of *RA* extracts based on the resistance-in-series model. The kinetics of various resistances, including adsorption, pore blocking and cake layer resistances, are quantified as functions of time or time and TMP. The models developed can be successfully applied to predict the fluxes in UF or US-assisted UF processes, respectively.

(6) The mechanisms of US irradiation on the membrane fouling are demonstrated by comparing the kinetics of different resistances during UF and US-assisted UF processes. The adsorption resistances increases gradually, and they are almost identical in these two processes. The degree of pore blocking resistance can be affected by US irradiation jointly with TMP in the filtration process. By analyzing the effects of US irradiation on the hollow fiber membrane, acoustic cavitation, bubble collapse and micro-jet are believed to be the main mechanisms for membrane fouling reduction and flux improvement.

Chapter 9

Future Studies

Results of this study demonstrate that US technique can be applied to the membrane filtration process of natural products. Our study gives the fundamental and useful knowledge using for reference. Based on these satisfactory findings, there are some subsequent works recommended for future investigation:

(1) Feasibilities and effects of US technique on other membrane filtration modules and membranes can be investigated, such as tubular, spiral wound membrane modules made from some other polymeric or inorganic materials. Polymeric membranes, including PES flat sheet and PS hollow fiber, were used in our study, and it was found PS hollow fiber membrane without supporter was breakable to US irradiation. Additionally, according to our knowledge, there is no study reported on applying US to other membrane modules, except flat sheet and hollow fiber.

(2) The manner of coupling US technique to membrane modules should be further improved. In the present study, the membrane modules were just immersed in an ultrasonic field. The US intensity inside the module was attenuated to about 10% only of the original US and this is energy consumption. Thus, it is necessary to find other more reasonable methods to couple US apparatus and membrane modules.

(3) Based on our study in the lab scale, it is possible to scale up the system for

pilot application in natural products manufactures. Few studies applied the US technique to an industry of membrane filtration process. It is necessary to study the feasibility and worthwhile of US technique applying to the membrane filtration processes.